DETERMINATION OF THE DYNAMICAL PROPERTIES OF THE JOVIAN SYSTEM BY NUMERICAL ANALYSIS

by

John Frederick Chandler

S.B., Massachusetts Institute of Technology
(1973)

SUBMITTED IN PARTIAL FULFILLMENT OF THE
REQUIREMENTS FOR THE DEGREE OF

DOCTOR OF PHILOSOPHY

at the

(c) Massachusetts Institute of Technology

1979 August

Signature of Author.....
Department of Earth and Planetary Sciences

Certified by.....
Thesis Supervisor

Accepted by.....
Chairman, Department Committee

WITHDRAWN
FROM
MIT LIBRARIES
LIBRARIES

ABSTRACT

DETERMINATION OF THE DYNAMICAL PROPERTIES
OF THE JOVIAN SYSTEM BY NUMERICAL ANALYSIS

by

John Frederick Chandler

Submitted to the Department of Earth and Planetary Sciences
on August 31, 1979, in partial fulfillment
of the requirements for the degree of
Doctor of Philosophy.

Recent observations (1973-1978) of Jupiter and its Galilean satellites have been used in a program of numerical integration and least-squares parameter estimation to obtain new values for the positions, velocities and masses of the satellites, as well as the mass distribution of Jupiter itself. Corrections to the ephemerides for Jupiter and Earth have also been estimated. The masses and standard deviations obtained for satellites I-IV were (in units of 10^{-7} Jupiter mass) 394±24, 248±3, 819±11, and 530±17, respectively. The new values are in closer agreement with de Sitter's 1931 results than with the Pioneer spacecraft determinations. The satellite observations, all Earth-based, include radar Doppler shifts, photographic positions, and photometric mutual eclipses and occultations. The Jupiter data include ranges from Pioneer spacecraft tracking and meridian circle positions. The mutual satellite phenomena have been modeled to reduce the biases and theory dependence of previous treatments. The numerical technique has yielded smaller residuals than did a previous, long-time-span, analytical approach by Lieske for those observations included in both. The new results have yielded good predictions one year beyond the span of fitting.

Name and title of Thesis Supervisor:
Irwin I. Shapiro, Professor of Geophysics and Physics

ACKNOWLEDGMENTS

I would like to express my thanks to Irwin Shapiro for his constant and patient guidance in pursuing the problems of celestial mechanics and his attention to detail in reading and criticizing early drafts of this thesis. I am indebted to David Pierce, Jay Lieske, Dan Pascu, Phillip Ianna, Steven Ostro, and Myles Standish for supplying the observational data that made this work possible. Jay Lieske, Antonia Forni, and Kaare Aksnes have provided computer programs for computing the positions of the Galilean satellites from various theories. I wish to thank Robert Reasenberg and Robert King for their help and advice in using the Planetary Ephemeris Program and in finding ways to make an overgrown computer program do what I needed. I would like to thank Sergei Gourevitch and Peter Ford for devising a flexible system of software maintenance that made possible the large modifications of PEP with a minimum of effort. I am indebted to James Ryan and Thomas Clark for making large amounts of computer time available at the Goddard Space Flight Center for performing long numerical integrations. Last of all, and most of all, I thank my wife

Bonnie for enduring with unending patience my irregular hours and peregrinations in search of computer time and for understanding and support during the preparation of this work.

This work was supported financially by the National Science Foundation under grants MPS 72-05104 and 78-07760.

TABLE OF CONTENTS

ABSTRACT ii

ACKNOWLEDGMENTS iii

Chapter page

I. INTRODUCTION 9

Discovery and early observations of the Galilean satellites 9
Progress in satellite theory to the present . . . 12
The present investigation 14

II. MOTIVATION 20

Recent observational advances 20
Photographic observations 24
Summary of available data 25
Modeling the satellite motions 28

III. AVAILABLE SOFTWARE 32

Planetary Ephemeris Program (PEP) 32
Other utility programs 40
Limitations of existing software 42

IV. EQUATIONS OF MOTION 44

Notation 44
Newtonian n-body motion 46
General relativistic motion 51
Newtonian variational equations 60
General relativistic corrections to the variational equations 64
Accuracy requirements 66

V. SATELLITE MUTUAL EVENTS 72

Mid-event time 72
Minimum separation 79
Partial derivatives of the observations 82
Effect of solar phase angle 86
Model of the apparent offset due to phase defect . 89

Partial derivatives of the phase correction . . . 95

VI. DATA PROCESSING 99

Checking the software 99
Starting the least-squares fitting 106
Matching the integration with an analytical theory 117

VII. RESULTS 122

Data inconsistencies 123
Adjustments to parameters 125
Checking the results 131
Extrapolation to later epochs 135
Future work 137

Appendix page

A. ROTATION MATRIX FOR BODY-FIXED COORDINATES . . . 140

B. EXTENSION OF NORMAL EQUATION ERROR STATISTICS IN PEP 143

C. S-BODY TAPE FORMAT 153

D. STELLAR OCCULTATIONS 155

E. RELATIVE PHOTOGRAPHIC OBSERVATIONS 171

F. POST-FIT RESIDUALS 188

BIBLIOGRAPHY 200

BIOGRAPHICAL NOTE 206

LIST OF TABLES

Table		page
1.	Determinations of satellite masses	13
2.	Physical properties of the Jovian system	17
3.	Fundamental constants	19
4.	Summary of Data	27
5.	Relative forces on a Galilean satellite	69
6.	Function f of fractional phase correction	94
7.	Partial derivative test for Europa	102
8.	Initial conditions determined from mutual events	115
9.	Relative post-fit radar and optical residuals	124
10.	Final parameter values	128
11.	Comparison of data residuals	133
12.	Power spectrum of numerical-analytical residuals	135
13.	Global temperature means and ranges	177

LIST OF FIGURES

Figure		page
1.	Phase defect on obscurable body	86
2.	Occultation and eclipse geometries	87
3.	Partly obscured disk	90
4.	Phase correction geometry	93
5.	Histograms of integration-theory residuals	121
6.	Relationship of body-fixed and inertial frames	141
7.	Stellar occultation geometry	157
8.	Spherical occulter	158
9.	Non-spherical occulter	158
10.	Near occultation	161
11.	Distance to tangent	167
12.	Cross-section and tangent geometry	169
13.	Atmospheric refraction correction	180

Chapter I

INTRODUCTION

1.1 DISCOVERY AND EARLY OBSERVATIONS OF THE GALILEAN SATELLITES

Among the solar family the Jovian system is perhaps the most interesting to Earth-based observers if we overrule our forgivable bias in favor of the planet we inhabit. Aside from Earth, Jupiter was the first planet known to have satellites, and, aside from the Sun, it is by far the largest and most massive body in the solar system. Also, as of this date, it is the only planet, again aside from Earth, whose satellites can be detected by Earth-based radar.

It was because Jupiter's four major satellites are so near to being visible to the naked eye that they were discovered so early. Indeed, they were discovered independently about the same time by two pioneer telescope astronomers, Galileo Galilei in Padua and Simon Mayer (usually called Marius) in Brandenburg, both in January of 1610. Ever since then there has been controversy over the question, who made the discovery first. Galileo was the first

to publish the astounding news, but Marius later claimed to have preceded him by a few days. However, Brandenburg was a Protestant principality and had not yet adopted the Gregorian, or new style, calendar, and so its "clock" was nine days slow in the Seventeenth Century. Thus, the time Marius claimed actually followed that of Galileo.

The response to Marius' claims was largely negative. Galileo, as well as Galileo's followers accused Marius of arrant plagiarism although there is really no strong evidence for doubting the veracity of the German astronomer. Just as in the later dispute between Newton and Leibnitz about the invention of calculus, the name-calling changed nothing -- the credit for priority goes to the one, but the notation of the German has prevailed. Galileo christened the satellites the "Stars of Medici" in honor of his former pupil Cosimo di Medici, Duke of Tuscany. Now, however, they are known as the "Galilean Satellites" in honor of their discoverer, and their individual names are the ones suggested by Marius. Marius chose names from classical mythology in keeping with the customary names for the planets. Thus, the four major satellites are called in order of increasing orbital radius Io, Europa, Ganymede, and Callisto after four of Jupiter's paramours. These names are still

avoided by many purists (not out of Puritanism, but because of suspected plagiarism), but they are universally recognized. Further, they are likely to gain ground (now especially) because names are more evocative than Roman numerals, and the satellites are becoming more interesting to more people with the advent of space probes and new observational techniques.

At any rate, both Galileo and Marius made pioneering contributions to the study of the satellites. Galileo soon calculated the periods and published tables of predictions for observing the satellites. Marius made the important discovery of satellite eclipses by Jupiter and pointed out the possibility of mutual satellite eclipses and occultations (see Chapter 5). In the succeeding century increasingly accurate observations and predictions of the eclipses were made, and these made possible one of the most significant discoveries in modern astronomy, namely, Roemer's measurement of the speed of light from the systematic discrepancies between predictions and observations.

1.2 PROGRESS IN SATELLITE THEORY TO THE PRESENT

One of the spurs to improvement of the predictions of satellite ephemerides was the need for a universal time standard for geodesy. The comparison of local sidereal time with the absolute time of a satellite eclipse would provide a simple method of finding the longitude at any place on Earth. That goal, however, was elusive because of the complexity of the Jovian system. Along the way great advances were made in a variety of fields from empirical extrapolation to gravitational perturbation theory.

At first, tables of satellite positions were purely empirical, but soon theoretical models were being used for including the perturbing effects of the satellites. By the Eighteenth Century the satellite masses could be determined from their effects on each other. Until the advent of space probes that was, in fact, the only way of determining the masses. Table 1 shows some of the evolution of the satellite mass determinations.

In Table 1 all but the last line were obtained through the perturbations of the satellites upon each other. Although it might seem that the masses of the satellites were changing wildly over the last two hundred years, most of the

Table 1

Determinations of satellite masses

Mass determinations based on gravitational perturbations. On the left are listed the sources and dates of the results. In two cases the mass of Callisto was assumed, rather than measured; those values are indicated by parentheses. The uncertainties are not available for all of these values. Uncertainties are for the last place shown.

Determination	Masses (in Jupiter mass x 10^{-5})			
	Io	Europa	Ganymede	Callisto
Bailly, 1766	4.24	2.11	7.62	(5.)
Laplace, 1805	1.733	2.324	8.850	4.266
Damoiseau, 1836	1.688	2.323	8.844	4.248
Souillart, 1890	3.773	2.453	8.218	2.312
Adams, 1900	2.831	2.324	8.125	2.149
de Sitter, 1908	2.60	2.31	8.04	(4.248)
Sampson, 1921	4.497	2.536	7.988	4.504
de Sitter, 1931	3.81±40	2.48±7	8.17±13	5.09±53
Null, 1976	4.684±22	2.523±25	7.803±30	5.661±19

values reported were really much more uncertain than they appear to be. Indeed, of the three or four digits presented, only one or two are really significant given the uncertainties of the observations used. Still, Io and Callisto in particular show marked disagreements among the Twentieth Century mass estimates.

The last determination in Table 1 is fundamentally different from the others because it represents short-term perturbations on Pioneer 10 and 11, which passed through the Jovian system in 1973 and 1974, respectively. The accelerations were quite precisely measured by Doppler tracking (though only in one direction), and the results were applied in a parameter fitting scheme to estimate not only the masses of the satellites, but also Jupiter's gravitational harmonic coefficients and local corrections to the ephemerides for Jupiter and the satellites.

1.3 THE PRESENT INVESTIGATION

With the advent of high-speed digital computers and increasingly precise observations of Jupiter and its satellites it is now possible to carry out a program of improving the determinations of the dynamical properties of the system by means of direct numerical integration of the equations of motion and least-squares analysis of observations. Heretofore, progress has depended on the occasional major advances in the theory of the Galilean satellite motions based on reformulation and recalculation of the residuals for available observational data. An important aspect of any new work on the Galilean satellites should be the possibility of exten-

sion to include new data without the necessity of rederiving any formulas or constants. An integration may always be extended to cover the times of additional data, and the variational equations for the pertinent parameters allow continued improvement of the numerical representation of the motions. For such a project it is necessary to include all the most accurate data within the selected time span in order to take advantage of the power of the numerical techniques. In addition, the best available initial estimates of the physical parameters of the system must be used to make the resulting adjustments as small as possible.

Table 2 gives the best determinations of the masses and other dynamical properties of the Jovian system available prior to the writing of this thesis. The symbol M(S) represents the mass of the Sun, while M(s) is that of Saturn, and M(J) that of the Jovian system. The numbers given for the satellite masses appear to be somewhat smaller than those given in the last line of Table 1, but they actually represent the same values scaled by the ratio of the mass of Jupiter itself to that of the whole system. These determinations of the masses are undoubtedly the best to date, despite the difficulties of separating ephemeris effects from mass differences, since the two Pioneer spacecraft gave

independent results in fairly good agreement. Indeed, these results agree quite well with those of Sampson and de Sitter, except for Callisto and Io, respectively. The mass of the Jupiter system reported by Null, 1/1047.346±.004, is at variance with most of the recent determinations by conventional asteroid perturbation techniques. In light of that fact and the fact that the I.A.U. value is only twice the reported uncertainty away from Null's determination, the I.A.U. value was adopted initially for the present work. The differences among the several determinations are actually much larger than the individual reported errors.

The radius of Jupiter R(J) actually has no dynamical significance except that it scales the harmonic gravitational potential coefficients, which are dimensionless by convention. The satellite radii would act similarly except that the satellites' harmonic coefficients are all negligible. They do, however, enter into the computations of some of the observations and are, therefore, included with the dynamical parameters of the system. Io and Ganymede have rather precisely determined radii because of occultations of stars.

The orientation of Jupiter's pole in Table 2 was also adopted from Null (1976). Since the pole was determined

Table 2

Physical properties of the Jovian system

Values of physical properties adopted for use in the present work: masses, gravitational harmonic expansions, and radii. All are subject to adjustment from the results of data analysis. M(J) represents the combined Jupiter system mass. The (1) - (4) represent Io, Europa, Ganymede, and Callisto, respectively. The orientation of Jupiter's pole is given in reference to the 1950.0 mean equator-equinox system. See Chapter 4 for the definitions of J(n).

Parameter	Value
M(J)	1/1047.355 M(S)
M(1)	4.683×10^{-5} M(J)
M(2)	2.522×10^{-5} M(J)
M(3)	7.801×10^{-5} M(J)
M(4)	5.660×10^{-5} M(J)
M(s)	1/3499 M(S)
J(2) of Jupiter	1.4733×10^{-2}
J(3) of Jupiter	0.0
J(4) of Jupiter	-5.87×10^{-4}
δ of Jupiter's pole	64.504°
α of Jupiter's pole	267.998°
R(J)	71398 km
R(1)	1820 km
R(2)	1521 km
R(3)	2653 km
R(4)	2500 km

from gravitational effects, it is not, strictly speaking, the pole of rotation, but rather the principal pole of the moment-of-inertia ellipsoid. Certainly, any difference be-

tween the two poles would require a reformulation of the harmonic expansion of Jupiter's gravity field to include rotating tesseral terms. However, the difference can not be large for a rapidly rotating gaseous planet, and Null places only upper bounds on the tesseral harmonic coefficients, which represent the rotational asymmetry.

The important dynamical properties that are <u>not</u> listed in Table 2 are the initial conditions of the motions of the satellites and Jupiter. Obviously, orbital elements must be referred to some epoch, and there is no single time that is relevant to all or even most aspects of the dynamics of the Jovian satellites. Not only the longitudes but also the nodes and apsides are secular variables, that is, they all progress continuously. These initial conditions will, in fact, be the most susceptible to adjustment in this undertaking because of their critical importance in the motions of the satellites.

The constants used for conversion among systems of units are presented for reference in Table 3. The first item is the Gaussian gravitational constant. With the ephemeris day it serves to define the Astronomical Unit (see Allen, 1973). The value of c, the speed of light, is the I.A.U. standard

(*Transactions*, 1977). The equivalent of the AU in light seconds is based on inner-planet radar studies (Ash *et al.*, 1971).

Table 3

Fundamental constants

Constant	Value
$[GM(S)]^{0.5}$	$0.01720209895\ (AU)^{1.5}/day$
c	299792.458 km/s
1 AU	499.00478 light-sec.

Chapter II

MOTIVATION

2.1 RECENT OBSERVATIONAL ADVANCES

Methods of observing the Galilean satellites have improved markedly in recent years. Eclipses and, especially, occultations of the satellites by Jupiter are difficult to observe because the events in question are inherently tied to Jupiter, which is much brighter. Still, they remained the most precise available measurements until the mutual satellite-satellite events of 1973. These latter, including both occultations and eclipses, offer two distinct advantages in that they occur away from the limb of Jupiter -- the apparent velocities projected onto the plane of the sky are, thus, less than maximum, and the bright disk of Jupiter causes much less interference. Such events had been observed before and even successfully predicted. After all, their possibility had been known over three hundred years. Indeed, the British Astronomical Society had been publishing predictions regularly since 1931. However, in order to be useful beyond mere confirmation of the events, the observa-

tions practically require photometric techniques. It was only with the 1973 passage of Earth through Jupiter's equatorial plane that there was any concerted, international effort at predicting and observing the mutual events (Aksnes and Franklin, 1976). That time period was particulary favorable because Jupiter went through opposition in the middle of it.

Even more recently it has become possible to detect radar echoes from the Galilean satellites. Starting in 1975, experimenters using the radar at Arecibo Observatory in Puerto Rico have been bouncing signals off the satellites every year near opposition (Campbell et al., 1977 and 1978). The system, using a 2380 MHz transmitter (S-band) has been consistently able to obtain strong echoes from the outer three satellites and marginal returns from Io. In all cases the only useful information has come from continuous wave transmission and frequency analysis of the returned power. For the purposes of celestial mechanics these measurements can be reduced to a series of Doppler shifts, giving in effect the relative velocites of the observing site and the satellites during the observations.

Both of these recent methods of observing suffer from the same drawback, scarcity. The mutual satellite events can be observed from Earth only when Earth passes through the satellites' orbital plane, and only when Jupiter is in the night sky. Therefore, only about six months out of every six years (corresponding to Jupiter's "equinoxes") yield these events. Further, the most frequent events, Io occulting or eclipsing Europa, occur at best only once every three days. Callisto's orbit is slightly inclined to the others and of longer period, and so it participates in mutual events even less often than the rest.

In principle, radar observations could be going on all the time, but, in fact, only two facilities have apparently succeeded in getting echoes from any Jovian satellite. The first reported observation (Goldstein and Morris, 1975) was of Ganymede during the 1974 opposition and was based on six nights of observing at S-band. During the 1978 opposition detections were made at X-band at the same installation, but no other observatory besides Arecibo has made any detection. The experiment is intrinsically lengthy compared to the more common radar observations because of the more-than-one-hour minimum round-trip time. Further, detectability goes down as the fourth power of the distance, and so only the annual,

favorable times at opposition are likely to yield good results at present levels of radar system sensitivity.

These types of observations are not only scarce, but also strictly limited to the time span starting in 1973. It is, unfortunately, impossible to make up the lost experiments of the past. However, there are other data that do not suffer from the difficulties of Jupiter eclipses and occultations. Simple Earth-based photographic measurements of satellite right ascension and declination are not so precise as the mutual event timings or radar measurements, but they offer an independent source of data and an important contribution to sensitivity. It is inherent in both the mutual event mid-times and Earth-based radar observations that out-of-orbital-plane motions of the satellites have very little effect on the measurements. The only exception to this restriction is the measurement of minimum separation in a mutual occultation, and even there, the result is strongly coupled with the assumed radii of the satellites. Thus, such observations are sensitive primarily to longitudinal motion because all the bodies involved are moving in approximately the same plane. Measurements of declination, on the other hand, are directly affected by out-of-plane motion (actually a combination of declination and right ascension because of the obliquity of the ecliptic).

2.2 PHOTOGRAPHIC OBSERVATIONS

Photographic measurements fall into two categories, relative and absolute. The former are differences in the instantaneous apparent right ascension and declination between two objects, such as Jupiter and a satellite or two satellites. Generally, the equator of date is established on the photographic plate by trailing a star image, that is, by letting Earth turn the telescope about the instantaneous rotation axis. Thus, the orientation of the plate can be rather precisely fixed with respect to Earth's axis, and subsequent measurements of the plate can be readily converted into angular offsets in the true right ascension and declination of date (Pascu, 1977).

The so-called absolute photographic measurements of position are actually relative, too, but they are relative to a system of standard stars. When several cataloged stars appear on the same photographic plate as the object in question, the relative plate positions can be converted using some sort of parameter fitting scheme into an absolute position for the object within the reference frame of the catalog. Thus, the errors induced by refraction and aberration can be removed beforehand from the cataloged star positions

and, hence, from the measured planet or satellite positions. In practice and for historical reasons, the star catalogs give what are known as astrometric positions, that is, the constant term in the annual aberration is not removed (Brouwer and Clemence, 1961). This term represents the difference between Earth's true orbital velocity and the circular velocity for an orbit of the same period. It can easily be shown that to first order the difference is a constant velocity offset proportional to the orbital eccentricity and parallel to the orbit's minor axis.

2.3 SUMMARY OF AVAILABLE DATA

In sum, there is a body of observational data of widely varying types covering the span of the last six years. Actually, most of the data fall within two months of the oppositions of Jupiter each year, and there are large gaps completely devoid of data. Table 4 gives a summary of the available observational data in the time span 1973-1978. Interest in the outer planet satellites has bloomed during the past few years because of the rapidly expanding capabilities typified by the Earth-based radar detections and the space probes to the outer planets. Ranges to Jupiter derived from Pioneer 10 and 11 have been included along with

conventional meridian circle observations of Jupiter as an anchor for the satellite data.

The dates listed in Table 4 represent Julian date less 2439999.5. The first column "SITE" gives a four-letter code for the observatory with the exception of the mutual satellite eclipses and occultations, which were observed from 21 different sites all over the world. The codes have the following meanings: TABL - Table Mountain Observatory, USNO - United States Naval Observatory, AREC - National Astronomy and Ionosphere Center at Arecibo, Puerto Rico, LMCC - Leander McCormick Observatory, and MCDO - McDonald Observatory. The fourth column "NUMBER" shows the total number of independent observations of each type. Most of these actually represent two measured quantities per observation. The fifth column gives the observation type with the following abbreviations: "abs.opt" for absolute photographic position measurements, "ecl.occ." for mutual eclipse or occultation timings, "Doppler" for radar Doppler shifts, "range" for radio tracking delays, and "merid." for meridian circle right ascensions and declinations. The last column gives the mean uncertainty in the observations in comparable units. The Table Mountain observations (Peters, 1973) were not used in this work because they were too few to justify the extra year's integrations.

Table 4

Summary of Data

Number and accuracy of available data listed by date and observing site. All observations are of the Galilean satellites, except as noted.

SITE	DATES	YEAR	NUMBER	TYPE	UNCERTAINTY
TABL	1513-1585	(1972)	40	abs.opt.	300 km
(many)	1844-2031	(1973)	87	ecl.occ.	40 km
USNO	1954-1954	(1973)	4	abs.opt.	350 km
(geoc.)	2021	(1973)	1	range *	30 km
(geoc.)	2385	(1974)	1	range *	30 km
USNO	2617-2787	(1975)	79	merid. *	3000 km
AREC	2684-2794	(1975)	9	Doppler	7 m/s
LMCC	2686-2722	(1975)	175	abs.opt.	900 km
AREC	3071-3120	(1976)	11	Doppler	7 m/s
LMCC	3096-3132	(1976)	100	abs.opt.	1100 km
USNO	3009-3183	(1976)	73	merid. *	3000 km
MCDO	3051-3518	(1977)	24	abs.opt.	750 km
AREC	3463-3475	(1977)	8	Doppler	5 m/s
LMCC	3463-3540	(1977)	417	abs.opt.	750 km

* Jupiter observations

It should be clear from Table 4 that the photographic data far outweigh the other kinds in sheer numbers. On the other hand the greater precision of the mutual event and radar measurements make them especially useful. The two groups, in fact, should complement each other in determining the satellite motion; the widely spaced, precise measurements constrain the motions at a few points while the bulk of the data ties down the long-term behavior.

2.4 MODELING THE SATELLITE MOTIONS

Having seen the availability of observational data, we may now attempt to tie them together by developing a model of the behavior of the Galilean satellites. In any kind of modeling there are two basically different ways of proceeding, namely analytical and numerical. Let us consider each in the context of the Galilean satellites. First, and potentially simplest, is the analytical approach. It is innately more satisfying to write down a simple equation describing some complex phenomenon than to tabulate "all" of the relevant data. The closed-form solution admits of easy calculation of the state variables at any epoch. The difficulty arises when no closed-form solution exists; then the expressions describing the satellite motions are no longer simple except through imaginative notation. Still, a series solution is sufficient for straightforward calculations and shares the important property that it applies to any epoch. Thus, widely spaced observations can be compared on an equal footing with such a model just as easily as densely packed ones.

In practice, analytical theories of the motions of the Galilean satellites require time series with many different

characteristic periods. For each satellite the main departure from circular motion is what is called the "equation of the center", namely that of a Keplerian ellipse. The so-called "proper" eccentricities of the Galilean satellites are very small (less than one percent), but they also have eccentricity-like terms ("forced" eccentricities) due to the gravitational perturbations of the other satellites. Generally, the coefficients are expressed in terms of expansions in small parameters such as the eccentricities and inclinations. Thus, the presentation of an analytical theory requires many pages of expressions and coefficient values, none of which are tied directly to simple physical quantities. Indeed, the refinement of a theory by fitting to additional data requires that the partial derivatives of the theoretical positions with respect to the basic physical parameters be calculable. The magnitude of the task is such that high-speed digital computers must be used to perform most of the manipulations (Lieske, 1974, 1977a).

A further drawback is the necessity of truncating the expansions of the disturbing functions. In effect, the fitting of the theory to the data must be done after the solution is known sufficiently to decide what terms may be dropped from the disturbing function.

Numerical methods offer rather different assets and liabilities. The primary problem with numerical integration as a means of determining satellite orbits is the large amount of computer time needed to accomplish anything. If, for example, the available data are concentrated in short spans of time with large gaps in between, the integrator must do all the work to bridge the gaps without any benefit from them. On the other hand, the process of integrating the equations of motion yields as a by-product a tabulation of the positions and velocity of the integrated body for all times within the overall time span. Therefore, the evaluation of coordinates within that range can always be done by simple interpolation. In addition, the tabulation is directly equivalent to the input physical parameters through the laws of physics; there is no intermediate stage of series expansions and arbitrarily neglected terms. There is only the limitation on accuracy imposed by computation.

In point of fact there is no complete physical parameterization of the Universe or of the Solar System. Thus, there can be no rigorous equivalence between reality and any simulation, especially one with a reasonably small number of parameters. Still, we are concerned in the final analysis with measurable phenomena. Since we may compute upper

bounds on the errors associated with ignoring any given physical effect, we may limit consideration to those terms in the equations of motion which might have observable consequences and still have an adequate, if not rigorous, representation of reality. Thus, we may hope to obtain a better and more physical model of the satellite motions by numerical integration.

Chapter III

AVAILABLE SOFTWARE

3.1 PLANETARY EPHEMERIS PROGRAM (PEP)

There is a computer program called PEP (for Planetary Ephemeris Program) which has been under development during the past fifteen years. The basic structure of PEP is fairly simple. There are four main sections of the program, one to perform each of the following tasks: integrate differential equations, compute expected values of observations based on tabulated integration results, perform weighted, linearized least-squares analysis of observation residuals in order to adjust parameters, and calculate post-fit residuals based on parameter adjustments. The first three sections form an iterative loop that may be used to form a sequence of parameter estimates converging to the true least-squares estimate regardless of the non-linearity of the problem (as long as the initial parameter values do not lead to a secondary minimum or a diverging sequence). For convenience, safety, and economy the intermediate results are saved on peripheral storage at several places in the

processing, and computation may always be resumed at such places by reading the saved quantities back.

The first section, called the PLANET link, begins with the set of parameters controlling the motions of interest, including the initial conditions at some epoch, and integrates the equations of motion and the variational equations for a selected set of parameters. The results may be both printed out on a line printer and written on magnetic tape although either of these may be omitted. The output consists of a tabulation of the coordinates in phase space and their partial derivatives in one of two standard formats recognized by other parts of PEP as well as by an assortment of auxiliary programs associated with PEP.

One of these formats features a variable tabular interval and a variable number of orders of time derivatives of each spatial coordinate. This format is primarily intended for space probes which may experience a wide range of accelerations. The step size is continually adjusted during the integration to keep it as large as possible within the constraints of integration stability and required accuracy. However, most objects in the solar system (comets excepted) travel in nearly circular orbits and experience approxi-

mately constant accelerations. Therefore, a single, constant integration step size and constant tabular interval usually suffices throughout. The second output format, thus, contains data at constant intervals.The information is arranged in a structure that also permits a variable number of orders of time derivatives, but only the position and velocity coordinates are actually included.

As a result of the generality of the integration subroutines, more than one motion may be integrated at a time. Thus, for example, the motions of the planets (or any set of up to 11 bodies, for that matter) may be integrated simultaneously although at present this capability does not extend to the variational equations. The existing software, thus, offered two possible approaches to the task of integrating the motions in the Jovian system, that is, simultaneously integrating all the satellites (requiring the addition of a facility for handling the variational equations at the same time) or integrating the satellites one at a time within an overall iterative scheme. It must be borne in mind that the adjustment of paramters is, of necessity, an iterative process anyway. Therefore, the penalty of performing four steps in the second method for every one in the first is only one of a little extra bookkeeping, and the independent process-

ing of each satellite adds the possibility of dealing with special problems of one without re-integrating all. Perhaps the strongest argument for adopting the second approach lies in the amount of alteration to PEP necessary for implementing each of the two possibilities. The software associated with the integration of the motion of individual bodies already included coding for several important physical phenomena not programmed in the so-called N-body integrator, and the cumulative experience of PEP programmers shows that the fewer changes needed for a contemplated capability the more reliable the results.

The second main section, called the COMPAR link, is responsible for computing the theoretical values of observations based on the results of integrations (either produced on the same iteration of the parameter adjustment loop, or saved from some previous runs, or even a combination of both). These values are then used to form observation residuals, which may be printed out and written on magnetic tape along with the observations themselves.

Observations are divided into five major categories for the purposes of computation and handled separately by different (and parallel) sections of the COMPAR link. These

categories are radar/radio tracking, optical/photographic angular measuring, transit/occultation timing, and interferometric tracking. Within these overall divisions there are sub-classes depending on a variety of criteria, such as the location of the observation site -- non-Earth-based observations are processed separately from Earth-based. This structure allows the implementation of a large number of distinct observable types, and, indeed, many types have been incorporated in PEP. However, many others have been merely envisaged. For example, lunar occultations of stars are assigned to the transit/occultation section of the COMPAR link. Because of the similarity of those observations to the mutual event timings, some code for stellar occultations was added in the course of the present investigation (see Appendix D). The occultation code, however, was not completely tested because it is not needed for this work.

For most observable types, that is, for any observable that is not the time of an event, PEP has the facility to compute the predicted value of observations on the basis of the available ephemerides. Such "dummy" observations are processed in just the same way as real ones with just two exceptions. First, the times are supplied by stepping in constant intervals over a selected time range or ranges,

and, second, the computed observable is substituted for the observed value of real observations, and the residuals are, therefore, all zero. The results of the dummy processing may be saved on tape just the same as real observations.

At any rate, the output format for the COMPAR link is uniform from category to category and includes the value actually observed along with the uncertainty, the observed-minus-computed, the partial derivatives of the computed value with respect to selected parameters, and a variety of numbers used along the way in calculating the theoretical value. As in the case of the integration output this format is recognized by other sections of PEP and some other associated programs. The immediate use of this output, called an observation library, is in the formation of the normal equations of least-squares parameter estimation in the ANALIZ, or third, section. See Appendix B for a discussion of the normal equations.

The normal equations can be formed from any combination of observation library tapes and old saved normal equations and input a priori parameter estimates and correlations. The result is a symmetric coefficient matrix and a so-called right-hand-side vector. These, along with the nominal val-

ues of the parameters, can be printed out or saved on magnetic tape for later use. Once the matrix is formed, it is inverted (that is, the normal equations are solved), and the solution vector is then applied to the adjustable parameters. Incidental information such as the cross-correlation matrix and the statistics of the observation residuals is then printed out with the parameter adjustments.

After the completion of the least-squares adjustment procedure in the ANALIZ link, the entire process may be repeated from the beginning of the integration step. At the end of a least-squares iteration, each parameter adjustment is tested for "convergence," that is, it is compared with the standard deviation of the parameter. For a small enough adjustment, the parameter may be deemed to have reached its "final" value, and on any subsequent iterations such a parameter is held fixed. Iteration continues until some maximum number of steps or until all parameters have converged on their "final" values, whichever happens first.

After the last least-squares iteration, any or all of the observation residuals that went into the solution (or even those that did not) may be reviewed in light of the new parameter values. Since the observation library tapes include

the partial derivatives of the observables (and thus of the residuals) with respect to the chosen parameters, a linear correction to the residuals may be performed using the adjustments from the last iteration. The resulting post-fit residuals may be printed out or written on magnetic tape in the same format as an observation library tape. Although the observables are not really linear in the parameters, the truncation of the Taylor series to first order yields very good post-fit residuals in practice except where the adjustments are very large compared to the standard deviations of the parameters. The PRDICT link, which forms these post-fit residuals, accepts a batch of observation library tapes and generates a copy of each with all the same data but with post-fit instead of pre-fit residuals. Even if the observations were not used in the fit, the program can predict what the post-fit residuals will be, based on the partial derivatives stored on each observation library tape.

At any point in the processing where observational data are read by PEP, the data may be edited by control cards supplied in the input stream. The editing may change the errors associated with individual measurements or time spans of measurements, or it may delete bad or suspect points altogether. Indeed, whole series of observations may be re-

weighted or deleted in this manner. Besides this explicit editing there is an automatic exclusion mechanism that rejects any residuals that exceed in absolute value some multiple of the associated error. Naturally, this multiple is adjustable according to the nature of the observation type and the quality of the ephemerides.

3.2 OTHER UTILITY PROGRAMS

Plotting of the residuals on observation tapes (or reasonable facsimiles) may be performed by a separate program called ABC. This program can also plot any of the saved quantities on an observation library tape, such as the observable itself or the uncertainty or one of the partial derivatives against any other such quantity or against the time of reception.

Other utility programs, namely CPLNTM and CPYNBDY, exist for copying all or part of single body or multi-body integration tapes, respectively. CPYNBDY can also copy out the coordinates of the Moon onto a single-body tape which masquerades as an integration. Unfortunately, the format of the multi-body tapes previously implemented in PEP is inadequate for short-period bodies such as satellites. Thus, any

serious study of a system of satellites must include the writing of a new set of utilities or a rewriting of the old to include the capability of copying multi-satellite tapes. In order to distinguish between the two kinds of multi-body tapes we will call them N-body and S-body tapes, respectively. A description of the S-body tape format appears in Appendix C. Since the present effort does not include the integration of the motion of all the satellites at once, there must be some way of making an initial S-body tape for use in computing the gravitational perturbations of each satellite by the others. In addition, we should be able to combine any number of individual integrations with an old S-body tape to obtain a new, updated S-body tape or to copy out the coordinates of a single body from the multi-body tape. The simplest starting point for making the first S-body tape would be a circular or elliptical orbit model. In fact, PEP already had the ability to compute the satellite perturbations based on static Keplerian orbits, and the next level of improvement on that sort of precision is the inclusion of extra eccentricity and precession terms, in short, of an analytical theory. Several different theories have been used in the course of this project, but all have been based on the work of R.A. Sampson, who published a succes-

sion of tables and revisions in the early part of this century. The bulk of computations have been done using a modern version of Sampson's theory furnished by J.H. Lieske. This theory follows Sampson's formulation, but includes the equivalent of the variational equations of a numerical model and has been extended and fit to more recent observations.

3.3 LIMITATIONS OF EXISTING SOFTWARE

One problem with PEP's handling of both integrations and observations has been the implicit assumption that all satellites in the solar system have negligible masses with the sole exception of Earth's Moon. Thus, the planetary mass used in the integration of a satellite's motion was actually the mass of the whole system. Further, the position of a planet relative to the Sun used in either integrations or calculations of observations was actually that of the planet's system barycenter. As a result, the central force terms were all off by a small factor, and the gravitational effects of the Sun in particular and of any out-of-system body in general were computed on the basis of offset coordinates. Indeed, this approximation was adequate for previous work because Jupiter had not been treated as other than a simple mass point.

Another approximation imbedded in PEP was in the calculation of the partial derivatives of Doppler shift measurements. Terms of the order of v/c relative to the partials were ignored because of a peculiarity of the program. In practice, that level of approximation has proven adequate for the sort of least-squares parameter adjustment proposed for the present work.

In the course of this investigation the new observables described in Chapter 2 were added to PEP, and some of the other limitations of the program were corrected. In particular, the planetary mass used in integrations was made to take massive satellites into account, and the position of a planet was adjusted for the offset from the system barycenter. That offset was not applied to positions used in integrations because the inverse-square law of gravity makes the gravitational correction much less important than the observational correction. Indeed, the correction is observable only in the Doppler shifts of the Galilean satellites, being on the order of 10 Hz at S-band (2 GHz).

Chapter IV

EQUATIONS OF MOTION

4.1 NOTATION

Throughout this thesis equations and formulas will appear with the following conventions. Vectors will be denoted by underscored symbols while scalars will be represented by ordinary characters. In some discussions where tensors play an important role it may be necessary to cast all equations in scalar form with tensor and vector elements represented by super- and subscripts. Because of type-font limitations all subscripts will appear in parentheses rather than below the line. Note that there is, therefore, no intrinsic distinction in the notation between subscripts and arguments of functions. In fact, some variables will be defined with both subscripts and arguments, but the distinction will be clear in each definition. Subscripts will precede arguments whenever both appear for one variable. In that sense there is a distinction between subscripts and arguments because an exponent on a function will precede the arguments while an exponent on a variable will follow any subscripts.

We now introduce the notation for unit vectors. The same symbol $\underline{u}$ will be used for the vector function that produces a unit vector in the direction of a given vector, and also for some other unit vectors that will be defined from time to time. The use of the function $\underline{u}$ will be clear from its vector argument. In the following notational definitions we let $\underline{x}$ be any vector.

$$
\begin{aligned}
x &= (\underline{x}\cdot\underline{x})^{0.5} \\
\underline{u}(\underline{x}) &= \underline{x}/x \qquad\qquad (4\text{-}1) \\
x' &= \underline{u}(\underline{x})\cdot\underline{x}'
\end{aligned}
$$

A prime added to a variable name will always indicate the total derivative with respect to the apropriate independent variable. In nearly all cases this independent variable is either explicitly or implicitly time. Indeed, the only exceptions to this rule are the Legendre polynomials and functions, which are functions of a dimensionless variable. Spatial derivatives which might be represented by the gradient operator (grad or ∇) would be confusing because of the multiplicity of coordinate vector variables. Therefore, any vector derivative will, instead, be written as though it were a partial derivative with respect to the apropriate vector variable. Thus, we would write in Cartesian coordinates

$$\partial f/\partial \underline{x} = (\partial f/\partial x(1))\underline{u}(1) + (\partial f/\partial x(2))\underline{u}(2) + (\partial f/\partial x(3))\underline{u}(3) \tag{4-2}$$

where x(i) are the components of $\underline{x}$, and $\underline{u}(i)$ are the coordinate unit vectors. That notation may not fit the rigorous development of the derivative as the limit of the ratio of small increments, but it is certainly more concise than the gradient notation.

4.2 NEWTONIAN N-BODY MOTION

Consider a system of bodies labeled 0, 1, 2, and so on, each with an associated body-fixed coordinate system and harmonic gravitational potential expansion

$$V(i) = -(Gm(i)/r)(1- \sum_{n=2}^{n} (a(i)/r)^{n} [J(n,i)P(n,\sin \phi) - \sum_{h=1}^{n} (C(nh,i)\cos h\theta + S(nh,i)\sin h\theta) P(nh,\sin \phi)]) \tag{4-3}$$

where P(n) and P(nh) are the Legendre polynomials and functions, respectively; J(n,i) and C(nh,i) and S(nh,i) are, respectively, the zonal and tesseral cosine and sine gravitational harmonic coefficients of body i defined with radius a(i); m(i) is the mass of body i and G is the gravitational

constant; (r, ϕ, θ) are the body-fixed spherical polar coordinates relative to body i. Now we write the coordinates of body j in the system of body i as $(r(ji), \phi(ji), \theta(ji))$, and, thus, the total gravitational potential energy of the system is

$$U = -\sum_{i<j} Gm(i)m(j)/r(ij) + \sum_{i} Gm(i) \sum_{j\neq i} m(j)\varrho(ji)/r(ji) \tag{4-4}$$

where

$$\varrho(ij) = \sum_{n}(a(i)/r(ji))^{n} [J(n,i)P(n,\sin \phi(ji)) - \sum_{h=1}^{n} (C(nh,i)\cos h\theta(ji) + S(nh,i)\sin h\theta(ji)) P(nh,\sin \phi(ji))] \tag{4-5}$$

It will be convenient to use rectangular coordinates along with the polar systems we have already set up. Thus, we define

$$\begin{aligned} x(ji)^1 &= r(ji)\cos \phi(ji) \cos \theta(ji) \\ x(ji)^2 &= r(ji)\cos \phi(ji) \sin \theta(ji) \\ x(ji)^3 &= r(ji)\sin \phi(ji) \end{aligned} \tag{4-6}$$

That gives the reverse transformation

$$r(ji) = (x(ji)^k x(ji)^k)^{1/2}$$

$$\phi(ji) = \sin^{-1}(x(ji)^3/r(ji)) \tag{4-7}$$

$$\theta(ji) = \tan^{-1}(x(ji)^2/x(ji)^1)$$

where repeated superscripts are to be summed from 1 to 3. At the same time we need some overall inertial frame of reference, and we define the coordinates of body i in that frame as $(z(i)^1, z(i)^2, z(i)^3)$ and let $\underline{z}(ji) = \underline{z}(j)-\underline{z}(i)$. Then there is a rotation matrix T(i) such that we can transform to the body-fixed system with

$$x(ji)^k = T(i)^{kl} z(ji)^l \tag{4-8}$$

For details of the transformation see Appendix A. It is now simple to write the equation of motion

$$\begin{aligned} z''(j)^k &= -(1/m(j))(\partial U/\partial z(j)^k) \\ &= -\sum_{i\neq j} (Gm(i)/r^2(ji)) [z(ji)^k/r(ji) \\ &\qquad -H(ji)^k - r(ji)\partial[\varrho(ji)/r(ji)]/\partial z(j)^k] \end{aligned} \tag{4-9}$$

where

$$
\begin{aligned}
H(ji)^{k} &= -r(ji)\ \partial[\Omega(ji)/r(ji)]/\partial z(j)^{k} \\
&= \sum_{n=2}^{n} (a(i)/r(ji))\ [J(n,i)((n+1)z(ji)^{k}/r(ji) \\
&\qquad P(n,\sin\phi(ji)) \\
&\qquad -[r(ji)\partial(\sin\phi(ji))/\partial z(ji)^{k}]P'(n,\sin\phi(ji)) \\
&\qquad +\sum_{h=1}^{n} ([C(nh,i)\cos h\theta(ji) + S(nh,i)\sin h\theta(ji)] \\
&\qquad [-(n+1)/r(ji)\ z(ji)^{k}\ P(nh,\sin\phi(ji)) \\
&\qquad + r(ji)\partial\sin\phi(ji)/\partial z(j)^{k}\ P'(nh,\sin\phi(ji))] \\
&\qquad +h[-C(nh,i)\sin h\theta(ji) + S(nh,i)\cos h\theta(ji)] \\
&\qquad P(nh,\sin\phi(ji))r(ji)^{k}\ \partial\theta(ji)/\partial z(j)\ \ )]
\end{aligned}
\tag{4-10}
$$

However, we note that $\Omega(ij)/r(ij)$ is a function of position only in terms of $r(ij)$, so we have

$$
\begin{aligned}
\partial[\Omega(ij)/r(ij)]/\partial z(j)^{k} &= \partial[\Omega(ij)/r(ij)]/\partial z(ij)^{k} \\
&= -\partial[\Omega(ij)/r(ij)]/\partial z(i)^{k}
\end{aligned}
\tag{4-11}
$$

and we may rewrite equation (4-9) as

$$z''(j)^{k} = -(1/m(j))(\partial U/\partial z(j)^{k})$$

$$= -\sum_{i \neq j} (Gm(i)/r^2(ji)) \, [z(ji)^{k}/r(ji) \qquad (4\text{-}12)$$

$$-H(ji)^{k} + H(ij)^{k}]$$

Now we have

$$\sin \phi(ji) = T(i)^{3k} z(ji)^{k}/r(ji)$$

$$\partial \sin \phi(ji)/\partial z(j)^{k} = T(i)^{3k}/r(ji) - T(i)^{3n} z(ji)^{n} z(ji)^{k}/r^3(ji)$$

$$(4\text{-}13)$$

$$r(ji)\partial \sin \phi(ji)/\partial z(j)^{k} = T(i)^{3k} - [z(ji) \sin \phi(ji)^{k}]/r(ji)$$

and

$$\theta(ji) = \tan^{-1}[(T(i)^{2n} z(ji)^{n})/(T(i)^{1m} z(ji)^{m})]$$

$$r(ji) \, \partial\theta(ji)/\partial z(j)^{k} = [\cos \theta(ji) \, T(i)^{2k} \qquad (4\text{-}14)$$

$$-\sin \theta(ji) \, T(i)^{1k}]/\cos \phi(ji)$$

If we examine equations (4-9) to (4-14), we see that all coordinates are expressed as one body relative to another with the sole exception of $\underline{z}(j)$. Indeed, it is convenient in general to recast the equations of motion so that all co-

ordinates are relative to the reference body, say, body 0. Thus, we have

$$
\begin{aligned}
z''^{k}(j0) &= z''^{k}(j) - z''^{k}(0) \\
&= -G(m(0)+m(j))/r^2(ji) \\
&\quad [z^{k}(j0)/r(j0) - H^{k}(j0) + H^{k}(0j)] \\
&\quad + \sum_{\substack{i\neq j \\ i\neq 0}} Gm(i)\,[z^{k}(0i)/r^3(0i) - z^{k}(ji)/r^3(ji) \\
&\qquad + (H^{k}(ji) - H^{k}(ij))/r^2(ji) \\
&\qquad - (H^{k}(0i) - H^{k}(i0))/r^2(0i)]
\end{aligned}
\tag{4-15}
$$

4.3 GENERAL RELATIVISTIC MOTION

Naturally, for a system of masses as small and spread out as those in the Jovian system, the full general relativistic equations of motions will be very nearly the same as the purely Newtonian equations. In other words, the so-called post-Newtonian or first-order relativistic terms will be nearly negligible. In truth, the full equations can not be solved for even two bodies, but the method of solving for the zeroth and first-order terms gives results as precise as we are able to use. Landau and Lifshitz (1962) give a de-

rivation of the covariant metric tensor in harmonic coordinates for a system of point masses using the Einstein field equations to leading order in the small parameters GM/Rc^2 and v^2/c^2.

$$g(ij) = -(1+2U(b))\ \delta(ij)$$

$$g(j4) = g(4j) = 0.5 \sum_a W(ba)[7V^j(a)-V^k(a)R^{kj}(ba)] \qquad (4\text{-}16)$$

$$g(44) = 1-2U(b)+2U^2(b)+\sum_a[2W(ba)\Omega(a)-3W(ba)V^2(a)]$$

where

$$V^k = dz^k/dz^2 = z'^k/c$$

$$U(b) = (G/c^2) \sum_{a \neq b} m(a)/r(ba)$$

$$A^k = d^2z^k/(dz^2)^2 = z''^k/c^2$$

$$W(ba) = (G/c^2)\, m(a)/r(ba) \qquad (4\text{-}17)$$

$$f(ba)^k = -Gm(a)z(ba)^k/c^2r^3(ba)$$

$$F(b)^k = \sum_{a \neq b} f(ba)^k$$

$$\Omega(a) = \sum_{b \neq a} W(ab)$$

$$ds^2 = dz^\alpha dz^\beta g(\alpha\beta)$$

$$R(ba)^{kj} = z(ba)^k z(ba)^j/r^2(ba)$$

We will follow the conventions that Roman superscripts range from 1 to 3 while Greek superscripts range from 1 to 4, and $z^4 = ct$. Thus, the contravariant metric tensor is (again to leading order)

$$g^{ij} = -(1-2U(b))\ \delta(ij)$$

$$g^{j4} = g^{4j} = 0.5 \sum_a W(ba)[7V(a)-V(a)R(ba)^{j}{}_{k}{}^{kj}] \tag{4-18}$$

$$g^{44} = 1+2U(b)+U^2(b)-\sum_a W(ba)[2\Omega(a)-3V^2(a)]$$

The Christoffel symbols of the second kind may be evaluated from the metric tensor and its derivatives as follows

$$\left(\begin{matrix}\alpha\\ \beta\gamma\end{matrix}\right) = 0.5\ g^{\alpha\mu}\ (g(\beta\mu)_{,\gamma} + g(\gamma\mu)_{,\beta} - g(\beta\gamma)_{,\mu}) \tag{4-19}$$

where a comma-subscript indicates the partial derivative with respect to the corresponding coordinate, e.g.

$$g(\beta\mu)_{,\gamma} = \partial g(\beta\mu)/\partial z^{\gamma} \tag{4-20}$$

Thus, to leading order in the small parameters we get

$$(4)_{(44)} = \sum_a f(ba)V^k(a)^k$$

$$(4)_{(4s)} = -F^s + \sum_a f(ba)^s \left(\Omega(a)-1.5(V(a))^2\right)$$

$$(s)_{(44)} = -(1-4U(b))F^s(b) + \sum_a [f(ba)^s \left(\Omega(a)-2(V(a))^2\right)$$

$$+f(ba)V^t(a)^t(3V^s(a)+1.5\ V^k(a)R^{ks}(ba)\ )$$

$$-W(ba)(3.5\ A^k(a)+.5\ A^k(a)R^{ks}(ba)\ )\ ]$$

$$(4)_{(st)} = \sum_a [f(ba)^t\ (1.5\ V^s(a)+.75\ V^s(a)R^{ks}(ba)\ )$$

$$+f(ba)^s\ (1.5\ V^t(a)+.75\ V^t(a)R^{kt}(ba)\ ) \qquad (4\text{-}21)$$

$$-1.5\ f(ba)V^k(a)^k\delta(st)\ ]$$

$$(s)_{(4s)} = \sum_a [f(ba)^t\ (2V^s(a)+.75\ V^s(a)R^{ks}(ba)\ )$$

$$+f(ba)^s\ (2V^t(a)+.75\ V^t(a)R^{kt}(ba)\ )$$

$$-f(ba)V^k(a)^k\delta(st)\ ]$$

$$(s)_{(rt)} = \delta(rs)^t F(b) + \delta(st)^r F(b) - \delta(rt)^s F(b)$$

Using these values we may proceed to the equation for a space-like geodesic

$$d^2 z^{\alpha}/ds^2 + (\beta\gamma)^{(\alpha)} (dz^{\beta}/ds)\, dz^{\gamma}/ds = 0 \qquad (4\text{-}22)$$

and obtain the equations of motion. First, we need to be able to express the derivatives in terms of time derivatives d/dz^4 instead of interval derivatives d/ds.

$$d/ds = (dz^4/ds)\, d/dz^4 \qquad (4\text{-}23)$$

$$d^2/ds^2 = (dz^4/ds)^2\, d^2/(dz^4)^2 + d^2z^4/ds^2\, d/dz^4$$

Then, we get

$$d^2 z(b)^j/(dz^4)^2 = 1/c^2\, z''(b)^j \qquad (4\text{-}24)$$

$$= -[(st)^{(j)} z'(b)^s z'(b)^t/c^2 + 2(4s)^{(j)} z'(b)^s/c$$

$$+ (44)^{(j)} + s'^2/c^2\, d^2z^4/ds^2\, z'(b)^j\ ]$$

$$
\begin{aligned}
z''^{j}(b) = c^2 F^{j}(b) - c^2 \sum_a \Big[& f^{j}(ba) \, (4U(b) - V^2(b) - 2V^2(a) + \Omega(a) \\
& + 4V^{k}(a) V^{k}(b) + 0.5 \, A^{k}(a) z^{k}(ba) \\
& + 1.5 \, (V^{k}(a) z^{k}(ba))^2 / r^2(ba) \;) \\
& + V^{j}(b) \, (3f^{k}(ba) V^{k}(a) - 4V^{k}(b) f^{k}(ba) \;) \\
& + V^{j}(a) \, (4f^{k}(ba) V^{k}(b) - 3V^{k}(a) f^{k}(ba) \;) \\
& + 3.5 \, A^{j}(a) W(ba) \; \Big]
\end{aligned}
\tag{4-25}
$$

Clearly, the first term in equation (4-25) is just the Newtonian gravitational acceleration, and the rest of the terms account for the first-order post-Newtonian effects. If we now look again at equation (4-15), we are reminded that we actually want the differenced acceleration. Let us use the subscripts s, o, and b for a three-body system of point masses. Then, we get the post-Newtonian term:

$$
\begin{aligned}
\Delta \underline{z}''(bo) = {} & Gm(s)/c^2 \; [(\underline{z}(bs)/r^3(bs)) \; (G(4m(s)+m(b))/r(bs) \\
& \quad + G(4m(o)+3.5\; m(b))/r(bo) \\
& \quad +Gm(o)/r(os)-z'^2(b) \;) \\
& \quad -(\underline{z}(os)/r^3(os)) \; (G(4m(s)+m(o))/r(os) \\
& \quad + G(4m(b)+3.5\; m(o))/r(bo) \\
& \quad +Gm(b)/r(bs)-z'^2(o) \;) \;] \\
& +G/c^2 \; [\underline{z}(bo)/r^3(bo) \\
& \quad (G(4m^2(o)+10m(o)m(b)+4m^2(b))/r(bo) \\
& \quad +Gm(s)[(4m(o)+m(b))/r(bs) \\
& \qquad +(4m(b)+m(o))/r(os)] \\
& \quad -(2m(o)+m(b))z'^2(o)-(2m(b)+m(o))z'^2(b) \\
& \quad +4(m(o)+m(b)) \; \underline{z}'(b)\cdot\underline{z}'(o) \\
& \quad +1.5\; m(o)(\underline{z}'(o)\cdot\underline{z}(bo))^2/r^2(bo) \\
& \quad +1.5\; m(b(\underline{z}'(b)\cdot\underline{z}(bo))^2/r^2(bo) \\
& \quad -.5\; Gm(s)m(o) \; \underline{z}(os)\cdot\underline{z}(bo)/r^3(bo) \\
& \quad +.5\; Gm(s)m(b \; \underline{z}(bs)\cdot\underline{z}(bo)/r^3(bs) \;) \\
& \quad +\underline{z}'(b) \; (4m(s)\underline{z}(bs)\cdot\underline{z}'(b)/r^3(bs) \\
& \qquad +[\underline{z}(bo)/r^3(bo)]\cdot[(4m(o)+3m(b))\underline{z}'(b) \\
& \qquad +(4m(b)+3m(o))\underline{z}'(o)] \;) \\
& \quad +\underline{z}'(o) \; (4m(s)\underline{z}(os)\cdot\underline{z}'(o)r^3(os) \\
& \qquad +[\underline{z}(bo)/r^3(bo)]\cdot[(4m(o)+3m(b))\underline{z}'(b) \\
& \qquad +(4m(b)+3m(o))\underline{z}'(o)] \;) \;]
\end{aligned}
\tag{4-26}
$$

by substituting the Newtonian accelerations for the $\underline{A}$ terms in equation (4-25): Since these Newtonian values are correct to zeroth order, the resulting equation (4-26) is good to firstorder as we require. In the case of the Sun, Jupiter, and a Galilean satellite many of the terms in equation (4-26) are negligible compared to some of the others, and, at the same time, the general relativistic effect of the other satellites can also be treated as though it were purely Newtonian. Thus, we get the only important terms in equation (4-26).

$$\Delta \underline{z}''(bo) = [Gm(o)/c^2 r^3(bo)][\Phi \underline{z}(bo) + \Psi \underline{z}'(bo)] \qquad (4\text{-}27)$$

where

$$\begin{aligned} \Phi = {} & 4Gm(o)/r(bo) + 5Gm(s)/r(os) - z'^2(bo) + 2\underline{z}'(bo)\cdot\underline{z}'(os) \\ & + z'^2(os) + 1.5\ (\underline{z}'(os)\cdot\underline{z}(bo))^2/r^2(bo) \\ & - Gm(s)\underline{z}(os)\cdot\underline{z}(bo)/2r^3(os) \qquad (4\text{-}28) \\ \Psi = {} & \underline{z}(bo)\cdot(4\underline{z}'(bo) + \underline{z}'(os)) \end{aligned}$$

Note that we have used the same coordinates $\underline{z}(i)$ in our general relativistic development as in the preceding Newtonian expressions. The two are fundamentally different, but this convention is justified because the first term in equation (4-25) matches the Newtonian point-mass terms in equa-

tion (4-15). Thus, to zeroth order there is no difference, and so we will retain equation (4-15) as the equation of motion with just a correction term from equation (4-27).

4.4 NEWTONIAN VARIATIONAL EQUATIONS

The equation of motion contains an infinite set of parameters since each body has an infinite number of gravitational potential coefficients, but in practice only a limited set of these has any observable effect on the motions of a real system. Thus, we may realistically write a set of variational equations for all the parameters of interest corresponding to the equation of motion. Then, to integrate these equations we need $d[\partial \underline{z}(j0)/\partial p]/dt$ for $\partial \underline{z}(j0)/\partial p$ and $d[\partial \underline{z}'(j0)/\partial p]/dt$ for $\partial \underline{z}'(j0)/\partial p$. However, all the parameters are independent of time, and we may freely interchange the order of differentiation in these expressions. Thus, the time derivatives are just $\partial \underline{z}'(j0)/\partial p$ and $\partial \underline{z}''(j0)/\partial p$. Then, using the chain rule we may separate the partial derivatives into convenient parts.

$$\partial z''^{k}(j)/\partial p = (\partial z''(j)/\partial p)_{z,z'} + \Sigma_i[(\partial z''(j)/\partial z(i))_{p,z'}\, \partial z(i)/\partial p + (\partial z''^{k}(j)/\partial z'^{m}(i))_{p,z}\, \partial z'^{m}(i)/\partial p\,] \tag{4-29}$$

Now let us work as before and treat only the Newtonian approximation at first. Then there are no velocity-dependent terms in the force equation, and we may ignore the last term in equation (4-29). Thus, we write

$$\partial z''^{k}(j)/\partial z^{m}(j) = - \sum_{i \neq j} Gm(i)/r^3(ji) \, [\delta(km) - 3z^{k}(ji)z^{m}(ji)/r^2(ji) - K^{km}(ji) - K^{km}(ij) \,] \tag{4-30}$$

where

$$K^{km}(ji) = r^3(ji) \, \partial(H^{k}(ji)/r^2(ji))/\partial z^{m}(j) \tag{4-31}$$

Again, the simplification we used for equation (4-9) has been applied to the last term in equation (4-30). By the symmetry of indices we can see

$$\partial z''^{k}(j)/\partial z^{m}(i) = Gm(i)E^{km}(ji) \tag{4-32}$$

where

$$E^{km}(ji) = [\delta(km)-3z^{k}(ji)z^{m}(ji)/r^2(ji)-K^{km}(ji)-K^{km}(ij)] \tag{4-33}$$

Thus, we may write for the Newtonian approximation

$$\partial z''^{k}(j)/\partial p = (\partial z''^{k}(j)/\partial p)_z + \sum_{i \neq j} Gm(i)E^{km}(ji) \left(\partial z^{m}(i)/\partial p - \partial z^{m}(j)/\partial p\right) \tag{4-34}$$

and, therefore,

$$\partial z''^{k}(j0)/\partial p = (\partial z''^{k}(j0)/\partial p)_z - G(m(0)+m(j))E^{km}(j0)\partial z^{m}(j0)/\partial p + \sum_{\substack{i \neq j \\ i \neq 0}} Gm(i)[E^{km}(ji)\partial z^{m}(ij)/\partial p - E^{km}(0i)\partial z^{m}(i0)/\partial p] \tag{4-35}$$

In order to compute these partial derivatives we must evaluate K:

$$
\begin{aligned}
K^{km}(ji) = \sum_{n}^{n} & [a(i)/r(ji)] \, [J(n,i) \, (\delta(km)q(1n,ji)/r(ji) \\
& -((n+3)q(1n,ji) + q(2n,ji)\sin\phi(ji)) \\
& \quad z^{k}(ji)z^{m}(ji)/r^{3}(ji) \\
& +q(2n,ji) \, \mathrm{Sym}(\underline{T}^{3}(i),\underline{z}^{km}(ji)) \, /r^{2}(ji) \\
& -P''(n,\sin\phi(ji)) \, T^{3k}(i)T^{3m}(i)/r(ji) \,) \\
& - \sum_{h=1}^{n} (\, t(1nh,ji) \, [\delta(km)p(1nh,ji)/r(ji) \\
& -((n+3)p(1nh,ji) + p(2nh,ji)\sin\phi(ji)) \\
& \quad z^{k}(ji)z^{m}(ji)/r^{3}(ji) \\
& +p(2nh,ji) \, \mathrm{Sym}(\underline{T}^{3}(i),\underline{z}^{km}(ji)) \, /r^{2}(ji) \\
& -P''(nh,\sin\phi(ji)) \, T^{3k}(i)T^{3m}(i)/r(ji) \\
& +h^{2}r(ji) \, \partial\theta(ji)/\partial z^{k}(j) \, \partial\theta(ji)/\partial z^{m}(j) \\
& \quad P(nh,\sin\phi(ji)) \,] \\
& +t(2nh,ji) \, [\\
& \quad p(1nh,ji)\mathrm{Sym}(\partial\theta(ji)/\partial\underline{z}(j),\underline{z}^{km}(ji)) \, /r(ji) \\
& \quad -P'(nh,\sin\phi(ji))\mathrm{Sym}(\partial\theta(ji)/\partial\underline{z}(j),\underline{T}^{3\,km}(i) \,) \\
& -P(nh,\sin\phi(ji))r(ji)\partial^{2}\theta(ji)/\partial z^{k}(j)\partial z^{m}(j)]) \,]
\end{aligned}
\tag{4-36}
$$

where

$$q(1n,ji) = (n+1)P(n,\sin\phi(ji)) + \sin\phi(ji)\, P'(n,\sin\phi(ji))$$

$$q(2n,ji) = (n+2)P'(n,\sin\phi(ji)) + \sin\phi(ji)\, P''(n,\sin\phi(ji)) \qquad (4\text{-}37)$$

$$t(1nh,ji) = C(nh,i)\cos h\theta(ji) + S(nh,i)\sin h\theta(ji)$$

$$t(2nh,ji) = h[-C(nh,i)\sin h\theta(ji) + S(nh,i)\cos h\theta(ji)]$$

$$p(1nh,ji) = (n+1)P(nh,\sin\phi(ji)) + \sin\phi(ji)\, P'(nh,\sin\phi(ji))$$

$$p(2nh,ji) = (n+2)P'(nh,\sin\phi(ji)) + \sin\phi(ji)\, P''(nh,\sin\phi(ji))$$

$$\mathrm{Sym}(\underline{x},\underline{y})^{jk} = x^j y^k + x^k y^j$$

4.5 GENERAL RELATIVISTIC CORRECTIONS TO THE VARIATIONAL EQUATIONS

Next, we must consider the partial derivatives of the post-Newtonian correction terms. It is clear from equations (4-27) and (4-28) that we must deal with velocity-dependence. Thus, we have the partials with respect to the position and velocity of both body "b" and body "o".

$$\partial\Delta z''^{k}(bo)/\partial z^{j}(bo) = (Gm(o)/c^2r^3(bo))\ [\Phi\delta(jk) - R^{jk}(bo)\ (3\Phi$$

$$+4Gm(o)/r(bo)$$

$$+3(\underline{z}'(os)\cdot\underline{z}(bo))^2/r^2(bo)\ )$$

$$+3z'^{j}(os)z^{k}(bo)\ \underline{z}'(os)\cdot\underline{z}(bo)/r^2(bo)$$

$$-.5\ z^{j}(os)z^{k}(bo)\ Gm(s)/r^3z(bo)$$

$$+(4z'^{j}(bo)+z'^{j}(os))z'^{k}(bo)$$

$$-3z^{j}(bo)z'^{k}(bo)\ \Psi/r^2(bo)\ ] \qquad (4\text{-}38)$$

$$\partial\Delta z''^{k}(bo)/\partial z'^{j}(bo) = (Gm(o)/c^2r^3(bo))\ [-2z'^{j}(bo)z^{k}(bo)$$

$$+2z'^{j}(os)z^{k}(bo)+4z^{j}(bo)z'^{k}(bo)+\Psi\delta(jk)\ ]$$

$$\partial\Delta z''^{k}(bo)/\partial z^{j}(os) = (G^2m(o)m(s)z^{k}(bo)/c^2r^3(bo)r^3(os))$$

$$[-5z^{j}(os) + 1.5\ \underline{z}(os)\cdot\underline{z}(bo)z^{j}(os)/r^2(os)$$

$$-.5\ z^{j}(bo)\ ]$$

$$\partial\Delta z''^{k}(bo)/\partial z'^{j}(os) = (Gm(o)/c^2r^3(bo))$$

$$[z^{k}(bo)\ (2z'^{j}(bo)+2z'^{j}(os)$$

$$+3\underline{z}'(os)\cdot\underline{z}(bo)z^{j}(bo)/r^2(bo)\ )$$

$$+z'^{k}(bo)z^{j}(bo)\ ]$$

With these expressions and the partial derivatives of the coordinates and velocities themselves we may apply the chain rule as in equation (4-29) to get the partial derivative accelerations for integrating the variational equations. One might argue that the general relativistic corrections to the partial derivatives should be ignored because they are on the order of v^2/c^2 while some omitted terms in the partial derivatives of observations are of order v/c. However, the inclusion of the general relativistic terms is no great added burden, and the observation partials may be corrected in the future.

4.6 ACCURACY REQUIREMENTS

It is appropriate to consider here the limiting accuracy needed in the equations of motion for this particular application. There are actually two kinds of cutoff that may be applied, the precision limit of the hardware that supports the program and the minimum offset of position or velocity that can be detected in the observations available. Indeed, if the hardware limit is more severe than the observational, it is clear that the undertaking requires new or different hardware. If, on the other hand, the observational limit dominates, then the "invisible" physical effects may be ignored in the interest of speed.

Upon inspecting the equations of motion presented in this chapter we may write down the gravitational effects that might have an observable bearing on the motions of the Galilean satellites. First of all is the effect of Jupiter considered as a mass point, but there is also the effect of the non-sphericity of Jupiter, that is, the gravitational potential harmonic expansion. Then, we have the point-mass and non-spherical perturbing effects of the satellites on each other and the effects of the perturbing satellites on the non-spherical distribution of Jupiter. These last must be included because the equations of motion are expressed in terms of the satellite coordinates relative to the center of mass of Jupiter. Next, we have the perturbing effects of the Sun and planets, particularly Mars and Saturn, and of the asteroid belt. We must also consider the interaction of the Sun with the non-spherical distribution of Jupiter. Finally, there is the correction that must be made for general relativity, which may be thought of as a perturbation upon the Newtonian problem. Indeed, there is no reason to reject non-gravitational forces out of hand, and, so, we should at least examine the solar wind and light pressure. In addition, the effect of Jupiter's magnetosphere should be considered at least for Io.

There is also a class of terms due to errors in the implementation of the equations of motion in PEP. The most significant of these is the ephemeris error for the position of the central body with respect to the rest of the Solar System which is due to the tabulation of coordinates of the center of mass of the whole system of planet-plus-satellites rather than those of the planet. This kind of term is of interest only if the magnitude of the error warrants its inclusion. Table 5 gives a summary of these forces with their relative magnitudes.

The formulas in Table 5 represent the forces approximately in terms of powers of the appropriate distance scales. Indeed, these distances are variable, and the listed forces are actually upper limits. The masses used in the formulas are as follows; (Sun) $M = 1$, (Jupiter) $m = 1.0\times10^{-3}$, (Saturn) $m(s) = 3\times10^{-4}$, (Mars) $m(m) = 3\times10^{-7}$, (typical Galilean satillite) $m(i) = 5\times10^{-8}$, (Amalthea) $m(A) = 10^{-12}$, (asteroid belt) $m(a) = 10^{-9}$. For the distance scales, r denotes the typical Galilean satellite semimajor axis (5×10^{-3} AU), and R represents that of Jupiter (5 AU). The gravitational harmonic coefficient terms are represented by the largest in each case. The magnetosphere terms, labeled "Lorentz" and "Jup. plasma", represent the forces due

Table 5

Relative forces on a Galilean satellite

The approximate magnitudes of the acceleration terms in the equations of motion for the Galilean satellites with the corresponding approximate formulas.

Name	Formula	log F
central	Gm/r^2	0 (by def.)
cnt.harm.	$GmJ(2)a^2/r^4$	-3
satellite	$Gm(i)/r^2$	-5
Sun	GMr/R^3	-6
gen. rel.	G^2m^2/c^2r^3	-8
sat.-c.hrm.	$Gm(i)J(2)a^2/r^4$	-8
Saturn	$Gm(s)r/R^3$	-9
Amalthea	$Gm(A)/r^2$	-9
Mars	$Gm(m)r/R^3$	-12
sat. hrm.	$Gm(i)J(2,i)a(i)^2/r^4$	-12
Sun-c.hrm.	$GMJ(2)a^2/R^4$	-13
ephem. err.	$GMm(i)r^2/mR^4$	-13
asteroids	$Gm(a)r/R^3$	-15
Lorentz	$qvB/m(i)$	-15
Jup. plasma	$\rho v^2\pi a(i)^2/m(i)$	-15
radiation	$La(i)^2/4R^2cm(i)$	-17
solar wind	$\rho v^2\pi a(i)^2/m(i)$	-17

to an assumed net charge on Io of 10^4 Coulombs in the co-rotating magnetic field of 0.03 gauss and to the drag of a co-rotating plasma of density 10^5 protons/cm^3. See, for example, Smith et al. (1975) and Fillius et al. (1975).

It remains now to decide where to cut off the consideration of terms in the equations of motion. We may note, first of all, that both non-gravitational forces in Table 5 are lost in the digital noise when combined with the central force term to the precision available to PEP. Still, that has no bearing on where the cutoff should be; if these terms could not be neglected, then either the presently available computer would have to be abandoned or the precision would have to be extended by extra software. Thus, some computation is needed for the offset in distance for each term. For example, the perturbing effect of Mars may be estimated by a straightforward calculation of the effect of the linear acceleration during a quarter of an orbital period for Callisto. Callisto experiences the greatest differential acceleration because it is farthest from Jupiter. This differential acceleration reaches a maximum of about 10^{-12} m/s^2, and its direction is constantly rotating as the satellite revolves about Jupiter. Thus, the time-averaged differential acceleration vanishes, and the only effect to consider is the linear displacement after about a quarter period of near maximum acceleration, namely about half a meter, or the velocity displacement, which comes to about 5×10^{-7} m/s. both of these are far below the sensitivities

of any presently available observations, and we conclude that Mars' effect may be ignored completely. A similar calculation yields the maximum linear offset of Io due to the differential attraction of Amalthea (we use Io for the worst case rather than Callisto) of about one meter. Again, the effect is far from detectable. Even the effect of Saturn is less than the precision of currently available observations (the same simple calculation gives about 400 m as the maximum offset). However, this is only two orders of magnitude below observability and is, therefore, a reasonable point to begin including terms in the equations of motion. Thus, everything in Table 5 from Saturn up should be included in the integrations. An interesting possible non-gravitational force has come to light with the Voyager photographic evidence of volcanic activity on Io, namely, self-propulsion. However, that is sure to be sporadic and negligible within the scope of this investigation. For example, a vent with an area of 5 km^2 spewing a gas of density 10^{-3} g/cm^3 at a velocity of 100 m/s would provide an acceleration on the order of 10^{-11} times the central force effect of Jupiter. Indeed, we simply can not expect to detect non-gravitational forces in the motions of such massive bodies as the Galilean satellites.

Chapter V

SATELLITE MUTUAL EVENTS

5.1 MID-EVENT TIME

Now we turn to the body of observational data. In order to make use of a given observation, we must be able to predict the observed value from the ephemerides. In addition, for the linearized least squares fitting technique we need the partial derivatives of the computed observable with respect to a variety of parameters. Thus, we must derive the expressions to be realized in subroutine form for any observables not previously implemented in PEP. Consider a mutual occultation, that is, of one satellite by another. The time of maximum obscuration is very nearly the same as the time of minimum apparent separation of their centers. Indeed, the two times would be identical except for two possible complicating factors, namely solar phase angle (incomplete illumination) and non-uniform reflectance. These will be discussed later.

The apparent angular separation θ is given by

$$\cos\theta = C \tag{5-1}$$
$$= \underline{u}(\underline{a})\cdot\underline{u}(\underline{b})$$

where

$$\underline{a} = \underline{r}(a,t2)-\underline{r}(o,t3)$$
$$\underline{b} = \underline{r}(b,t1)-\underline{r}(o,t3)$$
$$t2 = t3-a/c \tag{5-2}$$
$$t1 = t3-b/c$$

Here t3 is the instant of observation, $\underline{r}(o)$ is the position of the observer, and $\underline{r}(a)$ and $\underline{r}(b)$ are the positions of the occulting and occulted bodies. Note that this treatment is essentially the same as for the relative photographic observations, but the vectors $\underline{a}$ and $\underline{b}$ are directed away from, instead of toward, the observer. The bodies will be assumed spherical with radii of $\rho(a)$ and $\rho(b)$, respectively. Thus, the condition of minimum separation is given by

$$0 = F(t3,p) = \underline{u}(\underline{a})\cdot\underline{u}'(\underline{b})+\underline{u}'(\underline{a})\cdot\underline{u}(\underline{b}) \tag{5-3}$$

where p represents the parameters governing motions, and the prime notation represents the partial derivative with respect to t3. It should be borne in mind that equation (5-3) also applies at the time of maximum separation, but we may take advantage of the wide temporal separation between the

actual maxima and minima and restrict ourselves to the vicinity of minima confirmed by observation. By the same token, we can calculate the apparent separation and see if it is truly a minimum.

Since unit vectors and their derivatives figure prominently in this chapter, let us now present some formulas for unit vector derivatives.

$$\begin{aligned}
\underline{u}'(\underline{a}) &= (\underline{a}'-\underline{a}(\underline{a}\cdot\underline{a}')/a^2)/a \\
\underline{u}''(\underline{a}) &= [\underline{a}''-\underline{a}(\underline{a}\cdot\underline{a}'')/a^2-\underline{u}(\underline{a})(\underline{a}'\cdot\underline{u}'(\underline{a}))-2a'\underline{u}'(\underline{a})]/a \\
\partial\underline{u}(\underline{a})/\partial p &= [\partial\underline{a}/\partial p - \underline{a}(\underline{a}\cdot\partial\underline{a}/\partial p)/a^2]/a \\
\partial\underline{u}'(\underline{a})/\partial p &= [\partial\underline{a}'/\partial p-\underline{a}(\underline{a}\cdot\partial\underline{a}'/\partial p)/a^2 \\
&\quad -\underline{u}(\underline{a})(\partial\underline{u}(\underline{a})/\partial p\cdot\underline{a}') \\
&\quad -\underline{u}'(\underline{a})(\underline{u}(\underline{a})\cdot\partial\underline{a}/\partial p)-a'\partial\underline{u}(\underline{a})/\partial p]/a
\end{aligned} \tag{5-4}$$

Here it will be useful to introduce a simplification of notation by defining two vector functions.

$$\begin{aligned}
\underline{M}(\underline{a},\underline{v}) &= (\underline{u}(\underline{a})\cdot\underline{v})\underline{u}'(\underline{a})+(\underline{u}'(\underline{a})\cdot\underline{v})\underline{u}(\underline{a}) \\
\underline{P}(\underline{a},\underline{v}) &= (\underline{v}-\underline{a}(\underline{a}\cdot\underline{v})/a^2)/a.
\end{aligned} \tag{5-5}$$

Clearly, we may write for any vectors $\underline{x}$ and $\underline{y}$, $\underline{M}(\underline{a},\underline{x})\cdot\underline{y}=\underline{M}(\underline{a},\underline{y})\cdot\underline{x}$. and $\underline{P}(\underline{a},\underline{x})\cdot\underline{y}=\underline{P}(\underline{a},\underline{y})\cdot\underline{x}$. Thus, we have for equations (5-4)

$$\underline{u}'(\underline{a}) = \underline{P}(\underline{a},\underline{a}')$$

$$\underline{u}''(\underline{a}) = \underline{P}(\underline{a},\underline{a}'')-[\underline{M}(\underline{a},\underline{a}')+a'\underline{u}'(\underline{a})]/a$$

$$\partial\underline{u}(\underline{a})/\partial p = \underline{P}(\underline{a},\partial\underline{a}/\partial p) \qquad (5\text{-}6)$$

$$\partial\underline{u}'(\underline{a})/\partial p = \underline{P}(\underline{a},\partial\underline{a}'/\partial p)-[\underline{M}(\underline{a},\partial\underline{a}/\partial p) + a'\ \underline{P}(\underline{a},\partial a/\partial p)]/a$$

Since we have a scalar function of time F, which vanishes at mid-event, we may use Newton's method of extracting roots to calculate the time of mid-event. The first guess of this time may be the observed value of t3 for the event or, for that matter, any other estimate. Then, we simply evaluate the function and its time derivative using this first guess and form a correction via

$$\delta t3 = -F(t3^{(0)},p) \ / \ F'(t3^{(0)},p) \qquad (5\text{-}7)$$

Rather than deriving an expression for F', we will find it useful to obtain a general form for the derivative of F with respect to any variable p.

$$\partial F/\partial p = \partial\underline{u}(\underline{a})/\partial p\cdot\underline{u}'(\underline{b})+\partial\underline{u}'(\underline{a})/\partial p\cdot\underline{u}(\underline{b}) \qquad (5\text{-}8)$$
$$+\underline{u}'(\underline{a})\cdot\partial\underline{u}(\underline{b})/\partial p+\underline{u}(\underline{a})\cdot\partial\underline{u}'(\underline{b})/\partial p$$

This is a scalar expression, so let us derive some useful substitutions for the dot products based on equations (5-6).

$$\partial \underline{u}(\underline{a})/\partial p \cdot \underline{v} = \underline{P}(\underline{a},\underline{v}) \cdot \partial \underline{a}/\partial p$$

$$\partial \underline{u}'(\underline{a})/\partial p \cdot \underline{v} = \underline{P}(\underline{a},\underline{v}) \cdot \partial \underline{a}'/\partial p \qquad (5\text{-}9)$$

$$-[\underline{M}(\underline{a},\underline{v})+a'\underline{P}(\underline{a},\underline{v})] \cdot [\partial \underline{a}/\partial p]/a$$

Substituting into equation (5-8), we get

$$\begin{aligned}\partial F/\partial p = {} & \underline{P}(\underline{a},\underline{u}'(\underline{b})) \cdot \partial \underline{a}/\partial p + \underline{P}(\underline{a},\underline{u}(\underline{b})) \cdot \partial \underline{a}'/\partial p \\ & -[\underline{M}(\underline{a},\underline{u}(\underline{b}))+a'\underline{P}(\underline{a},\underline{u}(\underline{b}))] \cdot \partial \underline{a}/\partial p \ /a \\ & +\underline{P}(\underline{b},\underline{u}'(\underline{a})) \cdot \partial \underline{b}/\partial p + \underline{P}(\underline{b},\underline{u}(\underline{a})) \cdot \partial \underline{b}'/\partial p \qquad (5\text{-}10) \\ & -[\underline{M}(\underline{b},\underline{u}(\underline{a}))+b'\underline{P}(\underline{b},\underline{u}(\underline{a}))] \cdot \partial \underline{b}/\partial p \ /b\end{aligned}$$

but $\underline{P}(\underline{a},\underline{u}'(\underline{b})) = (\underline{u}'(\underline{b})-\underline{a}(\underline{a} \cdot \underline{u}'(\underline{b}))/a^2)/a$, so we may collect terms in $\underline{u}(\underline{a})$, and we have, finally,

$$\begin{aligned}\partial F/\partial p = {} & \underline{P}(\underline{a},\underline{u}(\underline{b})) \cdot \partial \underline{a}'/\partial p \\ & +[\underline{u}'(\underline{b})-C\underline{u}'(\underline{a})-F\underline{u}(\underline{a})-a'\underline{P}(\underline{a},\underline{u}(\underline{b}))] \cdot \partial \underline{a}/\partial p \ /a \\ & +\underline{P}(\underline{b},\underline{u}(\underline{a})) \cdot \partial \underline{b}'/\partial p \qquad (5\text{-}11) \\ & +[\underline{u}'(\underline{a})-C\underline{u}'(\underline{b})-F\underline{u}(\underline{b})-b'\underline{P}(\underline{b},\underline{u}(\underline{a}))] \cdot \partial \underline{b}/\partial p \ /b\end{aligned}$$

Using equation (5-11) we may get dF/dt3 in particular, and this expression is especially handy for calculating the partial derivatives of the computed value of t3. Now we can find the correction to t3 using equations (5-11) and (5-7). Obviously, the first guesses at t1 and t2 must also be corrected, but the form of the correction need not be the same.

If the first guesses were actually obtained from $t3^{(0)}$ by the light-time offsets b/c and a/c, then the corrections would be the same as $\delta t3^{(0)}$ to first order in v/c. However, finding the retarded times is an iterative procedure in itself, and we may converge toward all three times simultaneously provided that the errors in the first guesses are well below the characteristic times of the motions (that is, the orbital periods). Thus, the procedure begins with $t3^{(0)}$, $t2^{(0)}$, and $t1^{(0)}$, and we obtain the next approximation from a given one, designated $^{(*)}$, as follows.

$$
\begin{aligned}
\underline{a}^{(*)} &= \underline{r}(a,t2^{(*)})-\underline{r}(o,t3^{(*)}) \\
\underline{b}^{(*)} &= \underline{r}(b,t1^{(*)})-\underline{r}(o,t3^{(*)}) \\
\delta t3^{(*)} &= -[F(t3^{(*)},p)] \;/\; [F'(t3^{(*)},p)] \\
t3^{(*+1)} &= t3^{(*)}+\delta t3^{(*)} \qquad\qquad (5\text{-}12) \\
t2^{(*+1)} &= t3^{(*+1)}-a^{(*)}/c \\
t1^{(*+1)} &\doteq t3^{(*+1)}-b^{(*)}/c
\end{aligned}
$$

Once the correction $\delta t3$ becomes less in absolute value than some accuracy constant, the procedure may be said to have converged to that accuracy. In passing, we should mention some corrections which are ignored throughout this derivation. The first of these is aberration. Clearly, aberration may be ignored because we are dealing with a small

angular separation, and the differential aberration is at least four orders of magnitude less than the separation itself. In fact, in the case of Jovian satellites, the apparent separation (that is, the separation projected onto a plane normal to the line of sight) at mid-event is nearly perpendicular to the ecliptic. Since Earth's velocity vector lies in the ecliptic, the differential aberration is much smaller still. Another effect we omit is that of general relativity, which would introduce corrections to all of the (purely Newtonian) calculations here. For example, the apparent positions of the bodies are offset by the gravitational light bending due to any masses near the line of sight (primarily Jupiter). This bending is on the order of GM/Rc^2 at most, where M is the mass and R is the closest distance of the propagation path from the mass. For Jupiter this gives an angle of at most 10^{-8} radian, and, of course, we are really concerned with the differential bending, which is at least three orders of magnitude smaller. Again, the correction is much smaller than the resolution in angular separation (the separations themselves are typically 10^{-5} radian). Another relativistic correction involves the propagation delays that give the retarded times t2 and t1. Here the correction is on the order of GM/c^3. Again, for

Jupiter we get a negligible correction (10^{-8} second compared with the timing accuracy of about one second).

5.2 MINIMUM SEPARATION

The actual observable quantity during the occultation or eclipse is the light intensity, but processing convenience demands a reduction of the light curve to a few, easily interpreted parameters. The first of these is the mid-time, which we have already discussed. The mid-times presented by Aksnes and Franklin (1976) and used in this work were obtained by folding each light curve about some point and shifting that point to minimize the RMS deviation between the two resulting time series. The measurement uncertainties used in this work were obtained from the published normalized deviations by assuming that the measurement errors were proportional to those RMS deviations and scaling the errors to an overall mean of about 3 seconds. Such a procedure lacks the rigor of simultaneously fitting all parameters in a least-squares sense, but the strong bilateral symmetry evident in nearly all the published light curves indicates that very little information is lost by decoupling the mid-time determination from the other parameter fits.

The remaining information, then, must concern the shape and extent of the light curve. It would be most convenient to separate this into parameters involving just the motions of the bodies and parameters involving just the sizes, but the effects are strongly related. The present work is limited to a two-stage approach, however, and only parameters that are relatively insensitive to the motions of the two bodies may be used in the second stage, namely, fitting to the motions. Only one parameter meets this criterion, that is, the angular separation of the two objects as a fraction of the combined radii. This can be seen qualitatively by considering the effect on the light curve of changing the actual size of either of the two bodies. Since the brightness of each body is separately measurable, we need consider only the depth and width of the brightness dip that constitutes the event. Further, the width depends on both positions and velocities and is more easily degraded by noise in the signals than is the mid-time. At any instant during the occultation there is a total brightness for each body and, thus, a relative brightness defect or depth, which is a function of just the sizes of the bodies and the angular separation at that instant as long as we neglect the phase defect and the possibility of non-uniform reflectance.

Clearly, increasing the size of either body will increase the depth (and the reverse). If, however, the sizes and the separation scale equally, the depth will remain the same. Aksnes and Franklin report the angular separations at the best fit mid-times as well as the corresponding linear distances. These are easily converted into fractional separations. Thus, we have

$$s = \theta \ / \ [\rho(a)/a+\rho(b)/b] \qquad (5\text{-}13)$$

It is here that the possibility of non-uniform reflectance enters the problem, since we need to relate the brightness diminution to the apparent angular separation of the two bodies. Indeed, any unevenness in the reflectance could introduce asymmetry into the light curve, which could affect the apparent mid-time itself. However, all the Galilean satellites have relatively small orbital brightness variations, and that fact lends itself to the assumption that the observed mid-time is the same as the time of minimum separation. Indeed, the preliminary reports of brightness contrasts on the surface of Europa (for example, Vermilion et al., 1974) seem to have been due to errors in the ephemerides used in processing the light curves. Variations in the surface brightness because of the scattering law can

not be ruled out. Visual inspection of some of the photographs returned by the Voyager spacecraft reveals a suggestion of limb brightening, but nothing definite. Only a detailed and calibrated study of the photographs can establish the true degree of limb brightening or darkening. For the time being the uniform disk model will have to serve, although the variations of brightness from center to limb may, in fact, be large.

5.3 PARTIAL DERIVATIVES OF THE OBSERVATIONS

We have equation (5-3) as the condition for mid-event. Thus we may perform implicit differentiation to get the partial derivative of the time with respect to any parameter that enters into F.

$$\partial t3/\partial p = -[\partial F/\partial p] \;/\; [\partial F/\partial t3] \qquad (5\text{-}14)$$

Note that a general expression for $\partial F/\partial p$ was obtained in equation (5-11) and $\partial F/\partial t3$ comes from a simple substitution of t3 for p. Thus, we already have all the expressions necessary to evaluate equation (5-14).

$$\partial t3/\partial p = -\,[\underline{P}(\underline{a},\underline{u}(\underline{b}))\cdot\partial\underline{a}'/\partial p+\underline{V}(\underline{a},\underline{b})\cdot\partial\underline{a}/\partial p$$

$$+\underline{P}(\underline{b},\underline{u}(\underline{a}))\cdot\partial\underline{b}'/\partial p+\underline{V}(\underline{b},\underline{a})\cdot\partial\underline{b}/\partial p] \qquad (5\text{-}15)$$

$$/\ [\partial F/\partial t3]$$

where

$$\underline{V}(\underline{a},\underline{b}) = [\underline{u}'(\underline{b})-C\underline{u}'(\underline{a})-F\underline{u}(\underline{a})-a'\underline{P}(\underline{a},\underline{u}(\underline{b}))]/a$$

$$= [\underline{u}'(\underline{b})-C\underline{u}'(\underline{a})-a'\underline{P}(\underline{a},\underline{u}(\underline{b}))]/a \qquad (5\text{-}16)$$

since F vanishes.

The partial derivative of the minimum separation is slightly more complicated. By the chain rule we have

$$\partial s/\partial p = (\partial s/\partial t3)_p\ \partial t3/\partial p + (\partial s/\partial p)_{t3} \qquad (5\text{-}17)$$

but $\partial s/\partial t3$ (constant p) is simplified by the condition equation (5-3), since $\partial\theta/\partial t3$ (constant p) vanishes at mid-time. Using equation (5-1) we get

$$(\partial\theta/\partial p)_{t3} = -[\partial\underline{u}(\underline{a})/\partial p\cdot\underline{u}(\underline{b})$$

$$+\partial\underline{u}(\underline{b})/\partial p\cdot\underline{u}(\underline{a})]\ /\ \sin\theta \qquad (5\text{-}18)$$

$$= -[\underline{P}(\underline{a},\underline{u}(\underline{b}))\cdot\partial\underline{a}/\partial p+\underline{P}(\underline{b},\underline{u}(\underline{a}))\cdot\partial\underline{b}/\partial p]\ /\ \sin\theta$$

Let $D = \rho(a)/a + \rho(b)/b$; then we find

$$
\begin{aligned}
(\partial D/\partial p)_{t3} = & -[\rho(a)/a^2][\underline{u}(\underline{a})\cdot\partial\underline{a}/\partial p] \\
& -[\rho(b)/b^2][\underline{u}(\underline{b})\cdot\partial\underline{b}/\partial p] \\
& +[\partial\rho(a)/\partial p]/a+[\partial\rho(b)/\partial p]/b
\end{aligned}
\tag{5-19}
$$

and, thus,

$$
\begin{aligned}
\partial s/\partial p = (& -[\underline{P}(\underline{a},\underline{u}(\underline{b}))\cdot\partial\underline{a}/\partial p \\
& +\underline{P}(\underline{b},\underline{u}(\underline{a}))\cdot\partial\underline{b}/\partial p] \ / \ \sin\theta \\
& +s[[\rho(a)a'/a^2+\rho(b)b'/b^2]\partial t3/\partial p \\
& \quad +(\rho(a)/a^2)(\underline{u}(\underline{a})\cdot\partial\underline{a}/\partial p) \\
& \quad +(\rho(b)/b^2)(\underline{u}(\underline{b})\cdot\partial\underline{b}/\partial p)] \ ) \ / \ D
\end{aligned}
\tag{5-20}
$$

Equations (5-15) and (5-20) apply, of course, only to parameters that affect the motions and, thus, $\underline{a}$ and $\underline{b}$. All other partials are zero except $\partial s/\partial\rho(a)$ or $\partial s/\partial\rho(b)$, which are easily obtained from equation (5-19)

$$
\begin{aligned}
\partial s/\partial\rho(a) &= -s/Da \\
\partial s/\partial\rho(b) &= -s/Db
\end{aligned}
\tag{5-21}
$$

Now consider an eclipse of one satellite by another. The geometry is the same as in an occultation except that the logical center of the event is in the Sun instead of the observer. Obviously, the details of the obscuration are different because of the mixture of umbra and penumbra into the

event -- that fact follows from the extended nature of the "observer" in the Sun. In addition, the direction of light propagation is away from the logical center, but that only means a change in the logical order of calculating the retarded times. Indeed, there are now four events to juggle, namely, emission from the sun, passage by the obscurer, reflection (if any) from the obscured, and perception by the observer. Thus, in principle, we must keep account of the position of the Sun, but within the sensitivity of this sort of experiment we may carry out all calculations in the Sun-centered frame of reference rather than the system barycenter frame, and the Sun's position is, therefore, always at the origin. The necessary changes, then, are minimal. Let $\underline{a}$ and $\underline{b}$ represent the eclipsed and eclipsing bodies; then the definition equations (5-2) become

$$\begin{aligned} \underline{a} &= \underline{r}(a,t1) \\ \underline{b} &= \underline{r}(b,t2) \\ t1 &= t3 - |\underline{a}-\underline{r}(o,t3)|/c \\ t2 &= t3 - |\underline{b}-\underline{r}(o,t3)|/c \end{aligned} \qquad (5\text{-}22)$$

From there on, the expressions are identical with equations (5-3) to (5-21).

5.4 EFFECT OF SOLAR PHASE ANGLE

The effect of solar phase angle α on mutual satellite events is small but non-negligible, even though the Sun-Jupiter-Earth angle never gets above 11 degrees. Before we actually go to the trouble of calculating this effect in detail we should get some idea of its size. Figure 1 shows the disk of (spherical) body b as seen from Earth with the phase defect hatched off.

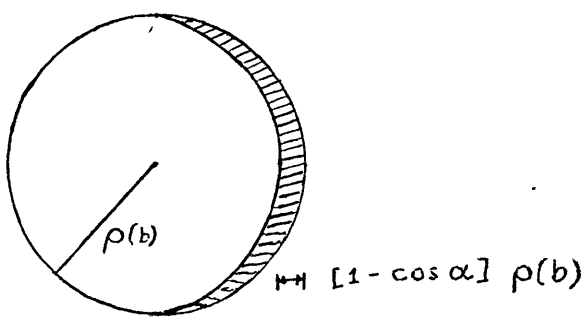

Figure 1: Phase defect on obscurable body

The visible disk at a small phase angle showing the projected maximum width of the unilluminated portion.

Cursory inspection reveals that the apparent center of the illuminated disk should be offset from the true center by about one-half of the maximum apparent width of the shadowed region, that is, by $[1-\cos\alpha]\,\rho(b)/2$ for a reasonably

small α. Thus, for the typical radius of 2000 kilometers and relative velocity of 10 kilometers per second the apparent time of mid-event might be shifted by as much as two seconds.

Such an effect can certainly not be ignored. We must make an effort to compute the time offset with a precision of at least 0.1 second. Here again, as we see in Figure 2, the geometry of eclipses and occultations is essentially the same except for the point of view.

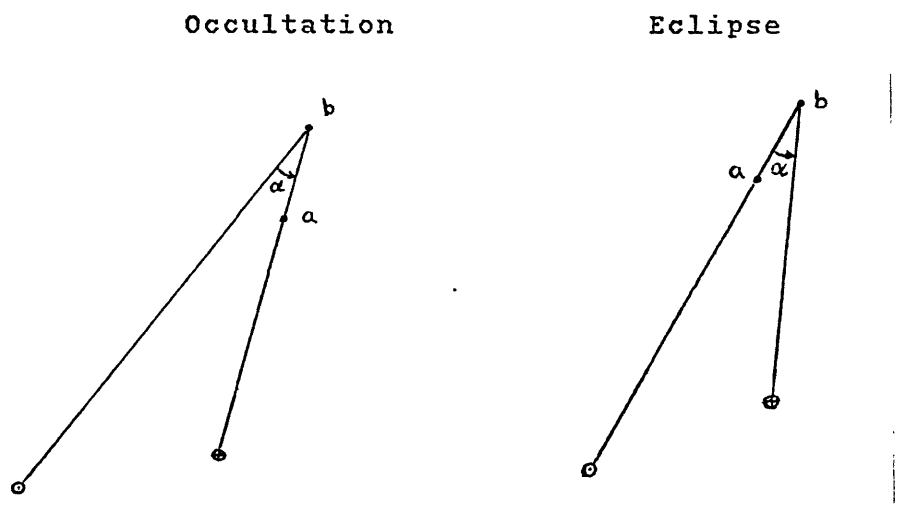

Figure 2: Occultation and eclipse geometries

Lines of sight for both cases illustrating the definition of "a" as the obscuring body and "b" as the obscured. For Jupiter satellites the phase angle α is no more than 11°.

For the purposes of generality, then, we shall define coordinates from two different points of view. We retain side by side the two different definitions of $\underline{a}$ and $\underline{b}$ from the discussion of the observables themselves, that is, geocentric and heliocentric, but we also need the positions of bodies relative to the Sun in either case, so let $\underline{A}$, $\underline{B}$, and $\underline{E}$ represent the corresponding positions of the obscurer, obscured, and observer. Thus, we note that in an eclipse $\underline{a}=\underline{A}$ and $\underline{b}=\underline{B}$, but in an occultation $\underline{a}=\underline{A}-\underline{E}$ and $\underline{b}=\underline{B}-\underline{E}$.

In both cases, then, we may form the shadow offset vector by projecting the obscurer to the distance of the obscured:

$$\underline{x} = (b/a)\underline{a}-\underline{b}$$

$$\underline{v} = (b/a)\underline{a}'-\underline{b}' \qquad (5\text{-}23)$$

Now we set up the observer's line of sight with $\underline{n}=\underline{B}-\underline{E}$ and define a notation for perpendicular components of vectors.

$$\underline{x}^* = \underline{x} - (\underline{x}\cdot\underline{u}(\underline{n}))\ \underline{u}(\underline{n}) \qquad (5\text{-}24)$$

We wish to find the projected impact parameter of the obscurer. Since satellite motions are approximately rectilinear on short time scales, we may obtain a very good estimate of the minimum apparent separation vector by taking the component of the offset vector perpendicular to $\underline{v}^*$.

$$H = |\underline{x}^* - [(\underline{x}^* \cdot \underline{v}^*)\underline{v}^*]/(v^*)^2| \tag{5-25}$$

so

$$H = [x^2 - (\underline{x} \cdot \underline{u}(\underline{n}))^2 - (n^2 \underline{x} \cdot \underline{v} - [\underline{x} \cdot \underline{n}][\underline{v} \cdot \underline{n}])^2 / (n^2 v^2 - (\underline{v} \cdot \underline{n})^2)\ ]^{0.5} \tag{5-26}$$

Similarly, we get the projected obscuration radius

$$\rho(0) = (b/a)\rho(a) \tag{5-27}$$

5.5 MODEL OF THE APPARENT OFFSET DUE TO PHASE DEFECT

Now we must set up a model of a mutual event that allows us to compute the effective apparent position of the obscured body as a function of the true positions of all the bodies concerned. What we need is the perceived brightness of the obscured body as a function of time during the event. Let us begin by making a number of simplifying assumptions, namely, (1) bodies a and b are spherical as already stated, (2) the illuminated portion of body b appears uniformly bright to the observer, (3) the position and velocity vectors of all bodies lie approximately in a single plane, and (4) the relative velocity vectors are constant during the

time interval of the event. The single plane of the geometry is, of course, the ecliptic. Thus, the brightness of the partially obscured object during the event is just some constant times the projected area inside the terminator with a circular zone cut out by the obscurer. Figure 3 shows a generalized picture of the illuminated portion of the visible disk.

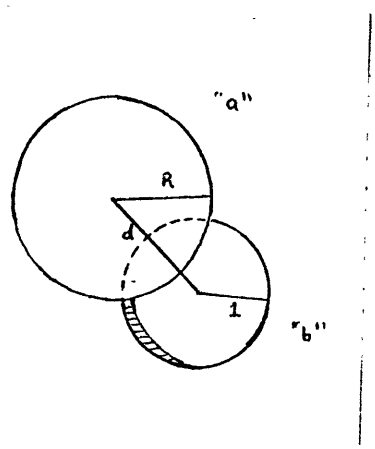

Figure 3: Partly obscured disk

Body b partly obscured by the disk (occultation) or shadow (eclipse) of body a.

Unfortunately, even this area cannot be described fully in terms of elementary functions unless the terminator coincides with the planet limb. In that limiting case, if we let the occulted disk have unit radius, let the occulter

have radius R and let the apparent distance between centers be d, we get for the area cut out just πR^2 if the occulter's disk appears entirely within the occulted disk, or π if the occulter completely covers the occulted, or $\cos^{-1}[(d^2+1-R^2)/2d] + R^2\cos^{-1}[(d^2-1+R^2)/2dR] - [4R^2-(R^2-d^2+1)^2]^{0.5}/2$ if the disks overlap only partly. It is a fairly straightforward matter to correct that occulted area for the phase defect by performing a numerical integration, but now the distance (d) between centers must be resolved into components parallel to and normal to the apparent relative velocity (x and y). Essentially, the problem is to determine the x offset that minimizes the visible illuminated area for any given value of the other parameters.

Strictly speaking, we should look for the offset that minimizes the RMS deviation between the two halves of the time series folded about the offset point. Since we are treating the velocity as constant, the time and x scales are linearly related. Further, since the y-axis is normal to the ecliptic (by assumption), the y offset of the centers is a constant (equal to $H/\rho(b)$ from equation (5-26)). Thus, the offsets in x were computed to minimize the RMS deviation of the folded time series for a variety of values of the parameters R, y, and α.

Inspection of those results showed that x is not exactly $(1 - \cos\alpha)/2$ (the rough guess). However, for all values of R and y, x is proportinal to $(1 - \cos\alpha)$, and the constant of proportionality f is about 1/2 for bodies of comparable sizes. Thus, we have the correction to $\underline{B}$ as follows:

$$|\Delta\underline{B}| = |f\,\rho(b)\,(1-\cos\alpha)| \qquad (5\text{-}28)$$

where $f = f(y, R)$.

Figure 4 illustrates the sense of the phase correction. It is clear from the figure that the correction $\Delta\underline{B}$ must be perpendicular to the line of sight $\underline{n}$ and must lie in the plane of $\underline{B}$ and $\underline{n}$. Also, the magnitude of $\underline{B}^*$ is just $B \sin\alpha$. Therefore, we may write

$$\begin{aligned}\Delta\underline{B} &= -f\rho(b)(1-\cos\alpha)\ \underline{u}(\underline{B}^*)\\ &= (f\rho(b)/B)([1-\cos\alpha]/\sin\alpha)((\underline{B}\cdot\underline{n})\underline{n}/n^2-\underline{B}) \qquad (5\text{-}29)\end{aligned}$$

The function f plotted on the R-y plane resembles an archway along the diagonal. The value drops to zero in the region where the disks do not actually overlap and varies between about 0.39 and 0.43 in the region representing a large obscurer and nearly total obscuration. The function may thus be approximated by a quadratic polynomial in R and

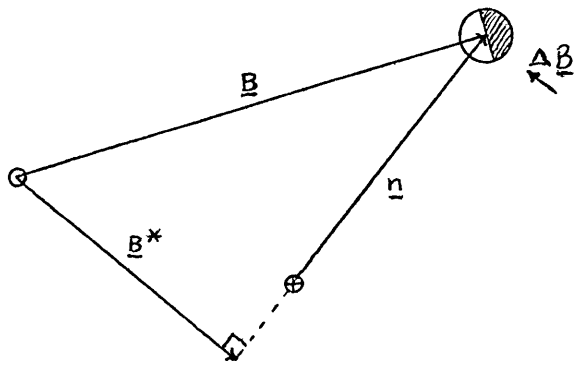

Figure 4: Phase correction geometry

y near the diagonal and by constants elsewhere. A least-squares fit on a grid of points at intervals of 0.3 in y and R gives the polynomial

$$f = -.08883631\ y^2 + .1785059\ Ry - .08996493\ R^2 - .1340744\ y + .1385038\ R + .3917556$$

within the region near the diagonal, that is, where R is less than 1.38 + 1.2 y and greater than y - 1. Numerical experiments with such a model reveal that the apparent off-set of the obscured body due to the phase defect is quite well represented by the combined polynomial and constants as can be seen in Table 6.

Table 6 gives the values of the function f at a selection of points on the R-y plane as actually determined from the

Table 6

Function f of fractional phase correction

The offset of the apparent position of the obscured body due to the solar phase angle as a fraction of the projected width of the un-illuminated portion of the disk. "R" represents the normalized radius of the obscuring body, and "y" the minimum separation of the centers. The offsets are computed from the folding point of maximum symmetry in the light curve assuming uniform brightness, following Aksnes and Franklin (1976).

Computed values

y= \ R=	0.3	0.6	0.9	1.2	1.5	1.8	2.1	2.4	2.7
0.6	.448	.400	.363	.281	.180	.000	.000	.000	.000
0.9	.439	.423	.397	.358	.290	.184	.000	.000	.000
1.2	.426	.440	.428	.403	.367	.291	.184	.000	.000
1.5	.420	.431	.441	.426	.409	.363	.290	.188	.000
1.8	.415	.423	.433	.439	.432	.410	.366	.293	.191
2.1	.419	.421	.424	.435	.439	.431	.404	.379	.292
2.4	.415	.414	.423	.424	.438	.438	.426	.407	.382
2.7	.410	.417	.413	.418	.426	.431	.439	.432	.406
3.0	.411	.409	.418	.418	.420	.424	.436	.441	.436
3.3	.414	.409	.411	.420	.414	.423	.426	.436	.444

Best fit values

y= \ R=	0.3	0.6	0.9	1.2	1.5	1.8	2.1	2.4	2.7
0.6	.426	.394	.346	.282	.202	.000	.000	.000	.000
0.9	.444	.428	.396	.348	.284	.204	.000	.000	.000
1.2	.444	.445	.429	.397	.349	.285	.205	.000	.000
1.5	.429	.445	.445	.430	.398	.350	.286	.206	.000
1.8	.410	.430	.446	.446	.431	.399	.351	.287	.207
2.1	.410	.398	.431	.447	.447	.431	.400	.352	.288
2.4	.410	.410	.399	.431	.448	.448	.432	.401	.353
2.7	.410	.410	.410	.399	.432	.448	.449	.433	.402
3.0	.410	.410	.410	.410	.400	.432	.449	.449	.434
3.3	.410	.410	.410	.410	.410	.400	.433	.449	.450

uniform disk model and as calculated from the combined quadratic polynomial and constants. The standard deviation between the two sets of values is just 0.012, which for any of the Galilean satellites corresponds to less than a tenth of a second in the time of an event. The maximum difference between corresponding members of the two sets of values is only .029, and most differences in the range of likely parameters are less than 0.005. In particular, the single most common event (Io occulting or eclipsing Europa) represents the case where R = 1.2, and the differences for that case in the range of y from 0.6 to 1.2 are all no more than 0.005.

5.6 PARTIAL DERIVATIVES OF THE PHASE CORRECTION

Ordinarily, the solar phase angle correction may be treated as a small, constant offset during an event. For the case of planetary satellites, the characteristic distances are large compared to the velocities and accelerations (in the time scale of the events). Thus, the function f is only very weakly dependent on time. Indeed, it is also insensitive to line-of-sight or line-of-motion offsets of the involved bodies; only a shift perpendicular to both gives rise to a significant change in y and, hence, in f. The phase correction must be applied to the true position of

the obscured body for the purposes of finding the mid-event time with sufficient accuracy, and a similar procedure must be used to correct the partial derivatives of the position with respect to any parameter affecting y.

We may rewrite equation (5-29) as follows.

$$\Delta \underline{B} = h(k\underline{n}-\underline{B}) \tag{5-30}$$

where

$$\begin{aligned} k &= \underline{b}\cdot\underline{n}/n^2 \\ g &= (1-\cos\alpha)/\sin\alpha \\ &= ([Bn-\underline{B}\cdot\underline{n}]/[Bn+\underline{B}\cdot\underline{n}])^{0.5} \\ h &= f\rho(b)\ g/B \end{aligned} \tag{5-31}$$

Now we must derive the partial derivatives of this correction with respect to its components.

$$(1/h)(\partial h/\partial \underline{B}) = -\underline{B}/B^2 + (1/f)(\partial f/\partial H)(\partial H/\partial \underline{B}) \tag{5-32}$$

$$+ (1/g)(\partial g/\partial \underline{B}) \tag{5-32}$$

where for this application f is computed as the quadratic function previously mentioned and fixed at 0 if H is greater than the sum of the two radii or at 0.41 if $\rho(0)$ is much bigger than $\rho(b)$. At mid-event we find

$$H = b\ |\underline{u}(\underline{a})-\underline{u}(\underline{b})| \tag{5-33}$$

Thus,

$$\partial H/\partial \underline{B} = (\partial/\partial \underline{B})(b[2-2\underline{u}(\underline{a})\cdot\underline{u}(\underline{b})]^{0.5})$$

$$= H\underline{b}/b^2-(b^2/H)\underline{P}(\underline{b},\underline{u}(\underline{a})) \qquad (5\text{-}34)$$

if we neglect the dependence of $\underline{b}$ on $\underline{E}$ in the case of an occultation. Recall the definition of $\underline{P}$ from equation (5-5). It should be obvious that observations of this sort are very insensitive to the position of the observer, so we will ignore any terms in the partial derivatives due to the site positions.

For example, for observations of Jupiter's satellites from Earth any lateral offset of the observer from the ephemeris position is reduced by three orders of magnitude relative to satellite offsets when all are expressed in jovicentric angles. If the satellite positions were precise to 100 meters, the corresponding Earth uncertainty could be as much as 100 kilometers without materially affecting the computations. Certainly geodesy has progressed beyond the point where timing Jovian events is useful in determining the observer's position on Earth.

Now,

$$(1/g)(\partial g/\partial \underline{B}) = \csc\alpha\ \partial\alpha/\partial \underline{B}$$

$$= -\csc^2\alpha\ [(\underline{n}+\underline{B})/Bn - \cos\alpha\ (\underline{b}/B^2+\underline{n}/n^2)] \qquad (5\text{-}35)$$

so

$$(1/h)(\partial h/\partial \underline{B}) = [(\underline{B}/B^2+\underline{n}/n^2)\cos\alpha - (\underline{n}+\underline{B})/Bn]/\sin^2\alpha$$

$$- \underline{B}/B^2 + (1/f)(\partial f/\partial H)[H\underline{b}/b^2-(b^2/H)\underline{P}(\underline{b},\underline{u}(\underline{a}))]$$

$$(1/h)(\partial h/\partial \underline{A}) = (1/f)(\partial f/\partial H)(\partial H/\partial \underline{a}) \qquad (5\text{-}36)$$

$$= -(1/f)(\partial f/\partial H)(b^2/H)\underline{P}(\underline{b},\underline{u}(\underline{a}))$$

and

$$\partial k/\partial \underline{B} = [\underline{B}+(1-2k)\underline{n}]/n^2 \qquad (5\text{-}37)$$

Thus, we may make corrections to the partials of $\underline{B}$:

$$\partial\Delta\underline{B}/\partial p = (1/h)[(\partial h/\partial \underline{B})\cdot(\partial \underline{B}/\partial p)+(\partial h/\partial \underline{A})\cdot(\partial \underline{A}/\partial p)$$

$$+\partial h/\partial p]\Delta\underline{B} \qquad (5\text{-}38)$$

$$+h[(k-1)\partial \underline{B}/\partial p+(\partial k/\partial \underline{B})\cdot(\partial \underline{B}/\partial p)\underline{n}]$$

where $\partial h/\partial p$ represents the partial derivative with $\underline{A}$ and $\underline{B}$ held fixed and, thus, vanishes for all parameters except the body radii.

Chapter VI

DATA PROCESSING

6.1 CHECKING THE SOFTWARE

Much of the PEP software needed for this undertaking did not exist, and much of that which did had never been tested. Thus, the newly developed or otherwise unverified sections of PEP had to be checked for errors at all levels. Aside from errors of punctuation or syntax that may be discovered by inspection of the code or compilation, there may always be errors of logic or the mapping of variables. In any case, the results should be checked by hand calculations to be sure the code is correct because errors are practically unavoidable otherwise.

The integration and data comparison sections of PEP are analogous. Each produces a tabulation of physical quantities (coordinates or observation residuals), and each item has an associated set of partial derivatives with respect to the relevant parameters. Leaving aside the physical quantities themselves for the moment, we must check the partial

derivatives in two ways. First, the expressions should be formally correct, and, more important, the limit of the ratio $\Delta x/\Delta p$, the change in physical quantity x to the change in parameter p, should approach the computed value of $\partial x/\partial p$ for small values of Δp. Unfortunately, a digital computer has inherent limits on the smallness of Δp, and a balance must be struck between digital noise and the nonlinearity of the physical quantities. In practice Δp should be chosen so that Δx lies midway between x and the digital noise (in a logarithmic sense). A generally adequate test is the following. Use the code to compute both x and $\partial x/\partial p$ for two values of p. Having thus obtained Δx and $\Delta(\partial x/\partial p)$, one may compute a truncated Taylor series expansion for Δx.

$$\Delta x = (\partial x/\partial p)\Delta p + (\partial^2 x/\partial p^2)(\Delta p)^2/2 + \ldots \qquad (6\text{-}1)$$

In lieu of the second derivative, which is not computed in PEP, we may use $\Delta(\partial x/\partial p)/\Delta p$ with the understanding that the resulting error for Δx will be about the same order of magnitude as the neglected higher order terms in equation (6-1), namely about $[\Delta(\partial x/\partial p)]^2\Delta p/(\partial x/\partial p)$. Thus, we may check whether the following inequality holds.

$$|\Delta x/\Delta p - \partial x/\partial p - \Delta(\partial x/\partial p)/2| < [\Delta(\partial x/\partial p)]^2/|\partial x/\partial p| \qquad (6\text{-}2)$$

In other words, the error in $\partial x/\partial p$ should be less than the omitted higher order terms. If this test is satisfied under reasonable conditions, then the corresponding partial derivative may be considered correct to within the accuracy of the machine.

Table 7 gives the results of some of the tests of the integration of partial derivatives. The parameters presented here were chosen to illustrate the variety of tests and to include the worst cases. For each parameter an integration was performed at least twice with different input values of that parameter, but all other held fixed. In most cases the initial position and velocity of the integrated body are independent of these values, and the corresponding initial values of the partial derivatives are all zero. However, the initial conditions themselves and the masses do have an effect on the position and velocity at the initial epoch. For such parameters the setup for the partial derivatives must be checked in the same way as the subsequent integrated values.

This same sort of test was applied to the partial derivatives of the observables. All new observation code must be accompanied by the corresponding partials code. The number

Table 7

Partial derivative test for Europa

For each parameter p the results of two integrations are compared. The integrated partial derivatives are checked by the difference method and the errors tabulated after 1-2 orbits. The estimated higher order terms (h.o.t.) in the expansions of $\partial x/\partial p$ are listed for comparison. Parameters include initial conditions, masses, and Jupiter gravity field expansion and orientation.

Parameter	$\partial x/\partial p$	Δp	$\Delta(\partial x/\partial p)$	h.o.t.	error
a(Io)	-3	-6	-5	-7	-9
M(Io)	-2	-6	-5	-8	-11
l(Cal)	-7	0	-7	-7	-9
e(Gan)	-6	-3	-9	-12	-14
M(J)	0	-9	-6	-12	-8*
J(2)	-4	-5	-10	-16	-13*
S(21)	-9	-2	-12	-15	-18
S(22)	-6	-4	-9	-12	-14
α pole	-8	0	-9	-10	-11
δ pole	-9	0	-10	-11	-13
rot.phase	-10	0	-11	-12	-14
rot.per.	-6	-3	-6	-6	-7
a(Jup)	-9	-3	-11	-13	-14
e(Jup)	-9	-3	-10	-11	-11
a(Eur)	1	-8	-5	-11	-9
e(Eur)	-3	-5	-7	-11	-11
Ω(Eur)	-3	-3	-7	-11	-11

* digital noise limit

of parameters that enter into the computation of observables is even greater than that for motions, but the task of

checking the partials is simplified by the fact that the partials are always computed via the chain rule. Thus, in principle, only one partial with respect to a parameter in any given body's motion need be tested. In addition, of course, there are parameters that do not affect motion at all but do affect the observations.

Checking the integration of the motion consists of two parts. The first is quite straightforward; it is the verification of the accelerations by hand calculation. The second, however, requires some ingenuity. The long-term stability of the integration depends on digital round-off effects, and the errors at the end of an integration must be tolerable if the integration is to have any value. Unfortunately, it is prohibitively expensive to perform long integrations just to test the stability of the integrator.

Several methods might be used to check the integrator. For example, the departure from closure may be checked for the special case where all perturbing forces are suppressed. Another method, which also serves as a test for the accelerations, is to integrate from one epoch forward to another and then take the final position and velocity as the initial conditions at the second epoch and integrate back to the

first. The differences between the two integrations laid side-by-side serve as a measure of the reliability of the integrator with any and all perturbing forces included.

Generally, integration errors display an oscillation within an envelope growing with time. The envelope does not usually grow linearly. In fact, depending on the circumstances it may grow exponentially with a power as high as 1.5 (King, 1979). Experiments must be carried out with a variety of integration step sizes to ascertain the best possible performance and whether, in fact, the best performance will suffice if extrapolated to the full span of the desired integration. One might expect that shortening the step size of the integrator would always improve the performance (aside from requiring more computation), but it is easily verified that for step sizes shorter than some optimum the discrepancies grow rapidly worse. This is easily understood in terms of the round-off errors beginning to dominate the Taylor series truncation errors inherent in a finite step-size integrator.

In the case of the Galilean satellites the usual optimum of about 360 steps per orbit proved to be about right, although the discrete choices of step size forced a decision

between 250 and 500 steps. All other factors being equal, the preferable step size is the largest because it requires the least computation. Integrating the motion of Europa forward and back 1800 steps at 250 steps per orbit produced a maximum discrepancy of only 100 μm. Extrapolating that result to a five-year time span by a $t^{1.5}$ law indicates that the maximum expected error due to the integrator should be no more than 200 cm for Io and proportionately less for the longer-period satellites.

Checking the computation of observables can be quite laborious because it involves iterative procedures. However, considerable savings may sometimes be effected when two different observables are closely related. For example, the relative photographic observable can easily be checked by computing the apparent positions of each of the two bodies at the same epoch and forming the difference. The simplest means of checking the occultation/transit observables is to supply idealized ephemerides that produce easily predictable event times, but another way of checking the validity of the computed time is to compute the relative positions of the two bodies over a range of times and interpolate to find the time of occultation or eclipse or any other such event. All of these tests have been applied to the relevant code in

PEP, some before and some concurrently with the processing of real data.

6.2 STARTING THE LEAST-SQUARES FITTING

One of the principles of iterative linearized least-squares data analysis is that all parameters must be given initial values that are reasonable. In other words, this technique is a means of refining or adjusting parameters, rather than generating them from scratch. Thus, we need not only the physical properties of the Jovian system (see Chapter 1), but also initial conditions for the satellite motions and ephemerides for computing the perturbing effects of all bodies of interest and also for computing the theoretical values of observations. The planetary ephemerides for this work were obtained from the PEP 311 ephemeris tape, one of a series of N-body integrations produced in the course of solar system parameter estimation using PEP. These ephemerides are the result of fitting to a large number of radar and optical observations, but all of the observations were made before mid-1969, and the positions for the epoch of 1973-1978 might, therefore, be expected to display noticeable and increasing discrepancies with reality. As a result, it may be necessary, and it is certainly possible,

to include the orbital parameters of Jupiter itself in the analysis for the satellite motions.

For the perturbing influences of the satellites on each other, the positions were taken from the E1S2 theory of J.H. Lieske (1977b and 1978). This theory is the latest of a series of versions of Sampson's theory used in this work. The first was the simplified version that has been used for the prediction ephemerides for the radar observations at Arecibo ("Quick Sampson"). The next two were obtained from K. Aksnes but were originally coded by J.H. Lieske; they were respectively the complete theory ("Sampson") and the theory with some orbital elements adjusted to fit the mutual event observations of 1973 (the "Revised Sampson" of Aksnes and Franklin, 1976). Finally, Lieske provided two versions of his extension of Sampson's work, namely "E1" and "E1S2". The two are identical in formulation and differ only in the values of the basic parameters. The former constitutes a fit to much of the same data that Sampson used in his original work, plus a small number of eclipse observations extending through 1974. The latter includes in addition the mutual event observations of 1973 and, thus, overlaps the data used in the present work. The theory consists of a set of coefficients for trigonometric series expansions of the

satellite positions. There is an accompanying computer program for evaluating the trigonometric series at any given Julian epoch, and the output is a set of coordinates of the satellites relative to the center of mass of Jupiter in the usual 1950.0 reference frame.

The initial conditions for the satellite motion integrations were obtained in two steps. The first and most obvious step was to evaluate the theory (or interpolate from a tabulation) to obtain a position and velocity for each satellite at the chosen epoch. Actually, for quasi-Keplerian orbits it is more meaningful to express the initial conditions as osculating elliptic elements. Indeed, the Cartesian and elliptic representations are equivalent, providing the gravitational constant and masses of the satellite and primary in question are fixed. Even when the masses are to be adjusted by least-squares fitting, the transformation of the elliptic elements can be linked in a straightforward manner with the mass adjustments.

It is a simple matter to generate elliptic elements from a theory. However, to the extent that the theory approximates or omits physical terms in its development, it will contain errors that may be rapidly magnified by a numerical

integration. While the theory is tied to the mean motion of the satellite by its dependence on trigonometric time functions, the mean motion of a quasi-Keplerian orbit depends critically on the initial semimajor axis. Actually, the osculating semimajor axis of the theoretical orbit varies by more than a tenth of a percent for each of the Galilean satellites on a time scale of the orbital period. In addition, the situation in a multi-body system is more complicated than in the Keplerian case. For example, one could compute the mean semimajor axis by averaging over an interval of many orbits and derive a Keplerian mean motion from this semimajor axis. This computed mean motion will not, however, agree with the motion implicit in the frequency of the principal trigonometric term of the theory. In particular, Sampson's theory gives a difference of about a part in 10^3 over a period of 100 days near the epoch of Julian date 2442600 for each of the satellites.

In any case, integration of the equations of motion from theory-derived initial conditions is almost certain to display increasing discrepancies with the theory as a result of the initial offset of the mean motion. Since the osculating elliptic elements vary with time, a suitable choice of the initial epoch might provide initial conditions that will

match the true mean motion of the satellite, but the same initial epoch would most likely not work for all four satellites. Further, there is nothing particularly useful about starting from initial conditions computed directly from the theory, since the purpose of the present undertaking is to adjust parameters.

Thus, the second step in producing the initial conditions is to tie them to the theory over a span of time rather than at a single point. That task can be accomplished by using the "dummy observation" facility of PEP in conjunction with the standard least-squares parameter adjustment technique. Observables can be predicted on the basis of the satellite theory, and these "observations" can serve as the input data to the fitting.

Before generating dummy observables in PEP it was necessary to implement the option of reading the satellite ephemerides from an S-body tape instead of from integration tapes. The result is analogous to the situation with regard to the major planets; under input stream control PEP can now read coordinates for any body from either the integration tape (if any) or from the N-body or S-body tape, as the case may be. Thus, in this work a Sampson's theory S-body tape was used to generate dummy observations of each of the sat-

ellites. For that purpose the "Revised Sampson" theory was chosen in order to match as closely as possible the mutual event observations of 1973 (Aksnes and Franklin, 1976).

The dummy observations themselves could be any set that sufficiently constrains the motions. The ideal observables would, in fact, be the Cartesian coordinates of the satellites direct from the theory. However, PEP is not designed to compare coordinates directly, but only indirectly through realizable observations. Thus, a set of 100 to 150 dummy optical observations was generated for each satellite evenly spaced over about three orbits. The observations consisted of astrographic right ascension and declination "measurements" from an arbitrary site on Earth. Each observation was assigned an uncertainty of 2.5×10^{-4} second of arc in both right ascension and declination, or about 800 meters at the distance of Jupiter. The uncertainties are, of course, arbitrary so long as they are uniform, but this value was chosen because it is just less than the target accuracy of Sampson's theory itself. Thus, a least-squares adjustment of numerical integration to the theoretical predictions should converge with a final goodness-of-fit of about unity. The goodness-of-fit as used in this thesis is formed by making a slight modification of the RMS (residual/error), that

is, the sum-squared normalized residual is divided by the number of data points minus the number of adjustable parameters, and then the square root is taken. For most cases these two are very nearly the same, and the terms will be used interchangeably whenever the difference is negligible.

As already described, PEP has the capability of iteratively integrating the differential equations, computing the observation residuals, and adjusting the parameters until they converge to their final values. Thus, the initial conditions were forced to fit the theory as represented by the dummy observations.

A typographical error in the initial conditions entered as input to this iterative fitting for Io provided an illustrative example of the consequences of unreasonable input parameter estimates for the iterative linearized least-squares adjustment technique. When the necessary adjustments stray outside of the linear region, the iterative procedure may begin to overshoot and actually diverge. In this case, the initial mean anomaly was given about 200° out of phase, and very little improvement took place during the first three iterations of the adjustment. The RMS (residual/error) remained on the order of 10^5, and the initial

mean anomaly made more than four complete revolutions. In the process, corrections to the eccentricity made it negative twice, but the program automatically uses the absolute value in such cases. Finally, an adjustment landed within 10° of the correct initial mean anomaly, and two more iterations resulted in convergence.

The sequence beginning with the initial conditions derived from a single point of an analytical theory and now tied to a span of the theory could, of course, be continued to longer spans to achieve a closer long-range fit, but the result would still be an integration tied to the theory rather than the observational data that went into the theory. Further, the main purpose of this procedure was to yield good beginning estimates of the initial conditions for fitting a numerical integration to real data. The primary need for the fit to a span of the theory was to obtain a reasonable initial mean motion for a longer time span integration.

The stage was therefore set for fitting an integration to a group of data from one opposition of Jupiter. Thus, the next step in producing improved initial conditions was to perform one iteration using the mutual event data of 1973

along with the few astrometric observations of the same opposition. At that time the relative photographic data were not available. Unfortunately, the coverage provided by the mutual events was rather spotty for the outer satellites. Thus, only 9 of the 91 events reported by Aksnes and Franklin (1976) involved Callisto, and only 27 involved Ganymede. As a result, Callisto's initial conditions were determined rather less reliably than the others. Only 19 measurements in all were used in determining those six initial conditions while 178 went into the total of 24 for all the satellites.

Table 8 shows the initial conditions and uncertainties from the fit to the six months of mutual event data. Actually these uncertainties are formal errors multiplied by the goodness-of-fit. The formal errors are simply the standard deviations of the parameter adjustments from the solution of the normal equations. Since no parameters were adjusted other than the initial conditions of the satellites, the uncertainties are somewhat arbitrary, but they do indicate that these values are reasonably close to the real initial conditions. Thus, the main purpose of fitting to a short span of data has been fulfilled.

Table 8

Initial conditions determined from mutual events

Osculating elliptic elements referred to the 1950.0 frame. Periapse (π) is measured from node (Ω) and longitude (l) from periapse. The base epoch is J.D. 2441842.5

	Io	Europa	Ganymede	Callisto
a (10^{-3} AU)	2.821046±3	4.486878±5	7.157099±3	12.58658±2
e (10^{-3})	4.5±1	9.39±6	0.66±3	7.4±1
i (deg)	25.49±6	25.13±4	25.38±5	25.43±6
Ω (deg)	358.1±1	358.76±8	358.37±9	358.3±1
π (deg)	5.±1	203.4±4	142.±3	334.3±1
l (deg)	262.±1	301.7±4	32.±2	332.5±1

After the fit to the six-month span of data in 1973 was completed there was no larger completely filled data arc for the next stage of processing. Although Jupiter is visible more than half of each year, observations are made primarily when it is high in the night sky. Thus, the next stage of fitting requires integrations of at least one and a half years to span two oppositions. At this point the tradeoff between saving computation on a single integration and on the entire project favors proceeding to the full integration span of 1973-1978 and using all the available data.

In general, when there are many mutually perturbing bodies whose parameters must all be adjusted, the fitting process must go through many iterations before it will converge. In this investigation the choice was made to integrate each body's motion separately using a composite perturbing body ephemeris drawn from the best preceding iteration or other sources. Thus, there are actually two levels of adjustment, single-body and perturbing-body. It may be necessary to hold the perturbing body ephemeris fixed through several iterations on the individual bodies before using the results to make a new version of the ephemeris. In particular, it makes sense to keep the same perturbing body coordinates when the errors in the integrations are due more to the individual body initial conditions than to the errors in the perturbing body ephemeris. The advantage in so doing is just the saving of time, rather than any rigorous requirement. Indeed, in the present investigation it is possible to perform only one long integration for each satellite because the perturbing ephemeris is supplied by a reasonably accurate analytical theory from the start. Thus, as long as the initial fit to six months of data suffices to bring the initial conditions in close agreement with the actual satellite motions, a single iteration with post-fit differential

corrections will converge adequately to the final values of all parameters.

6.3 MATCHING THE INTEGRATION WITH AN ANALYTICAL THEORY

An important test of the numerical integration technique is how well it can agree with a good analytical theory over a short span, say, one to twenty orbits. Unlike the process of determining the starting values for the initial conditions, this test requires that all non-adjustable physical parameters in the integration match those that went into the theory. Under those conditions any irreducible differences after fitting the integration to the theory must represent errors in one or the other. Thus, "dummy" observations of Europa were generated using the theoretical ephemerides, and then the residuals were formed on the basis of an integration very nearly converged to the theory. These residuals were used to adjust Europa's initial conditions, and the resulting differential corrections were applied to produce the post-fit residuals. Since the accuracy of the E1S2 theory is estimated to be about 1 km (Lieske, 1978), the uncertainties of the "dummy" observations were arbitrarily and uniformly set at 0.8 km to make the comparison simple.

A series of tests of this sort was carried out with a variety of observables, principally the conventional Earth-based measurements of photographic right ascension and declination and radar time-delay. These three form an approximately orthogonal system and should provide a well-determined solution. In addition, the corresponding rate observables were tested singly and in combination with the distance-type observables. The arbitrary measurement uncertainties for the rate observables were, again, set uniformly to the same fraction of the mean orbital velocity that 0.8 km is of the semimajor axis. The results showed some interesting anomalies. First of all the goodness-of-fit ranged from about 1.0 to about 6.6 depending on the particular combination of observables. Further, the post-fit mean residual for a single observation type ranged as large as twice the measurement uncertainty. In other words, there was sometimes an apparent bias in the observations even after fitting the integration to the theory. For a normal distribution of errors the mean residual should fall off as the inverse square-root of the number of measurements. Since there were about 500 data points of each observation type, the maximum post-fit mean should have been less than 5 percent of the measurement uncertainty unless there were

some systematic bias built into the comparison between the integration and theory.

In particular, the biases were large whenever a rate observable was combined with a distance observable, but small when only rate or only distance observables were used. This effect first appeared with the inclusion of Doppler shifts with the distance-type observables, and the fact that Doppler partial derivatives in PEP are incorrect by a part in 10^4 seemed at first to be a likely cause of the anomalies. However, the same behavior persisted even when there was substituted a pseudo-Doppler observable that did have the correct partial derivatives. There is no obvious reason to expect such behavior on the basis of differences in the treatment of velocity, although the theoretical velocity is the formal derivative of position while the integrated position is, literally, the integral of the velocity. Nevertheless, this result may still be attributed to the fundamental difference between the analytical and numerical approaches. The post-fit residuals display systematic variations rather than random noise, and the usual criteria of data analysis do not hold in so far as biases are concerned. Figure 5 shows the distribution of post-fit residuals that resulted from a combination of right ascension and declination rates

with declinations. It is clear that the residuals do not follow a normal distribution.

The large post-fit RMS residuals are a more significant indicator of errors. Indeed, the theory is not above suspicion either in that regard. A similar, but inverse, matching of theory with integration is reported by Lieske (1977a) in graphic form as a series of plots of cylindrical coordinate differences after fitting the theory to an integration. In fact, the discrepancies there were rather similar to those found in this investigation. The apparent biases in the coordinates ranged up to 3 km (4 times the arbitrary uncertainty), and the RMS up to 4 km. In the absence of real data of accuracy as fine as these differences it is impossible to distinguish conclusively the short-period accuracy of either theory or integration.

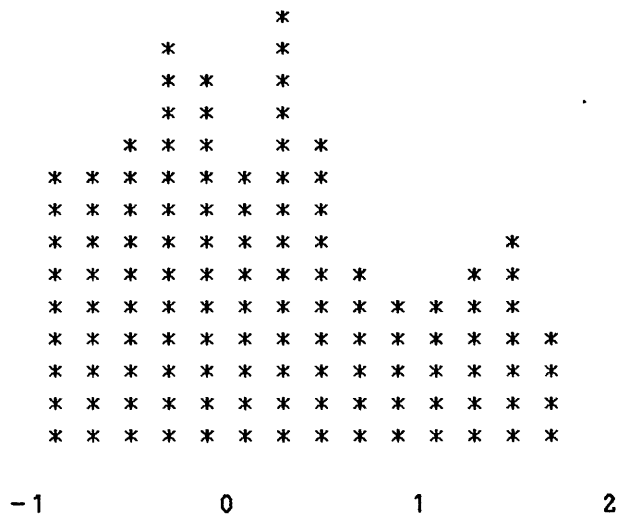

Normalized residual (declination)

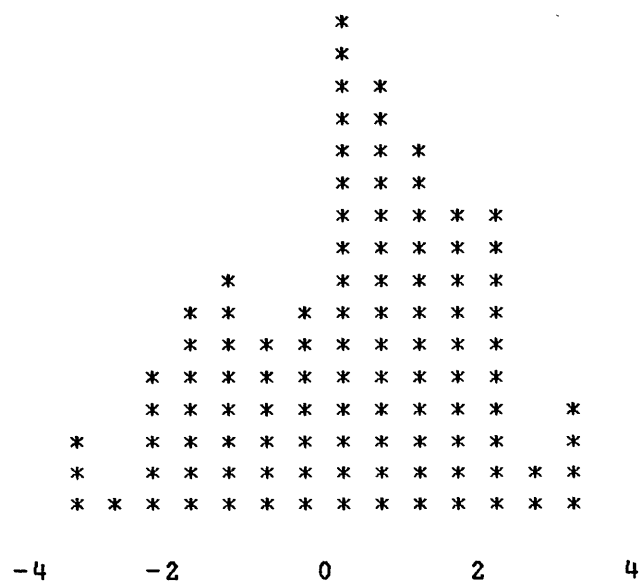

Normalized residual (declination rate)

Figure 5: Histograms of integration-theory residuals

Chapter VII

RESULTS

In essence, the process of numerical integration and least-squares parameter estimation consists of taking a set of basic input physical quantities and finding small corrections to those quantities. While the set of adjustments represents a best fit to the input observational data, the individual parameters may have widely varying uncertainties because of their different sensitivities to errors in the observations. Further, some pairs of parameters may be poorly resolved, even with an abundance of data, simply because the data may not provide enough information to break the near-degeneracies. Thus, the results of the fitting process consist of four sets of numbers, namely, the adjustments, the uncertainties, the cross-correlations, and the post-fit residuals. In addition, since the observations are not of uniform quality and the parameters not of uniform importance, the fitting may usefully be performed many times with different combinations of data and parameter subsets. The post-fit residuals from the final fit are presented in Appendix F.

7.1 DATA INCONSISTENCIES

In the course of the fitting, a relatively minor disagreement appeared between the radar and optical data. Table 9 shows the post-fit RMS residuals for the radar and principal optical data relative to the overall post-fit RMS for all data. As usual, the residuals have been normalized to the measurement errors. One must bear in mind that the radar figures represent only 29 measurements. Clearly, some allowances must be made for the "noisiness" inherent in such a small sampling of data, but the single entry that stands apart from the rest (and from the expected value of unity), Europa in 1975, represents three measurements and is, thus, no more noise-prone than the others. Further, one of the possible sources of error in the Doppler shifts, namely asymmetry in the reflection spectrum, was noticeably absent for that set of three observations. Besides, the formal errors from the spectrum template fits that gave the Doppler shifts were almost invariably much less than the reported two percent of the nominal limb-to-limb bandwidths of the radar echoes.

The radar observations are unique in that they measure velocities while all the other observables measure posi-

Table 9

Relative post-fit radar and optical residuals

Normalized post-fit residuals of radar and optical data from a fit to all data. The residuals are divided by the RMS normalized residual for the overall fit. An average of three measurements are represented by each radar entry.

Year	Io	Europa	Ganymede	Callisto
(radar AREC)				
1975	1.3	3.9	0.8	0.8
1976	2.1	2.1	0.6	0.9
1977	*	0.9	1.5	0.7
(optical LMCC)				
1975	1.0	1.3	1.1	0.9
1976	0.7	1.4	0.9	1.2
1977	0.7	1.6	0.7	0.5

* No observations available.

tions. Further, the combination of a very few, very precise measurements with many, less precise measurements leaves little room for direct comparison of the separate results because there are not enough radar observations to determine all the free parameters. The next best diagnostic device would be to vary the relative weights of the two kinds of data and examine the resulting post-fit residuals. Neither overweighting nor underweighting the radar observations

produced any systematic shifts in the post-fit radar residuals other than reducing or enlarging them, respectively. Further, the post-fit residuals for the optical observations showed no systematic changes at all.

7.2 ADJUSTMENTS TO PARAMETERS

Some of the parameters in the original set were excluded from adjustment because of insufficient resolution. Many of the parameters had strong cross-correlations, and if the data were not completely free of unmodeled biases, some of the "best" fit adjustments might be significantly in error. Indeed, we have seen that there are low-level disagreements among the data.

Along with the problem of correlations goes the question of parameter sensitivities. Some physical quantities were rejected in Chapter 4 as having no discernible effect on the satellite motions. In particular, the gravitational perturbations due to any bodies less massive than the Sun outside the Jovian system are marginal at best. Even within the system, only the central force and the perturbations of the Galilean satellites on each other are significant. Further, since the orbits are all nearly coplanar with Jupiter's equator, the effect of the zonal harmonic coefficients of

Jupiter's gravity field is essentially just the addition of some central force terms with non-inverse-square behavior. Since the orbits are all nearly circular, the effect is practically indistinguishable from a slight change in Jupiter's mass for any single satellite. It is only because there are four satellites that there is any sensitivity to the harmonic coefficients at all. Still, the outer satellites are so little affected by the gravity harmonics compared to Io that the separation of J(2) from the other harmonics by the different rates of falling off with distance from Jupiter is difficult. Indeed, the correlation between the adjustments to J(2) and J(4) when both were fitted amounted to about 92 percent. The value of J(3), which was assumed to be zero for the integrations, was also poorly determined for the same reason. The satellite radii were also adjustable through the effects they had on the mutual events, but the effects were not large. For example, a ten percent change in the radius of one of the satellites would make less than 0.2 second difference in the apparent mid-event time, and most of the events occurred fairly near opposition, where the effect vanished. Since the measurement errors were about one second or more, the adjustments to the radii would be subject to statistical buffeting from the errors.

To the remaining parameters from Tables 2 and 8 must be added the orbital elements of Jupiter and Earth to allow for ephemeris errors and a set of optical observation biases to allow for errors in the standard star catalogs used for the astrometric data. The final fits for all these parameters are presented in Table 10. All results are listed with their formal errors, which should be multiplied by the goodness-of-fit to make some allowance for the systematic errors. In this solution the overall normalized post-fit RMS residual, or goodness-of-fit, amounted to 1.36.

One interesting feature of the final parameter values is revealed by comparison with Table 1. The final masses are actually closer to de Sitter's 1931 determinations than to the Pioneer results that were used in the integrations. Since the Pioneer results were based on two separate flybys that gave fairly consistant values, it is difficult to explain the disagreement on the basis of ephemeris errors in the Pioneer processing. Jupiter's mass and J(2) in this fit are not significantly changed from the input values. However, a fit that allowed J(4) to vary as well as J(2) gave a solution for J(2) that agreed better with older determinations than with the Pioneer result. The uncertainty was, of course, larger because of the correlation with J(4),

Table 10

Final parameter values

a: Osculating elliptic elements referred to the 1950.0 frame. Periapse (π) is measured from node (Ω) and longitude (l) from periapse. The base epoch is J.D. 2441842.5 (see Table 8) Errors are given for the last place shown.

	Io	Europa	Ganymede	Callisto
a (10^{-3} AU)	2.82101±4	4.48682±7	7.1570±1	12.5860±2
e (10^{-3})	3.80±7	9.73±3	0.37±2	7.58±1
i (deg)	25.461±6	25.116±3	25.364±3	25.406±2
Ω (deg)	358.08±1	358.803±8	358.416±5	358.288±4
π (deg)	12.0±5	201.5±1	157.±1	333.50±7
l (deg)	255.6±5	303.4±1	17.±1	333.28±7

Planet epoch is J.D. 2440000.5

Jupiter: a=5.2029387±9 AU e=0.0481902±1 i=23.25312±1 °
Ω=3.26092±3 ° π=10.3750±1 ° l=141.1846±2 °

Earth-Moon: i=23.44371±6 ° Ω=5.7±2 x 10^{-5} °

b: Final adjusted masses and Jupiter J(2). (see Tables 1,2) To the precision given, M(J) is equivalent to Jupiter's mass for the values of M(1-4).

M(J)	1/1047.40±5 (M(S))
M(1)	3.94±24 (10^{-5} M(J))
M(2)	2.48± 3 (10^{-5} M(J))
M(3)	8.19±11 (10^{-5} M(J))
M(4)	5.30±17 (10^{-5} M(J))
Jupiter J(2)	0.014733±2

c: Equator-equinox corrections for optical observations (free parameters to allow for errors in the star catalog reference frames). Corrections coded by site.

Correction	LMCC 1975	LMCC 1976	LMCC 1977	MCDO
Δequinox (")	0.81±7	-1.41±34	-0.10±5	0.12±5
Δequator (")	4.20±62	-7.74±173	2.20±111	-1.46±41
Δlatitude (")	-0.66±19	6.15±140	-2.18±111	1.43±40

and, thus, the difference could not be taken as significant. In addition, the adjusted J(4) was roughly twice the value of older results, both from conventional methods and Pioneer reductions. Results from the Voyager spacecraft should help to resolve the discrepancies between the present work and the Pioneer determinations.

In all, twelve of the cross-correlations of the final fit were more than 99 percent, and the highest correlation (Ganymede periapse with Ganymede initial anomaly) was 99.999 percent. The high correlations between the periapsides and initial mean anomalies of the satellites stem from the fact that the eccentricities are all very low. Thus, the periapsides may be shifted by large amounts (with compensating changes for the mean anomalies to reflect the offsets of origin) without materially affect the osculating orbit. Concomitantly, the large uncertainties in all these elements of the orbits translate to small uncertainties in the actual satellite positions. The twelve largest correlations are as follows: $\pi(3)$ with $l(3)$, $\pi(1)$ with $l(1)$, LMCC 1976 Δequator with Δlatitude, LMCC 1977 Δequator with Δlatitude, $\pi(4)$ with $l(4)$, M(j) with a(1), M(J) with a(2), $\pi(2)$ with $l(2)$, LMCC 1976 Δequinox with Δequator, LMCC 1976 Δequinox with Δlatitude, MCDO Δequator with Δlatitude, and a(1) with a(2).

The optical observation bias model was designed for telescope mounting errors and could not be expected to duplicate exactly the type of errors present in a standard star catalog. However, catalog position determinations are relatively consistent locally to within the sort of rotation of coordinates represented by the latitude-equator-equinox corrections. Thus, since Jupiter moves rather slowly in apparent position in the sky, the catalog errors for astrometric observations within a short time period might be well modeled by a simple set of those corrections. So, the data from a single observatory during one opposition of Jupiter could reasonably be grouped together under a single set of corrections. Obviously, the number of bias parameters must remain small if the data are to yield information about the observed objects rather than just the observers. Still, the possibility of errors in the catalogs used in reducing the astrometric observations must be included in order to make a proper comparison between the radar and optical data. The values of the equator-equinox adjustments, however, should not be taken completely at face value. The equator and latitude corrections, especially, are strongly correlated, and the results from fitting are very sensitive to small errors in the data. Thus, it is not surprising that the correc-

tions are about an order of magnitude larger than the uncertainties in present star catalogs. In fact, the largest adjustments are paired opposite corrections for equator and latitude and, because of the high correlations, constitute very little change in the observation residuals. the sky, the residuals are not much affected.

7.3 CHECKING THE RESULTS

The question remained whether these results constitute an improvement in the knowledge of the Jovian system. That could be tested in two closely related ways. First, the post-fit residuals for the input observations could be compared with the corresponding residuals from Lieske's E1S2 theory. PEP could reprocess any and all of the input observations using the perturbing S-body tape for its ephemerides and derive residuals based on otherwise identical computations. The comparison was performed for the major portion of the data and the results are presented in Table 11. It is clear from the table that the post-fit residuals from the numerical analysis are significantly smaller than the theory-based residuals overall. In particular, the mutual events of 1973, which were included in the analysis that led to the E1S2 ephemeris as well as the present work, show con-

siderably smaller residuals with the numerical integration results. That is an important comparison because those data are, in fact, the only observations in common to the two systems of analysis. The straightforward comparison of residuals is actually not completely fair to the analytical theory because it was based on a much longer span of data than the numerical integration. Nevertheless, that is the only comparison possible. If the numerical results were not, in fact, better for the data used in this work, the entire method would be of little value.

The detailed comparison between the final results from the integration and Lieske's theory could be more easily investigated by using "dummy" observations at regular intervals. A series of round-trip delays between the centers of Io and Jupiter was generated at five-minute intervals over a period of five days using the theory tape. These were then reprocessed using an Io ephemeris differentially adjusted from the integration. The adjustment was carried out by an enhanced version of CPLNTM, the integration tape copier (see Chapter 3). Since the integration tapes contained partial derivatives of the positions and velocities with respect to all of the parameters that affected the individual body motions, the parameter adjustments could be applied linearly

Table 11

Comparison of data residuals

The RMS residuals for the mutual event observations and for the major optical and radar data are presented both from E1S2 and from this work post-fit. The residuals are normalized by the measurement errors.

YEAR	RMS: E1S2,POST-FIT			
	Io	Europa	Ganymede	Callisto
Radar (AREC)				
1975	1.6,1.6	4.8,5.1	1.2,1.1	2.0,1.1
1976	2.4,2.7	2.7,2.8	0.8,0.8	2.6,1.2
1977	*	1.4,1.2	1.7,2.0	2.9,0.9
Optical (LMCC)				
1975	4.2,1.3	3.3,1.7	4.1,1.5	3.7,1.2
1976	2.1,1.0	2.3,1.8	1.1,1.2	3.8,1.6
1977	2.0,1.0	2.1,2.2	2.5,1.0	2.1,0.6
Mutual Events				
1973	(all bodies)	4.5,1.9		

* No data available

to make a corrected pseudo-integration analogous to the predicted observation libraries from PEP. This feature of CPLNTM was, in fact, tested by using its pseudo-integration output as ephemerides in computing observation residuals and comparing these with the corresponding predicted residuals from the same parameter adjustments.

In any case, the "dummy" delays represented very nearly twice the radial distances of Io from Jupiter, and the residuals, therefore, gave a good indication of the differences between the numerical and analytical radius vectors. The RMS of these residuals was 1.9×10^{-4} light second, which corresponds to 44 km in one-way distance, and the average of the residuals was 1.7×10^{-5} light second, or 3 km one-way. The residuals themselves showed essentially a sinusoidal variation with Io's orbital period. The detailed behavior of this variation was examined by Fourier transforming the residuals over double the orbital period. Table 12 shows a portion of this power spectrum in the residuals covering 3.5 days.

The peak at zero frequency represents the non-zero mean residual but is not really significant because the mean is not much more than the expected mean of 1.5 km based on the number of points averaged. The secondary peak between 21- and 17-hour period is also of little interest because it represents just about half the orbital period of Io. The 44 km RMS difference between the numerical predictions and Lieske's theory is certainly much larger than the intended accuracy of ±1 km of the theory, but it is much smaller than the uncertainties of the bulk of the measurements that went

Table 12

Power spectrum of numerical-analytical residuals

512 "dummy" points at ten-minute intervals were Fourier transformed to yield a power spectrum for a period of 3.5 days. The first ten frequencies contain essentially all the information. The peak represents Io's orbital period.

Period d	h	m	Freq. (c/d)	Power
-	-	-	0.0	7.70141×10^{-7}
3	13	20	0.28	7.64063×10^{-9}
1	18	40	0.56	2.27387×10^{-5}
1	4	27	0.84	3.57051×10^{-10}
0	21	20	1.13	4.45219×10^{-9}
0	17	4	1.41	9.33417×10^{-9}
0	14	13	1.69	4.19782×10^{-10}
0	12	11	1.97	3.16197×10^{-10}
0	10	40	2.25	1.86754×10^{-10}
0	9	29	2.53	4.30256×10^{-11}

into these parameter adjustments (or any analytical theory, for that matter). Again, the discrepancies can not be finally resolved without much more precise observational data.

7.4 EXTRAPOLATION TO LATER EPOCHS

Another way of testing the results of this investigation is to extend the time span and attempt to predict later ob-

servations. Ideally, the best-fit parameter adjustments would be applied, and the entire integration would be redone with partial derivatives over the longer span. That, of course, would require a major infusion of computer time, and a much cheaper approach would be to extend the integration as it is, without partials. That, however, would fail to take advantage of the parameter adjustments and would entirely miss the point of testing. The next easiest approach would be to propagate the differential corrections to the positions and velocities through to the end of the integration span and then continue the integrations or to extend the present integrations with partial derivatives and then apply the differential corrections from the parameter fitting. To the extent that the corrections fall within the linear regime of least-squares adjustment, the two methods should be equivalent. The second would require more computation than simply integrating the motions, but it would provide results that are directly comparable to the post-fit residuals of the input observations. Indeed, if enough new observations became available beyond the original time span, the extension of the integrations would be desirable for including the new observations in a new overall fit.

The second method (that is, integrating and then adjusting) has been tested for a set of radar observations taken in February of 1979. Three Doppler shift measurements of Callisto taken at Arecibo Observatory (Ostro, 1979) were used as the test of accuracy, and the RMS normalized residual amounted to 1.9, which is comparable to the post-fit residuals for radar observations that actually were included in the fit. Indeed, the predictions were better than those of Lieske's theory, which yielded an RMS of 2.6. This provides the best confirmation available of the validity of the numerical integrations. Actually, one would expect from Table 11 that the Lieske-theory residuals for the other satellites might be smaller than those for Callisto, but this case by itself is sufficient to confirm the extensibility of the integrations.

7.5 FUTURE WORK

Now that the feasibility of numerical integration has been demonstrated for the Galilean satellites for a five-year time span, it is clear that further improvements in the ephemerides may be obtained through extension of the integrations and inclusion of more data, especially the highly accurate radar observations, beginning with those of 1979.

Although no radar range measurements are currently available, they may be so as early as the next opposition. With continued improvement in radar system sensitivity the radar should make an increasingly important contribution to the study of the satellite motions.

The power of the numerical integration technique remains in short, connected spans of data, and the combination of diverse data types must continue to be the rule. In the long run, the cost of computing will undoubtedly continue to fall, and it seems likely, then, that longer and longer integrations will become practical. It is especially important that the satellite mass determinations be re-examined because of the disagreement between these new values and the best previous results. Aside from the knowledge of the satellite motions and further refinement of the mass determinations, there is one other important contribution to be made by continued application of this technique, namely, the improvement of the ephemerides of Jupiter itself. The present investigation covered less than half of an orbital period of Jupiter, and that limited the resolution in the adjustments to Jupiter's orbital elements. Longer time spans should improve the determinations.

Relative photographic position measurements were not incorporated in the present work, but the bulk of the development and coding necessary for PEP to process such observations was carried out in anticipation of including them in the future (see Appendix E). The addition of relative positions may make a significant contribution to the results because of the large number of (as yet unpublished) data (Pascu, 1977).

Appendix A

ROTATION MATRIX FOR BODY-FIXED COORDINATES

To a good approximation any planet rotation can be expressed as a uniform rotation about a very slowly precessing axis. In the short run, then, the axis may be treated as fixed. In Figure 6 the (z^1,z^2,z^3) frame is any fixed inertial reference frame while (x^1,x^2,x^3) are the rotating body-fixed axes. Without loss of generality we may let x^3 be the fixed rotation axis and let x^1 and x^2 rotate about it in a counter-clockwise sense. Thus, we have $\phi = \phi(0)+\omega t$, where ω is the constant rotation rate. Further α and δ are the polar coordinates of x^3 in the (z^1,z^2,z^3) frame.

Clearly, the (z) axes can be obtained by three compounded rotations of the (x) axes, (a) by $-\phi$ about x^3 to give the intermediate axes (u^1,u^2,x^3), (b) by $\delta-\pi/2$ about u^1 to give (u^1,v^2,z^3), and, (c) by $3\pi/2-\alpha$ about z^3 to give (z^1,z^2,z^3). The mathematical representation of these transformations is as follows.

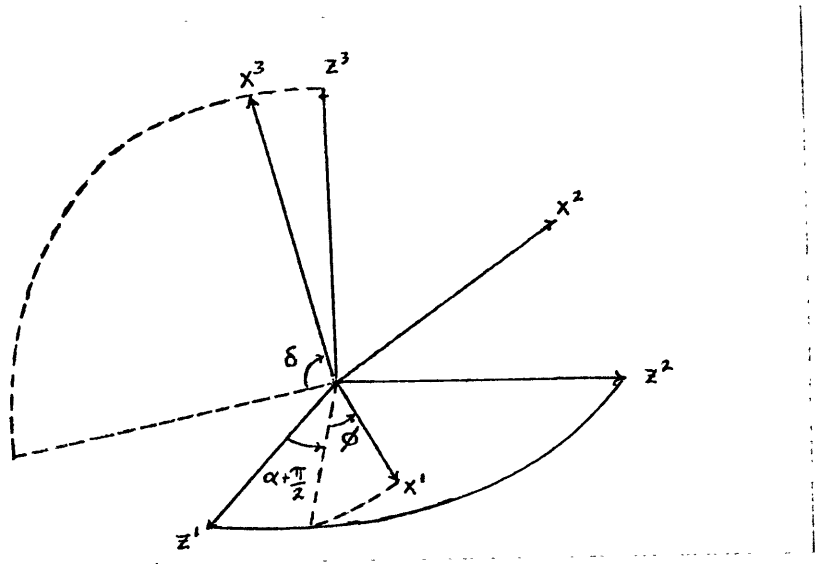

Figure 6: Relationship of body-fixed and inertial frames

$$
\begin{aligned}
&\text{a)} \quad u^1 = x^1\cos\phi - x^2\sin\phi \\
&\qquad\;\; u^2 = x^1\sin\phi + x^2\cos\phi \\
&\text{b)} \quad v^2 = u^2\sin\delta - x^3\cos\delta \\
&\qquad\;\; z^3 = u^2\cos\delta + x^3\sin\delta \\
&\text{c)} \quad z^1 = -u^1\sin\alpha - v^2\cos\alpha \\
&\qquad\;\; z^2 = u^1\cos\alpha - v^2\sin\alpha
\end{aligned}
\tag{A-1}
$$

The reverse transformations are similar.

$$
\begin{aligned}
&\text{a)} \quad x^1 = u^1\cos\phi + u^2\sin\phi \\
&\qquad\;\; x^2 = -u^1\sin\phi + u^2\cos\phi \\
&\text{b)} \quad u^2 = v^2\sin\delta + z^3\cos\delta \\
&\qquad\;\; x^3 = -v^2\cos\delta + z^3\sin\delta \\
&\text{c)} \quad u^1 = -z^1\sin\alpha + z^2\cos\alpha \\
&\qquad\;\; v^2 = -z^1\cos\alpha - z^2\sin\alpha
\end{aligned}
\tag{A-2}
$$

Thus, the composite rotation may be expressed in terms of the three angles.

$$
\begin{aligned}
z^1 &= x^1(-\cos\phi \sin\alpha - \sin\phi \cos\alpha \sin\delta) \\
&\quad +x^2(\sin\phi \sin\alpha - \cos\phi \cos\alpha \sin\delta) \\
&\quad +x^3(\cos\alpha \cos\delta) \\
z^2 &= x^1(\cos\phi \cos\alpha - \sin\phi \sin\alpha \sin\delta) \\
&\quad +x^2(-\sin\phi \cos\alpha - \cos\phi \sin\alpha \sin\delta) \\
&\quad +x^3(\sin\alpha \cos\delta) \\
z^3 &= x^1(\sin\phi \cos\delta) \\
&\quad +x^2(\cos\phi \cos\delta) \\
&\quad +x^3(\sin\delta)
\end{aligned}
\tag{A-3}
$$

Again, the inverse is similar; indeed, the inverse of any rotation matrix is just its transpose. Thus, we have

$$
\begin{aligned}
x^1 &= z^1(-\cos\phi \sin\alpha - \sin\phi \cos\alpha \sin\delta) \\
&\quad +z^2(\cos\phi \cos\alpha - \sin\phi \sin\alpha \sin\delta) \\
&\quad +z^3(\sin\phi \cos\delta) \\
x^2 &= z^2(\sin\phi \sin\alpha - \cos\phi \cos\alpha \sin\delta) \\
&\quad +z^2(-\sin\phi \cos\alpha - \cos\phi \sin\alpha \sin\delta) \\
&\quad +z^2(\cos\phi \cos\delta) \\
x^3 &= z^3(\cos\alpha \cos\delta) \\
&\quad +z^3(\sin\alpha \cos\delta) \\
&\quad +z^3(\sin\delta)
\end{aligned}
\tag{A-4}
$$

Appendix B

EXTENSION OF NORMAL EQUATION ERROR STATISTICS IN PEP

The following is a memorandum written and distributed by the author to the other users of the Planetary Ephemeris Program (PEP) on July 17, 1978. It refers to three other memoranda that had been distributed to the same group by R.D. Reasenberg. The notation differs from that of the main body of this thesis in that vectors are not underscored, but rather treated as n-by-1 matrices. Also, the prime added to a variable does not indicate differentiation, but rather denotes the best-fit value of the variable from the solution of the normal equations. The transpose of any matrix x is denoted by x^+.

References:

1. Reasenberg, R.D. (1974). on "Convergence Indicator in PEP", PEP Memo 74-1 (1974 Jan 24).
2. ---------- (1975a). on "The PEP A Priori Facility", PEP Memo 75-2 (1975 Jul 28.

3. ---------- (1975b). on "Partial Prereduction of the Normal Equations", PEP Memo 75-3 (1975 Jul 29).

At present, the formation or restoration of normal equations for parameter estimation in PEP produces an n-by-n coefficient matrix B, an n-vector right-hand side u, and the sum, sum absolute and sum-squared weighted residuals. These are sufficient for solving for adjustments to parameters and predicting the post-fit sum-squared and, thus, also the root-mean-squared (RMS) weighted residuals, but not for predicting the post-fit sum or sum absolute weighted residuals. Indeed, the sum of absolute values of the residuals after fitting (or before, for that matter) can be found only by going thfough the observations one by one. However, the sum of weighted residuals is a simple linear combination of observables and computed values and the post-fit sum can be predicted by applying a correction to the prefit sum.

Let us begin with a brief development of the least-squares estimation technique. Consider a set of observations represented as an m-vector z with associated errors ν. Suppose we have a set of parameters α such that we can com-

pute the theoretical values $H(\alpha)$ for the observations, given the nominal values α_0. A convenient approach is to form differenced variables based on the nominal parameter values as follows.

$$
\begin{aligned}
x &= \alpha - \alpha_0 \\
y &= z - H(\alpha_0) \\
A &= \partial H / \partial \alpha \\
R &= \langle \nu \nu^+ \rangle \\
W &= R^{-1}
\end{aligned}
\tag{B-1}
$$

In general, the error cross correlation matrix R must be used for a maximum likelihood estimation of parameter adjustments x. In practice, however, the errors are assumed uncorrelated -- if necessary, they are made so by modeling observation biases in $H(\alpha)$. Thus, both R and W are diagonal, and the least-squares fit is maximum likelihood. First, we linearize the problem by expanding to first order about α_0 and express the sum-squared weighted residuals in terms of x and y.

$$
\begin{aligned}
z - H(\alpha) &= y - Ax \\
S(x) &= (y-Ax)^+ W (y-Ax) \\
&= y^+ W y - 2x^+ A^+ W y + x^+ A^+ W A x
\end{aligned}
\tag{B-2}
$$

The least-squares solution x' is given by

$$\partial S(x)/\partial x = 0 \quad (\text{for } x=x')$$

$$A^{+}WAx' = A^{+}Wy \tag{B-3}$$

$$Bx' = u$$

where $B = A^{+}WA$ and $u = A^{+}Wy$. Thus, the best-fit parameter values are

$$\alpha' = \alpha_0 + x' \tag{B-4}$$

$$= \alpha_0 + B^{-1}u$$

and the post-fit residuals are

$$y' = z - H(\alpha') \tag{B-5}$$

$$= y - Ax'$$

The pre- and post-fit sum-squared weighted residuals are $S(0)$ and $S(x')$, and we find, by substituting into equation (B-2)

$$S(0) = y^{+}Wy \tag{B-6}$$

$$S(x') = S(0) - x'^{+}u$$

Note that $x'^{+}u$ is just the norm-square (N^2) of the adjustment as derived in Reference 1.

Now we turn to the sum of weighted residuals and define the corresponding quantities analogous to equation (B-2).

$$G(x) = (y-Ax)^{+}\omega \qquad \text{(B-7)}$$

$$k = A^{+}\omega$$

where ω is the vector of the reciprocals of the errors ν. In terms of the generalized maximum likelihood weighting matrix W, ω could be expressed as a projection into a vector of the square-root of W, but this reduces to just the reciprocal errors for the individual observations for uncorrelated errors. The vector k is, thus, a weighted sensitivity vector, that is, a weighted projection of the partial derivative matrix. Substituting into equation (B-7) we find the pre- and post-fit sums.

$$G(0) = y^{+}\omega \qquad \text{(B-8)}$$

$$G(x') = G(0) - x'^{+}k$$

The realization of the prediction of post-fit average weighted residuals, then, requires only the accumulation of the vector k, quite analogously with the right-hand side u. In particular, we note that k may be considered as extended with arbitrarily many zeroes for parameters that have no effect on the observations. Further, we may combine observation sets directly by just adding the k vectors componentwise. Consider two sets of data (1) and (2) already

processed separately. Each has a saved set of quantities B, u, S(0), G(0), and k, but, of course, the original solutions involved separate y, A, W, and ω. Now,

$$y = \begin{pmatrix} y_1 \\ y_2 \end{pmatrix}, \qquad A = \begin{pmatrix} A_1 \\ A_2 \end{pmatrix}$$

$$W = \begin{pmatrix} W_1 & 0 \\ 0 & W_2 \end{pmatrix}, \qquad \omega = \begin{pmatrix} \omega_1 \\ \omega_2 \end{pmatrix} \tag{B-9}$$

So, we get

$$\begin{aligned} G(0) &= y_1{}^t\omega_1 + y_2{}^t\omega_2 \\ &= G_1(0) + G_2(0) \\ k &= A_1{}^t\omega_1 + A_2{}^t\omega_2 \\ &= k_1 + k_2 \end{aligned} \tag{B-10}$$

and $G(x') = G(0) - x'^t k$ in just the same way as before.

PEP parameter estimation has a number of features which depart from the straightforward solution via equations (B-1) to (B-4), notably the inclusion of a priori information in the normal equations (see Reference 2). A priori input unfortunately destroys the simplicity of predicting post-fit RMS residuals. If we let (d) represent the data portions and (a) represent the a priori, we have

$$
\begin{aligned}
B &= B(d) + B(a) \\
u &= u(d) + u(a) \\
u(a) &= B(a)x(a) \qquad\qquad (B\text{-}11) \\
x(a) &= \alpha(a)-\alpha_0 \\
x &= [B(a)+B(d)]^{-1}[u(a)+u(d)]
\end{aligned}
$$

Further, we have

$$
\begin{aligned}
S(x') &= y^{+}Wy - 2x'^{+}A^{+}Wy + x'^{+}A^{+}WAx' \\
&= S(0) - 2x'^{+}u(d) + x'^{+}B(d)x' \\
&= S(0) - N^2 + x'^{+}[2u(a)-B(a)x'] \qquad\qquad (B\text{-}12) \\
&= S(0) - N^2 + x'^{+}B(a)[2x(a)-x']
\end{aligned}
$$

However, since k is unaffected by a priori information and G is linear in x, no such problem exists for predicting average residuals.

The partitioning of the parameter set α for partial prereduction of the equations (see Reference 3) likewise presents no difficulty. The technique is primarily a computational shortcut. In brief, a sub-matrix of B for part of the parameters is inverted once, and the solution is applied to the remainder of the elements of B and u to produce a smaller set of normal equations for the remaining parameters. The vector k is simply an n-vector of sensitivities

and may be partitioned in the same way as u. Thus, the saved sum of reduced residuals can formed analogously with the reduced sum-squared residuals. Let

$$u = \begin{pmatrix} u_1 \\ u_2 \end{pmatrix}, \quad B = \begin{pmatrix} C & F \\ F^+ & D \end{pmatrix}$$

$$x = \begin{pmatrix} x_1 \\ x_2 \end{pmatrix} \tag{B-13}$$

Then we get

$$\begin{aligned} u_1 &= Cx_1' + Fx_2' \\ u_2 &= F^+x_1' + Dx_2' \\ x_2' &= D^{-1}(u_2 - F^+x_1') \end{aligned} \tag{B-14}$$

The reduced normal equations appear as

$$\underline{u}_1 = \underline{C}x_1' \tag{B-15}$$

where

$$\begin{aligned} \underline{u}_1 &= u_1 - FD^{-1}u_2 \\ \underline{C} &= C - FD^{-1}F^+ \end{aligned} \tag{B-16}$$

Examining the sum-squared residuals, we find

$$\begin{aligned} S(x') &= S(0) - x_1'^+u_1 - x_2'^+u_2 \\ &= S(0) - \underline{x}_2^+u_2 - x_1'^+\underline{u}_1 \end{aligned} \tag{B-17}$$

where $\underline{x}_2 = D^{-1}u_2$. Thus, we may define a reduced sum-squared quantity

$$\underline{S}(x_1) = S(0) - \underline{x}_2{}^+u_2 \tag{B-18}$$

The sum of residuals yields a similar result.

$$\begin{aligned} G(x') &= G(0) - x_1'^+k_1 - x_2'^+k_2 \\ &= G(0) - u_2{}^+D^{-1}k_2 + x'^+D^{-1}k_2 - x_1'^+k_1 \\ &= \underline{G}(0) - x'_1{}^+\underline{k}_1 \end{aligned} \tag{B-19}$$

where

$$\underline{k}_1 = k_1 - FD^{-1}k_2 \tag{B-20}$$

$$\underline{G}(x_1) = G(0) - \underline{x}_2{}^+k_2$$

In some applications it may be desirable to transform the normal equations by changing the nominal parameter values α_0 (for example, to add two sets of equations with different nominals). The procedure bears some similarity to the inclusion of a priori parameter estimates in that the right-hand side u must be adjusted by $-B\Delta\alpha_0$. At the same time the error statistics must also be adjusted to reflect the new computed values of observations.

$$y^* = y - A\Delta\alpha_0 \qquad \text{(B-21)}$$

$$u^* = u - B\Delta\alpha_0$$

First, we have the sum-squared residuals

$$S^*(x) = S(x+\Delta\alpha_0)$$

$$\begin{aligned} S^*(0) &= S(0) - 2\Delta\alpha_0{}^+A^+Wy + \Delta\alpha_0{}^+A^+WA\Delta\alpha_0 \\ &= S(0) - 2\Delta\alpha_0{}^+u + \Delta\alpha_0{}^+B\Delta\alpha_0 \qquad \text{(B-22)} \\ &= S(0) - \Delta\alpha_0{}^+[u+u^*] \end{aligned}$$

Then, the summed residuals become

$$G^*(x) = G(x+\Delta\alpha_0) \qquad \text{(B-23)}$$

$$G^*(0) = G(0) - \Delta\alpha_0{}^+k$$

We have seen that the maintenance of the sensitivity vector k can be accomplished with a relatively simple set of operations and, further, that it is <u>necessary</u> for the proper handling of error statistics in nominal value shifting. The implementation of this feature will make possible the prediction of post-fit average weighted residuals without predicting the residuals themselves.

Appendix C

S-BODY TAPE FORMAT

Record 1: Title, 128 bytes. Consists of the 8-character type descriptor " S-BODY " and 120 characters of arbitrary description.

Record 2: Header information, variable length. 276+116n bytes, where n is the number of bodies represented.

Name	Offset	Length	Meaning
NAST	0	2	Number of bodies
NPL(n)	2	n*2	Body number for each.
NCP(n)	2n+2	n*2	Central body number for each.
INT(n)	4n+2	n*2	Tabular interval for each. (=INT if >0, 2**INT if <0)
JD1	6n+2	4	Julian day, beginning of tape
JD2	6n+6	4	Julian day, end of tape
JD0(n)	6n+10	n*4	Julian day number for initial conditions for each.
BETA(6,n)	10n+10	n*6*8	Initial condition for each.
NAME(6,n)	58n+10	n*6*4	24-byte name for each.
NA1	82n+10	2	Number with min. interval.
NA4	82n+12	2	Number with 4 times min.
NA8	82n+14	2	Number with 8 times min.
INTR	82n+16	4	Min. interval (see INT).

RSRV	82n+20	96	Reserved integration flags.
MASS1(n)	82n+116	n*8	Mass for each (Sun=1.).
RELFT(n)	90n+116	n*8	Relativity motion factor.
RSRV	98n+116	160	Reserved integration flags.
ICND(n)	98n+276	n*2	Kind of I.C. for each.
MASSC(n)	100n+276	n*8	Mass of primary for each.
FR0(n)	108n+276	n*8	Fraction of day past JD0 for each.

Subsequent records: Data, variable length. Each record spans 40 times the minimum tabular interval and is labeled with the time of its first point. The coordinates are grouped by point and then by body. The length depends on the number of coordinates included for each class of body specified on each record: 24 + 8*(max(1,NA1*40*IVL1) + max(1,NA4*10*IVL4) + max(1,NA8*5*IVL8))

Name	Offset	Length	Meaning
JD	0	4	Julian day number.
FR	4	8	Fraction of day past JD.
IVL1	12	4	Number of coordinates per body for min. int (3 or 6).
IVL4	16	4	Number per body for 4 times min.
IVL8	20	4	Number per body for 8 times min.
BODY	24		Coordinates

Appendix D

STELLAR OCCULTATIONS

Let us consider the occultation of a star by a relatively nearby object. We will assume that the star's position is fixed and known relative to the Sun. For our purposes, a star is fixed if its apparent angular velocity as seen from Earth is negligible compared to that of the occulting body. This angular velocity is not just the star's proper motion, of course, but includes the parallax effect due to Earth's orbital motion. Here we note that even Pluto, the most sluggish of planets, appears to move about seventy arc seconds per day while stars move only a few arc seconds per year at most. Similarly, stars are so far away that they appear as essentially point sources. This is not strictly true for occultations by bodies in the outer solar system, since stellar images may be as much as .01 second of arc in diameter, and the corresponding time needed for Pluto to cover such a disk would be about twelve seconds. Even Jupiter would take more than one second to occult such a star. However, the Moon would occult any star in much less than a

second. Thus the light cutoff at occultation appears to be instantaneous in the case of the Moon, especially since the Moon has no atmosphere. For other occulting bodies, the situation may be more complicated, but we will assume some light-curve fitting may be done to obtain the time of immersion or emersion. Thus, we will consider occultations (both immersions and emersions) as instantaneous phenomena.

Now we set up t3 as the coordinate time when the occultation event is observed on Earth and t2 as the time when the observed light ray grazes the occulter. We have the polar coordinates of the star (R,α,δ) with respect to the Sun, and we may define the unit vector from the Sun toward the star in a fixed reference frame, such as the 1950.0 mean equator-equinox system with origin at the solar system barycenter. Figure 7 shows the geometry of a stellar occultation.

$$\underline{u}(s) = \begin{pmatrix} \cos\delta\cos\alpha \\ \cos\delta\sin\alpha \\ \sin\delta \end{pmatrix} \qquad \text{(D-1)}$$

The observer is labeled with the position vector $\underline{o}(t3)$, and the corresponding unit vector $\underline{u}(o,t3)$ from the observer to the star may also be treated as a constant.

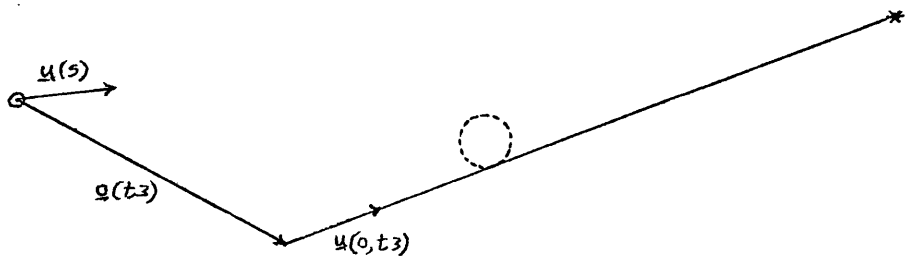

Figure 7: Stellar occultation geometry

$$\underline{R}^*(t3) = R\underline{u}(s) - \underline{o}(t3)$$

$$\underline{u}(o,t3) = \underline{R}^*(t3)/R^*(t3) \qquad \text{(D-2)}$$

$$= \underline{u}(s)-\underline{o}(t3)/R+\underline{u}(s)(\underline{u}(s)\cdot\underline{o}(t3)/R)+ \ . \ . \ .$$

Here the higher order terms in $\underline{o}/R$ amount to no more than about 10^{-12} for a typical star.

Next we define the position of the occulter $\underline{a}(t2)$. Let us now consider the geometry of a simple case, namely that of a spherical occulter. Here the spatial coordinates of the observer, the center of the occulter, and the point of grazing tangency on the occulter form a right triangle, and the mathematical description is very straightforward, as can be seen in Figure 8.

However, since the bodies we will need to deal with are not exactly spherical, we must modify this simple picture to something like Figure 9. A perpendicular to the light ray

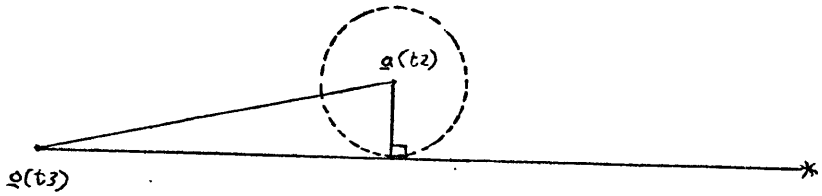

Figure 8: Spherical occulter

at the point of grazing tangency does not necessarily pass through the center of figure (or mass) of the occulter. Therefore, let us retain as much as possible of the simple picture and define the vector h(t3) as the perpendicular from the occulter's center of mass to the path of the light ray that reaches the observer at epoch t3.

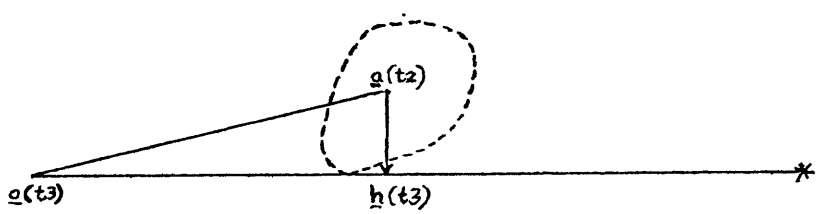

Figure 9: Non-spherical occulter

Next we define the vector from the observer to the center of the occulter

$$\underline{r}(t3) = \underline{a}(t2)-\underline{o}(t3) \qquad \text{(D-3)}$$

Clearly, the propagation distance from the point of tangency to the observer is nearly the same as from the occulter's center, provided that the occulter is relatively small or distant:

$$|\underline{r}+\underline{h}| = r(1-h^2/2r^2) \qquad \text{(D-4)}$$

so we have approximately

$$t2 = t3 - r(t3)/c \qquad \text{(D-5)}$$

In the case of the Moon this approximation is in error by about 13 microseconds, which corresponds to less than one centimeter difference in the Moon's position. In other cases the differences are even smaller. At this point we must consider the limits of observation - timing measurements for occultations can not realistically be made with precisions better than a millisecond. Thus, we may use equation (D-5) as our basis of relating t2 to t3.

With this in mind we may now generalize all the time arguments for the vectors we have defined. Let t be any time near the epoch of interest t3. Then we get a recursive definition to replace equation (D-3).

$$\underline{r}(t) = \underline{a}(t-r(t)/c) - \underline{o}(t) \qquad \text{(D-6)}$$

Also, $\underline{h}(t)$ may be defined as the perpendicular vector from $\underline{a}(t-r(t)/c)$ to the light ray path that reaches $\underline{o}(t)$. Clearly, this is consistent with our definition of $\underline{h}(t3)$ although the light ray in question grazes the occulting body only for t=t3. At any other epoch the length h(t) is different from the apparent radius of the occulter. Let us, therefore, define a new quantity $\rho(t)$ as follows. We construct a line tangent to the occulter's surface (at epoch t-r/c) and in the plane containing $\underline{h}(t)$ and $\underline{r}(t)$. This line must intersect the vector $\underline{h}(t)$, and we may define $\rho(t)$ as the distance along $\underline{h}(t)$ to the point of intersection. Thus, $\rho(t)$ is the effective radius for the occulting body. With this definition it is easy to see that the magnitude $h(t3)=\rho(t3)$ for a spherical body is exactly the body's radius.

Now we return to the geometric description of an observation at time t near t3. Our right triangle gives us

$$r^2(t) = C^2(t)+h^2(t) \qquad \text{(D-7)}$$

where $C(t) = \underline{r}(t)\cdot\underline{u}(o,t)$. Note again that the unit vector $\underline{u}(o,t)$ may be treated essentially as a constant. Even

though it is not, its variation is due to changes in small correction terms, namely the Earth parallax and, in some cases, the gravitational light bending, which we will discuss later. If this derivation were applied to occultations of satellites or other nearby objects, then $\underline{u}(o,t)$ could no longer be treated as a constant. In any case, Figure 10 shows this geometry, which forms the basis of a method of finding the time of occultation.

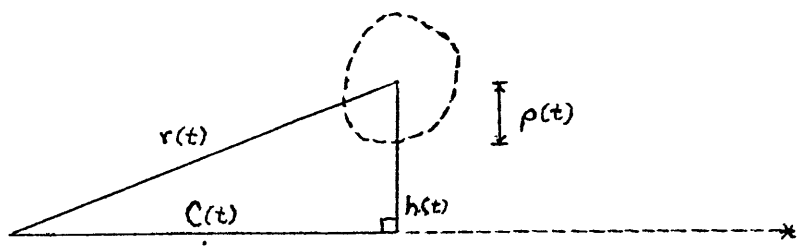

Figure 10: Near occultation

Generalization of the geometry of an impending or just past occultation showing an obvious method for computing the event time.

We may characterize the instant of occultation by defining a function

$$F(t) = [r^2(t)-C^2(t)]^{0.5} - \rho(t) \qquad \text{(D-8)}$$

that vanishes at t=t3. Thus, if we specify $\underline{r}(t)$ and start with a reasonable first estimate of t3, say $t3^{(0)}$, we may apply Newton's method for extracting roots to compute the theoretical time of the event. The procedure is as follows. We begin with $t3^{(0)}$, which may be, for example, the observed time of the occultation. We get $t2^{(0)}$ from equation (D-5), and we can now evaluate $F(t3^{(0)})$ and its time derivative F'. It will prove useful to derive the general partial derivative $\partial F/\partial p$, where p is any parameter. Thus, we have

$$\begin{aligned}\partial F/\partial p &= [\underline{r}(t)\cdot\partial\underline{r}(t)/\partial p - C(t)\underline{u}(o,t)\cdot\partial\underline{r}(t)/\partial p \\ &\quad - C(t)\underline{r}(t)\cdot\partial\underline{u}(o,t)/\partial p]/[r^2(t)-C^2(t)]^{0.5} \\ &\quad - \partial\rho(t)/\partial p \qquad\qquad (D\text{-}9) \\ &= -\underline{u}(\underline{h},t)\cdot\partial\underline{r}(t)/\partial p - \partial\rho(t)/\partial p \\ &\quad - C(t)\underline{r}(t)\cdot\underline{P}(\underline{R}^*,\partial\underline{R}^*/\partial p)\end{aligned}$$

The time derivative is just a special case of equation (D-9), and the physical interpretation is quite straightforward. The value of F' is just the component of the relative motion of the occulter perpendicular to the observer's line of sight (with a very small correction due to the changing apparent radius as a result of any non-sphericity of the occulter).

$$F' = -\underline{u}(\underline{h},t)\cdot\underline{r}'(t)-\rho'(t)$$
$$-C(t)\underline{R}^{*\prime}\cdot\underline{P}(\underline{R}^*,\underline{r}(t)) \qquad \text{(D-10)}$$

With the values of $F(t3^{(0)})$ and $F'(t3^{(0)})$ we may form a next estimate of the value of t3, namely,

$$t3^{(1)}=t3^{(0)}-F(t3^{(0)})/[F'(t3^{(0)})] \qquad \text{(D-11)}$$

At this point we re-enter the loop and find successive approximations $t3^{(2)}$, and so on until we reach some convergence criterion. For example, we might stop when the adjustment from one approximation to the next is less than a predetermined accuracy constant.

For least-squares error analysis we need to be able to form the partial derivatives of the computed time t3 with respect to any of the set of relevant parameters. Here we find another use for equation (D-9). Since F(t3)=0 to our desired accuracy, we may use implicit differentiation through F to get the partial derivatives of t3 with respect to any parameter entering into F.

$$\partial t3/\partial p = -(\partial F/\partial p) \;/\; F' \qquad \text{(D-12)}$$

Clearly, any parameter not entering into F, either explicitly or implicitly, can have no effect on t3.

Before we leave the topic, we should consider the effects of general relativity theory on this (so far) purely Newtonian discussion. There are two primary effects due to the passage of the light ray near to the occulting body, first, the gravitational deflection of the ray and, second, the propagation time correction. Both corrections are small and easily made. In the limiting case of infinitely distant bodies the bending angle is given by $B = 4G\ m/c^2h$, where m is the mass of the occulting body. For nearby objects the angle is actually smaller, being given by the formula $B = 2G\ m/c^2r \tan \theta/2$, where θ is the angle between the star and the observer as seen from the occulter's center. For an infinitely distant star this becomes just the same as the old formula, and even for a nearby object viewed close to the occulter's limb the old expression needs only to be multiplied by the ratio between the distances from the object to the occulter and observer. Thus, we must add a small term to the unit vector $\underline{u}(o)$ to obtain the corrected direction of the star

$$\underline{u}(o) \rightarrow \underline{u}(o)\cos B + \underline{u}(\underline{h})\sin B \qquad \text{(D-13)}$$

However, since B is so small (in the case of the Moon B is about 10^{-10} radian), cos B and sin B are negligibly differ-

ent from unity and B, respectively. Thus, we may in practice use an approximation for $\underline{u}(o)$

$$\underline{u}(o) \rightarrow \underline{u}(o)+\underline{u}(\underline{h})B \qquad \text{(D-14)}$$

Indeed, for the Moon this correction amounts to only 50 microseconds in the time of occultation and can be neglected altogether. For the major planets, whose masses are very much greater and whose apparent proper motions are very much smaller, the corrections in time can be large compared to a second and should not be ignored. For example, Jupiter's proper motion is typically 5×10^{-3} arc second per second, and the bending of light at the limb is about 0.017 ". Thus, the correction can be three seconds or more, but we should note that moons have masses several orders of magnitude smaller than Jupiter's.

The propagation time correction affects only the epoch t2 relative to t3, since we are assuming the star's position is fixed. Thus, we find the relativistic time correction for the epoch t2 from $\delta t = 2G\ m\ \ln(2r/h)/c^3$. For the Moon, this amounts to a few picoseconds, which is far less than an effect we have already ignored, and even for Jupiter this effect is only about a microsecond. Consequently, we may ignore this time correction completely. There is also a

correction term due to the Sun's mass, but this, too, is negligible because the line of sight to a star being occulted by a planet does not pass near the sun.

The simplest model of the visible disk of a planet is just a circle. For many applications that is sufficient, but most planetary bodies are better represented by oblate spheroids than by spheres. Let us examine the effect of the three-dimensional shape of a body on its projected (apparent) disk. Rather than limit the discussion to spheroids, let us consider ellipsoids with arbitrary axis lengths. The additional complication is small compared to that introduced by abandoning the sphere.

Consider an ellipsoid with center at the origin and principal axes aligned with the coordinate axes. For complete generality we must investigate the apparent radius at any position angle from any aspect. Another way of characterizing this information is to express the apparent radius along any given direction. More precisely, we wish to find the distance from the center of the ellipsoid to the tangent plane which is perpendicular to any given unit vector, as shown in cross-section in Figure 11.

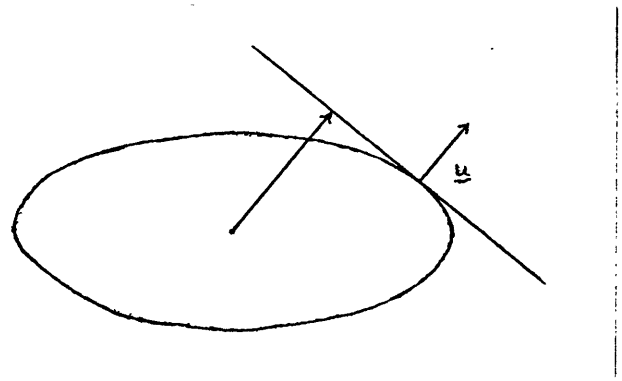

Figure 11: Distance to tangent

Let us write the equation for a generalized ellipsoid such as we have described. If the principal axis lengths are A, B, and C, then we may write $x^2/A^2+y^2/B^2+z^2/C^2=1$. A section through the ellipsoid parallel to the x-y plane can then be described by the equation $x^2/A^2+y^2/B^2=f^2$, where f^2 lies in the range from zero to one. Clearly, the section at a given value of z is given by $f^2=1-z^2/C^2$. Actually, the equation describes a pair of sections (at $\pm z$), but we need only consider one of them. Suppose we have a unit vector $\underline{u}$ and the tangent plane (actually, one of two symmetrically placed planes) perpendicular to $\underline{u}$. For consistency, let us use the plane for which $\underline{u}$ is an outward normal. Let us denote the point of tangency by $\underline{T}=(X,Y,Z)$.

We can simplify the geometric problem of relating $\underline{T}$ to $\underline{u}$ by constructing an x-y plane through $\underline{T}$. We will call it

plane TZ. The equation for the intersection of the ellipsoid and plane TZ is just

$$x^2/A^2+y^2/B^2 = F^2 \qquad \text{(D-15)}$$

where $F^2=1-Z^2/C^2$. Let us call this ellipse XY. The intersection of the tangent plane and plane TZ is a line which is, in turn, tangent to ellipse XY. In terms of algebra, this tangent line is described by the simultaneous equations giving, for each plane, a point and a unit normal.

$$(\underline{R}-\underline{T})\cdot(u(1)\underline{i}+u(2)\underline{j}+u(3)\underline{k}) = 0 \qquad \text{(D-16)}$$

$$(\underline{R}-\underline{T})\cdot\underline{k} = 0$$

where u(1) u(2), and u(3) are the Cartesian components of $\underline{u}$, and $\underline{i}$, $\underline{j}$, and $\underline{k}$ are the coordinate unit vectors. Since the tangent line must lie in both planes, its direction can easily be derived from the two equations by taking the cross product of the two perpendiculars, that is, $u(2)\underline{i}-u(1)\underline{j}$. Considering ellipse XY as a plane figure in plane TZ, then, we see that the slope of the ellipse at $\underline{T}$ must be $-u(1)/u(2)$, but we know from elementary calculus that the slope is $-XB^2/YA^2$. Thus, we have $X=A^2u(1)Y/B^2u(2)$, and we may plug this into equation (D-15) to get

$$Y^2 = B^2F^2/(1+A^2u(1)^2/B^2u(2)^2). \qquad \text{(D-17)}$$

This gives us the following results

$$Y = \pm B^2 Fu(2)/\gamma \qquad \text{(D-18)}$$

$$X = \pm A^2 Fu(1)/\gamma$$

where $\gamma = [A^2u(1)^2+B^2u(2)^2]^{0.5}$. Figure 12 shows the orientation in space of the ellipsoid along with the tangent plane and plane TZ.

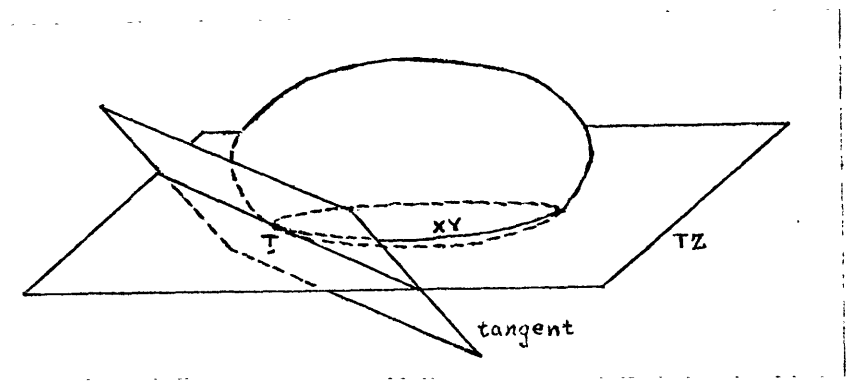

Figure 12: Cross-section and tangent geometry

The ellipsoid is cut by plane TZ in ellipse XY. TZ intersects the tangent point T.

The symmetry of the equation for an ellipsoid shows that we can apply the same procedure using x-z sections and get a result in the same form, that is,

$$Z = \pm C^2 Gu(3)/\beta \qquad \text{(D-19)}$$

$$X = \pm A^2 Gu(1)/\beta$$

where $\beta = [A^2u(1)^2+C^2u(3)^2]^{0.5}$ and $G^2=1-Y^2/B^2$. A comparison of the results for X shows that $G/\beta=\pm F/\gamma$ and substituting this and equation (D-17) into the definition of G^2 gives

$$F^2(A^2u(1)^2+B^2u(2)^2+C^2u(3)^2) = A^2u(1)^2+B^2u(2)^2 \qquad \text{(D-20)}$$

Combining all the equations for X, Y, and Z with our expression for F gives the following.

$$\begin{aligned} X &= \pm A^2u(1)/D \\ Y &= \pm B^2u(2)/D \\ Z &= \pm C^2u(3)/D \end{aligned} \qquad \text{(D-21)}$$

where $D=[A^2u(1)^2+B^2u(2)^2+C^2u(3)^2]^{0.5}$. Obviously, these signs must be all plus or all minus because there are only two possible tangent planes for any given direction. Further, we have made a unique choice -- note that our unit vector $\underline{u}$ points outward for only one of the two. Thus, we choose the plus signs. Finally, we get the distance from the center of the ellipsoid to the tangent plane (the same regardless of which signs we use) by evaluating the dot product of $\underline{T}$ and $\underline{u}$, and we find $\underline{T}\cdot\underline{u}=D$.

Appendix E

RELATIVE PHOTOGRAPHIC OBSERVATIONS

All real observations involve the propagation of the observed signal, and we must, therefore, associate a different time tag with each body involved in the observation event. Thus, if the observer is labeled with the position vector $\underline{r}(o)$ and the observed body with $\underline{r}(b)$, we may define the apparent vector from "b" to "o" at the observer's time t by

$$\underline{b}(t) = \underline{r}(o,t)-\underline{r}(b,t-b(t)/c) \qquad \text{(E-1)}$$

It should be clear from the time arguments on the right-hand side of equation (E-1) that the position of body "b" is taken at the time such that a light signal from there will reach the observer at time t. This is evidently a recursive definition, since b(t) appears on both sides of the equation. What makes this definition at all usable is the fact that c (the velocity of light) is large compared to the velocities of the bodies. Consequently, we may break equation (E-1) into two parts by defining T = t-b(t)/c and proceed to

compute T iteratively. With an initial estimate $T^{(0)}$ (such as $T^{(0)}=t$) we may apply the following iterative routine

$$\underline{b}^{(*)}(t) = \underline{r}(o,t) - \underline{r}(b,T^{(*)})$$

$$T^{(*+1)} = t - b^{(*)}(t)/c \qquad \text{(E-2)}$$

This procedure must converge rapidly because body "b" moves relatively little in the interval between successive estimates of T. Obviously, we need to continue the iterative process only until we obtain a value of T accurate enough for our purposes, that is, at least an order of magnitude more accurate than the observations themselves. At present, photographic observations seem to have no better than 0.1 arc second accuracy, and at a distance of five A.U. that angle includes a chord of 37 kilometers. Thus, at a typical planetary velocity of 30 kilometers per second the best accuracy amounts to about a second of time in T.

With the same sort of procedure we may obtain the vector from the reference object (which we will call body "a") to the observer "o".

$$\underline{a}(t) = \underline{r}(o,t)-\underline{r}(a,t-a(t)/c) \qquad \text{(E-3)}$$

From these vectors we may compute the normalized offset vector which describes the apparent separation of the two bodies as seen by the observer. First, we obtain the separation angle cosine.

$$C = \underline{u}(\underline{a})\cdot\underline{u}(\underline{b}) \tag{E-4}$$

Next we make the definition

$$\underline{w} = \underline{u}(\underline{a})-\underline{u}(\underline{b})/C \tag{E-5}$$

In words, $\underline{w}$ is the projection (onto the plane of the sky) of the apparent offset of the observed body from the reference, normalized so that $|\underline{w}|$ is the tangent of the separation angle.

Since the offset $\underline{w}$ is constrained to lie in the plane normal to $\underline{a}$, it is convenient to express $\underline{w}$ in terms of right ascension and declination offsets (actually $\Delta\alpha \cos\delta$ and $\Delta\delta$). That is, we may write

$$\underline{w} = (\underline{w}\cdot\underline{u}(\alpha))\underline{u}(\alpha)+(\underline{w}\cdot\underline{u}(\delta))\underline{u}(\delta) \tag{E-6}$$

where $\underline{u}(\alpha)$ and $\underline{u}(\delta)$ are the local coordinate unit vectors in the plane of the sky normal to $\underline{a}$. Let $\underline{u}(P)$ represent the pole of reference for the coordinate system; then we have

$$\underline{u}(\alpha) = [\underline{a} \times \underline{u}(P)] \,/\, |\underline{a} \times \underline{u}(P)| \qquad \text{(E-7)}$$

$$\underline{u}(\delta) = \underline{u}(\alpha) \times \underline{u}(\underline{a})$$

There are two primary corrections to this simple picture necessary to account for actual observations, namely, atmospheric refraction and "stellar" aberration (Brouwer and Clemence, 1961). Both of these enter as differential corrections and in some cases may, therefore, be negligible. The stellar aberration is simply due to the velocity of the observer relative to the inertial reference frame, and its direct effect can be as much as 20 arc seconds, but the differential aberration for objects separated by half a degree is no more than 0.2 arc second. Atmospheric refraction varies over the sky with zenith angle, but for objects at least 30 degrees above the horizon, the apparent shift is at most 200 arc seconds, and the differential shift for objects only half a degree apart is at most 2 arc seconds. In fact, astrometric photographs are seldom made closer to the horizon because of seeing problems, and are ordinarily made as close to the zenith as possible.

The aberration correction may be made by changing the apparent position of the observer relative to the observed bodies. To well within the required accuracy, we may ap-

proximate the correction by replacing $\underline{a}(t)$ with $\underline{a}(t)+a(t)\underline{r}'(o,t)/c$. Henceforth, we will assume that the vectors $\underline{a}$ and $\underline{b}$ have been corrected for the apparent aberration.

In principle the refraction correction is also very simple. However, it depends on not just one parameter (as does the aberration), but on the entirety of Earth's atmosphere along the line of sight from the observer to the objects. The correction can still be made straightforwardly, but only because it can be applied differentially to the vector $\underline{w}$ defined in equation (E-5). Thus, we may neglect most of the complexity of the atmosphere and treat the refraction as due to a single bending at a plane boundary between air and vacuum. Further, we construct a simple geographical model of mean temperature and pressure to calculate a single value for the refractive index of the atmosphere. In this model we write for the local temperature and pressure

$$\begin{aligned} T &= T(1) + T(2)\cos\phi + T(3)\cos\phi\sin\omega(t-t(d)) \\ &\qquad + T(4)\phi\sin\Omega(t-t(y)) + Lh \\ &= T(s) + Lh \qquad\qquad (E-8) \\ P &= P(0)\,(T/T(s))^{-3.5} \end{aligned}$$

where T(1) represents the global mean temperature, T(2) the difference between the mean equatorial and polar temperatures, T(3) the equatorial daily temperature amplitude, T(4) the polar yearly temperature amplitude, L the adiabatic temperature lapse rate in the troposphere, P(0) the mean sea-level pressure, T(s) the local sea-level temperature, and ϕ and h the geodetic latitude and altitude of the observer. The symbols ω, t(d), Ω, and t(y) represent the daily and yearly angular velocities and time origins. The functional form of this model is largely arbitrary, being constrained mainly to give the correct mean equatorial and polar temperatures and amplitudes. The values of the parameters were chosen to give a least-squares fit to global mean temperatures and ranges from Table 13 (Brooks, 1969). In fact, the vagaries of weather introduce considerable variations from the mean temperatures, and if the atmospheric temperature made a large contribution to observations (through the refraction correction or otherwise), it would be necessary to gather and use local meteorological data as part of the observing program. Indeed, one of the primary advantages of the so-called "absolute" position measurement by means of plate scale constant solutions is that all the relative corrections for such effects as refraction (or aberration, for that matter) are made automatically.

Table 13

Global temperature means and ranges

Annual mean sea-level temperatures and temperature ranges by latitude.

LAT. (deg)	MEAN (deg F)	AMP.	LAT. (deg)	MEAN (deg F)	AMP.
5	79	2	-5	79	3
15	80	7	-15	78	6
25	78	16	-25	73	12
35	69	29	-35	65	12
45	57	49	-45	54	11
55	42	49	-55	42	14
65	30	63	-65	28	31
75	14	59	-75	11	50
85	1	70	-85	-4	70

The adopted best fit values of the coefficients are as follows.

$$
\begin{aligned}
T(1) &= 249.7257 \text{ K} \\
T(2) &= 51.27402 \text{ K} \\
T(3) &= 7.9365 \text{ K} \\
T(4) &= 11.40036 \text{ K} \\
L &= -9.759547 \text{ K/km} \\
P(0) &= 1.013 \text{ bar}
\end{aligned}
\qquad \text{(E-9)}
$$

The last two coefficients, L and P(0), are just the dry adiabatic temperature gradient in the troposphere and the mean sea-level atmospheric pressure. The coeffecients are expressed here with much more than the needed precision for

such a global model, but that fact will not materially affect the computations. The index of refraction may be written as $n = 1 + \mu$, and we may approximate the refraction constant μ as follows (Allen, 1973).

$$\mu = (A+B\nu^2+C\nu^4)P[1+P(D+ET)]+F)/T$$

$$A = 7.74935 \times 10^{-2}$$

$$B = 4.85766 \times 10^{-33}$$

$$C = 4.63989 \times 10^{-64} \qquad \text{(E-10)}$$

$$D = 4.0041 \times 10^{-6}$$

$$E = -1.1778 \times 10^{-8}$$

$$F = 1.0735 \times 10^{4}$$

where ν is the frequency (in Hertz) of the light being refracted, and the coefficient units are combinations of Hertz, bars, and degrees K.

Given the refraction constant μ we may proceed to write the correction to the apparent offset in terms of the zenith angle. Since the two observed objects are assumed close together in the sky we will use a single zenith angle, namely that of the reference body. Let $\underline{u}(n)$ be the local upward vertical unit vector, and H be the reference body's zenith angle. Then we write

$$\cos Z = -\underline{u}(n)\cdot\underline{u}(\underline{a}) \qquad \text{(E-11)}$$

$$\underline{z} = \underline{u}(n) + \underline{u}(\underline{a}) \cos Z$$

Note that $\underline{u}(\underline{a})$, like $\underline{a}$, is directed toward the observer, but that $\underline{u}(n)$ is directed away.

With the assumption that atmospheric refraction can be modeled by a single vacuum-to-air interface with one characteristic refractive index, Snell's law states

$$(1+\mu) \sin(Z+\Delta Z) = \sin Z \qquad \text{(E-12)}$$

This gives (to first order in μ) the following value for ΔZ.

$$\Delta Z = \mu \tan Z \qquad \text{(E-13)}$$

Figure 13 shows the geometry of the refraction correction.

In Figure 13 we see the salient points of atmospheric refraction. In particular, refraction tends to squeeze apparent positions together toward the zenith. In this model the assumed symmetry requires that the change in the apparent position due to refraction be purely in the direction of the zenith, and we may obtain the correction to $\underline{w}$ by differentiating equation (E-13) with respect to Z and multiplying by the zenith component of $\underline{w}$.

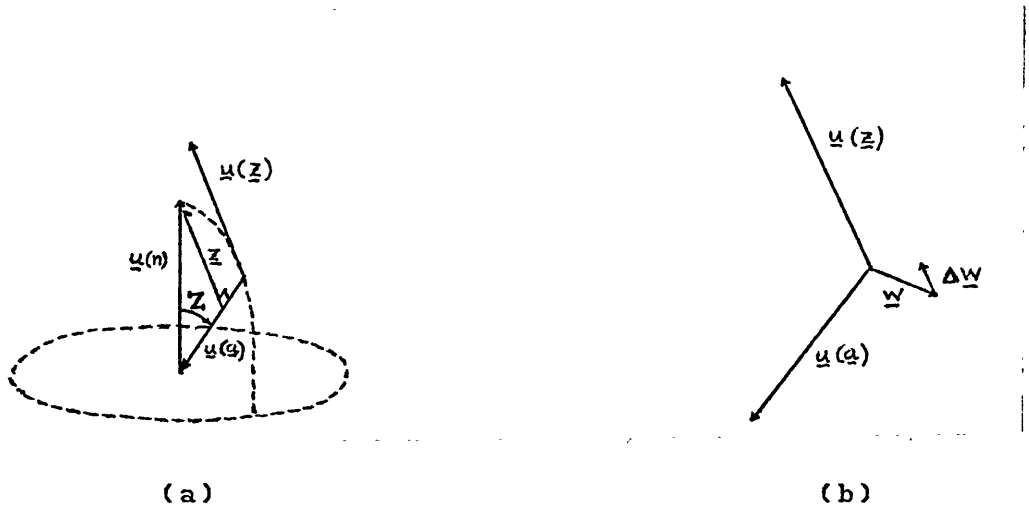

(a) (b)

Figure 13: Atmospheric refraction correction

(a): The topocentric geometry of the line-of-sight, local vertical, and zenith unit vectors. (b): A magnification of (a) showing the uncorrected offset vector and the sense of the refraction correction.

$$\begin{aligned} \Delta\underline{w} &= -\underline{u}(\underline{z})[\underline{u}(\underline{z})\cdot\underline{w}\mu\sec^2 Z] \\ &= -\underline{z}[\underline{z}\cdot\underline{w}\ \mu\ \sec^2 Z\ \csc^2 Z] \qquad \text{(E-14)} \\ &= -\underline{z}[\underline{u}(n)\cdot\underline{w}\ \mu\ \sec^2 Z\ \csc^2 Z] \end{aligned}$$

Since the correction is perpendicualr to the reference line of sight $\underline{u}(\underline{a})$ (as is $\underline{w}$ itself), we may still decompose the corrected vector as in equation (E-6). In practice the orientation of the right ascension unit vector $\underline{u}(\alpha)$ is determined by trailing a star on the photographic plate. Thus, it is merely the <u>apparent</u> unit vector and is corrupted by atmospheric refraction in the same way as $\underline{w}$, and we must replace the first equation (E-7) by

$$\underline{u}(\alpha) = \underline{u}(\ \underline{a}x\underline{u}(P) - \underline{z}[\underline{u}(n)\cdot\underline{a}x\underline{u}(P)]R\ ) \qquad \text{(E-15)}$$

where $R = \mu \sec^2 Z \csc^2 Z$. With this new definition we have the final mathematical description of the observable quantities as $\underline{\omega}\cdot\underline{u}(\alpha)$ and $\underline{\omega}\cdot\underline{u}(\delta)$, where $\underline{\omega}$ is just $\underline{w}+\Delta\underline{w}$. These are the offsets on a photographic plate in an X-Y coordinate system defined by the apparent instantaneous rotation of Earth and multiplied by the assumed focal plane plate scale factor for the telescope.

The partial derivatives of these observed offsets with respect to the observed body coordinates are easily obtained. First, we note

$$\partial C/\partial\underline{b} = (\underline{u}(\underline{a})-C\underline{u}(\underline{b}))/b \qquad \text{(E-16)}$$

Now, reference to equations (E-7) and (E-15) shows that the sky-plane coordinate vectors are perpendicular to $\underline{u}(\underline{a})$, whether corrected for refraction or not. Let us make use of this fact in finding the corresponding derivatives of the components of $\underline{w}$. Suppose we have a vector $\underline{v}$ such that $\underline{v}\cdot\underline{u}(\underline{a})$ is zero. Then we have from equation (E-5)

$$\underline{w}\cdot\underline{v} = -\underline{u}(\underline{b})\cdot\underline{v}/C \qquad \text{(E-17)}$$

and, as long as $\underline{v}$ is independent of $\underline{b}$,

$$\partial(\underline{w}\cdot\underline{v})/\partial\underline{b} = -[\underline{v}-(\underline{u}(\underline{b})\cdot\underline{v})\underline{u}(\underline{b})]/bC$$
$$+ \underline{u}(\underline{b})\cdot\underline{v}\ (\underline{u}(\underline{a})-C\underline{u}(\underline{b}))/bC^2$$
$$-(\underline{v}-\underline{u}(\underline{a})[\underline{u}(\underline{b})\cdot\underline{v}/C])/bC \qquad \text{(E-18)}$$
$$= -(\underline{v}+\underline{u}(\underline{a})[\underline{w}\cdot\underline{v}])/bC$$

This simple result may be applied to the computation of the derivative of $\underline{\omega}$, the vector corrected for refraction. We have, from equation (E-14)

$$\underline{\omega}\cdot\underline{v} = \underline{w}\cdot\underline{v}-(\underline{z}\cdot\underline{v})(\underline{z}\cdot\underline{w})R$$
$$= \underline{w}\cdot\underline{e} \qquad \text{(E-19)}$$

where $\underline{e} = \underline{v}-(\underline{z}\cdot\underline{v})\underline{z}R$. It is evident from the definition of $\underline{z}$ that it (and, therefore, also $\underline{e}$) is perpendicular to $\underline{u}(\underline{a})$, and we may now use the result from equation (E-18) to get

$$\partial(\underline{\omega}\cdot\underline{v})/\partial\underline{b} = -(\underline{e}+\underline{u}(\underline{a})[\underline{w}\cdot\underline{e}])/bC$$
$$= -(\underline{v}-(\underline{z}\cdot\underline{v})\underline{z}R+\underline{u}(\underline{a})(\underline{\omega}\cdot\underline{v}))/bC \qquad \text{(E-20)}$$

When we substitute $\underline{u}(\alpha)$ or $\underline{u}(\delta)$ for $\underline{v}$ in equation (E-20), we get the partial derivatives of the observables with respect to the coordinates of the observed body. We may use the chain rule to find the partial with respect to any parameter p which affects the motion of body "b".

Now we must consider the partial derivatives with respect to parameters that affect the motion of the reference body "a". In the case of observations of a satellite relative to its central body such parameters also affect the observed body in just the same way as they do the reference, simply because the motion of the satellite is naturally expressed relative to its central planet. These differential observations are, therefore, quite insensitive to the parameters that affect the central body. Nevertheless, for completeness we should derive the expressions for the partial derivatives.

First of all, we have

$$\partial C/\partial \underline{a} = (\underline{u}(\underline{b})-C\underline{u}(\underline{a}))/a$$
$$= -C\underline{w}/a \qquad \text{(E-21)}$$

Next, we must break the partial derivative into two pieces because the sky-plane coordinate unit vectors are functions of $\underline{a}$. Thus, we write

$$\partial[\underline{w}\cdot\underline{v}]/\partial\underline{a} = (\underline{v}\cdot\partial/\partial\underline{a})\underline{w})+(\underline{w}\cdot\partial/\partial\underline{a})\underline{v} \qquad \text{(E-22)}$$

where, again, $\underline{v}$ represents one of the unit vectors.

The first term in equation (E-22) is analogous to the partial derivative already obtained in equation (E-18), and we get

$$
\begin{aligned}
(\underline{v}\cdot\partial/\partial\underline{a})\underline{w} &= [\underline{v}-\underline{u}(\underline{a})[\underline{u}(\underline{a})\cdot\underline{v}]-[\underline{u}(\underline{b})\cdot\underline{v}]\underline{w}/C]/a \\
&= [\underline{v}-(\underline{u}(\underline{b})\cdot\underline{v})\underline{w}/C]/a \qquad \text{(E-23)} \\
&= [\underline{v}+(\underline{w}\cdot\underline{v})\underline{w}]/a
\end{aligned}
$$

We can redo this result for the refraction-corrected offset $\underline{\omega}$ by using equation (E-19) just as we we did in obtaining equation (E-20).

$$
\begin{aligned}
(\underline{v}\cdot\partial/\partial\underline{a})\underline{\omega} &= [\underline{e}+(\underline{w}\cdot\underline{e})\underline{w}]/a \\
&= [\underline{v}-(\underline{z}\cdot\underline{v})\underline{z}R+(\underline{\omega}\cdot\underline{v})\underline{w}]/a \qquad \text{(E-24)}
\end{aligned}
$$

For the second term of equation (E-22) we must use explicit values of the unit vectors $\underline{u}(\alpha)$ and $\underline{u}(\delta)$ in place of the general $\underline{v}$. For ease of evaluation we now rewrite equations (E-7)

$$
\begin{aligned}
\underline{u}(\alpha) &= \underline{u}(\underline{a}) \times \underline{u}(P) \;/\; Y \\
\underline{u}(\delta) &= [\underline{u}(P)-\underline{u}(\underline{a})(\underline{u}(\underline{a})\cdot\underline{u}(P))] \;/\; Y \qquad \text{(E-25)}
\end{aligned}
$$

where $Y = [1-(\underline{u}(\underline{a})\cdot\underline{u}(P))^2]^{0.5}$. Now we evaluate the derivative of the common factor in both unit vectors.

$$\partial(1/Y)/\partial\underline{a} = (\underline{u}(P)-\underline{u}(\underline{a})[\underline{u}(\underline{a})\cdot\underline{u}(P)])(\underline{u}(\underline{a})\cdot\underline{u}(P))/aY^3$$

$$= \underline{u}(\delta)(\underline{u}(\underline{a})\cdot\underline{u}(P))/aY^2 \qquad \text{(E-26)}$$

Next, we treat the right ascension component. We have

$$(\underline{w}\cdot\partial/\partial\underline{a})\underline{u}(\alpha) = (\partial/\partial\underline{a})[\underline{w}\cdot\underline{u}(a)\times\underline{u}(P)/Y] \qquad \text{(E-27)}$$

where $\underline{w}$ is treated as a constant. Thus, we may permute the triple product and use equation (E-26) to write

$$\begin{aligned}(\underline{w}\cdot\partial/\partial\underline{a})\underline{u}(\alpha) &= [\underline{u}(P)\times\underline{w}-\underline{u}(\underline{a})(\underline{u}(\underline{a})\cdot\underline{u}(P)\times\underline{w}) \\ &\qquad +(\underline{u}(\underline{a})\cdot\underline{u}(P))(\underline{u}(\underline{a})\cdot\underline{u}(P)\times\underline{w})\underline{u}(\delta)/Y] \;/\; aY \\ &= [\underline{u}(P)\times\underline{w}-\underline{u}(\underline{a})(\underline{u}(\underline{a})\cdot\underline{u}(P)\times\underline{w}) \\ &\qquad +(\underline{w}\cdot\underline{u}(\alpha))(\underline{u}(\underline{a})\cdot\underline{u}(P))\underline{u}(\delta)] \;/\; aY \\ &= \underline{u}(\alpha)(\underline{u}(\alpha)\cdot\underline{u}(P)\times\underline{w})/aY \qquad \text{(E-28)} \\ &= \underline{u}(\alpha)(\underline{w}\cdot\underline{u}(P))(\underline{u}(\underline{a})\cdot\underline{u}(P))/aY^2 \\ &= \underline{u}(\alpha)(\underline{u}(\underline{a})\cdot\underline{u}(P))(\underline{w}\cdot\underline{u}(\delta))/aY\end{aligned}$$

Next, we get

$$\begin{aligned}(\underline{w}\cdot\partial/\partial\underline{a})\underline{u}(\delta) &= [-\underline{w}(\underline{u}(\underline{a})\cdot\underline{u}(P) - \underline{u}(P)(\underline{u}(\underline{a})\cdot\underline{w}) \\ &\qquad +2\underline{u}(\underline{a})(\underline{u}(\underline{a})\cdot\underline{w})(\underline{u}(\underline{a})\cdot\underline{u}(P) \\ &\qquad +(u(a)\cdot u(\underline{P}))(w\cdot u(\underline{\delta}))u(\delta)] \;/aY \\ &= [-\underline{w}+(\underline{w}\cdot\underline{u}(\delta))\underline{u}(\delta)][\underline{u}(\underline{a})\cdot\underline{u}(P)/aY] \qquad \text{(E-29)} \\ &= -\underline{u}(\alpha)(\underline{w}\cdot\underline{u}(\alpha))(\underline{u}(\underline{a})\cdot\underline{u}(P))/aY\end{aligned}$$

If we now substitute into equation (E-22), we get

$$(\partial/\partial\underline{a})(\underline{w}\cdot\underline{u}(\alpha)) = [\underline{u}(\alpha)+(\underline{w}\cdot\underline{u}(\alpha))\underline{w} + (\underline{w}\cdot\underline{u}(\delta))\underline{u}(\alpha)\ \tan\delta]\ /\ a$$

$$(\partial/\partial\underline{a})(\underline{w}\cdot\underline{u}(\delta)) = [\underline{u}(\delta)+(\underline{w}\cdot\underline{u}(\delta))\underline{w} + (\underline{w}\cdot\underline{u}(\alpha))\underline{u}(\alpha)\ \tan\delta]\ /\ a \qquad \text{(E-30)}$$

Note that equations (E-28) and (E-29) treat the vector $\underline{w}$ as a constant, and the only restriction on $\underline{w}$ is that $\underline{w}\cdot\underline{a}$ be zero. Therefore, $\underline{\omega}$ can be substituted freely for $\underline{w}$, and we may now combine those equations with equation (E-24) to get

$$(\partial/\partial\underline{a})(\underline{\omega}\cdot\underline{u}(\alpha)) = [\underline{u}(\alpha)+(\underline{\omega}\cdot\underline{u}(\alpha))\underline{w}-\underline{z}\cdot\underline{u}(\alpha)\underline{z}R + (\underline{\omega}\cdot\underline{u}(\delta))\underline{u}(\alpha)\ \tan\delta]\ /\ a$$

$$(\partial/\partial\underline{a})(\underline{\omega}\cdot\underline{u}(\delta)) = [\underline{u}(\delta)+(\underline{\omega}\cdot\underline{u}(\delta))\underline{w}-\underline{z}\cdot\underline{u}(\delta)\underline{z}R + (\underline{\omega}\cdot\underline{u}(\alpha))\underline{u}(\alpha)\ \tan\delta]\ /\ a \qquad \text{(E-31)}$$

From the form of equations (E-20) and (E-31) it is clear that the motion of the observer has a direct effect on the observation through the explicit evaluation of $\underline{a}(t)$ and $\underline{b}(t)$. However, it approximately cancels out in just the same way as the motion of a reference body "a" which is the central body of the observed satellite. The only other parameter of interest in the computation of these differential observables is the assumed photographic plate scale. Instead of working directly with the plate measurements (typi-

cally in micrometers or millimeters) we are dealing with the offsets multiplied by the nominal plate scales. Thus, the observable is expressed as seconds of arc on the plane of the sky, and the most convenient parameterization of the plate scale is through a fractional deviation from the nominal value. In other words, the actual computed value X is $Y(1+\epsilon)$, where Y is the value described earlier in this chapter, and ϵ is the fractional deviation of the plate scale from its nominal. Thus, we may write for the partial derivative

$$\partial X/\partial \epsilon = Y \tag{E-32}$$

Actually, the nominal plate scale is variable during the course of one night because of temperature changes in the telescope, and the variations may be as large as a part in 10^4 (Pascu, 1977). Thus, there may be systematic variations in addition to any overall discrepancy in the nominal plate scale. In fact, the nominal plate scales are typically reported to only four or five significant digits, and the two effects are, therefore, likely to be inseparable.

Appendix F

POST-FIT RESIDUALS

The following are the post-fit residuals for all the observations that entered into the solution presented in this work. The residuals are presented in the sense of observed minus computed. Each observation has one or two independent measurements: Doppler for radar observations, right ascension and declination for meridian-circle or astrometric observations, mid-event time and minimum apparent separation (normalized by the sum of radii) for mutual event observations, and geometric round-trip delay for normal points. Astrometric positions are referred to the 1950.0 mean equator and equinox while meridian-circle positions are referred to the equator and equinox of date. The right ascension residuals are given in seconds of arc rather than in seconds of time and are not multiplied by the declination cosines. The observations are listed first by body and then by type. Observations are arranged chronologically within each category. The epoch is given for each observation in days (Julian date - 2440000), where each day is reckoned from noon.

The epochs are given in UT except for the normal points, which are given in Coordinate Time (here defined as Atomic Time (A1) plus 32.15 seconds). In the case of the mutual events, the epoch is actually the observable. The observing site is listed with each series except in the case of mutual event observations.

I O

Io Residuals
Radar (AREC)

EPOCH	Dop (Hz)
2794.444444	652.0
3077.776331	353.6
3097.708507	-34.0
3101.697049	275.9

Io Residuals
Astrometric (LMCC)

EPOCH	α (")	δ (")
2685.755556	-0.2558	0.0249
2685.758333	-0.0913	0.0116
2685.772222	-0.4914	0.0552
2685.775000	-0.0093	-0.1431
2714.649306	-0.1793	-0.1162
2714.652083	0.2395	0.1727
2714.654167	0.2046	0.0917
2714.658333	0.4198	0.0615
2714.660417	0.0606	0.1487
2714.662500	0.2991	0.1417
2714.667361	0.1198	0.2090
2714.669444	0.1680	0.0520
2714.671528	0.0530	-0.0137
2716.646528	0.8371	0.2361
2716.649306	0.6821	0.2672
2716.652083	0.3868	0.1729
2716.656944	0.3034	0.1744
2716.660417	0.3881	0.2709
2716.662500	0.4555	0.0711
2716.667361	0.6891	0.0478
2716.669444	0.3221	0.1191
2716.671528	0.2334	0.0316
2716.688194	0.4968	0.0392
2716.689583	0.1029	-0.0599
2716.691667	0.4620	0.1497
2717.658333	-0.2087	0.0272
2717.659722	0.2860	0.2078
2717.663194	-0.0784	-0.1640
2720.644444	1.2498	-0.1089
2720.651389	-0.0114	-0.1257
2721.638889	0.3432	-0.4276
2721.640972	-0.1338	-0.4269
2721.643056	-0.4962	-0.2543
2721.647917	-0.0406	-0.1013
2721.650000	0.0967	-0.7119
2721.652083	-0.3978	-0.4530
2721.658333	-0.4457	-0.1888
2721.660417	-0.0470	-0.6136
2721.662500	-0.3185	-0.4861
3095.733333	-0.4549	-0.1343
3095.739583	-0.2907	-0.2643
3099.698611	0.1406	-0.0680
3099.700694	0.2310	-0.1230
3099.702083	0.1986	-0.0778
3099.705556	0.1763	-0.0637
3099.706944	0.2111	-0.0584

3099.708333	0.2331	-0.0951
3101.691655	-0.1485	0.1595
3101.695833	-0.0375	0.3532
3101.700000	-0.0211	0.0903
3101.703472	-0.0909	0.2661
3113.678472	0.3439	-0.1374
3113.680556	0.3867	-0.1408
3113.682639	0.2333	-0.0486
3113.686806	0.3294	-0.1832
3113.688889	0.3555	-0.0680
3113.690278	0.2487	-0.0662
3131.639583	-0.1285	-0.1637
3131.641667	-0.2828	-0.2771
3131.643056	-0.1895	-0.3043
3131.650000	-0.2848	-0.3857
3131.651389	-0.0527	-0.2785
3131.652778	-0.0872	-0.4213
3462.797222	-0.0709	0.2664
3462.800000	-0.2146	0.1227
3462.802778	-0.2735	0.1682
3462.811806	0.0307	0.2197
3462.813889	-0.1042	0.1314
3462.815972	-0.1347	0.0898
3466.786111	0.0307	0.1859
3466.788194	-0.0051	0.1027
3466.790972	-0.0191	-0.0212
3467.786111	-0.1427	-0.0499
3467.805556	-0.3847	0.1314
3485.733333	0.1150	0.2076
3485.735417	-0.1436	0.2749
3485.746528	-0.0720	0.1992
3485.747917	0.0640	0.1704
3485.750000	0.0433	0.2069
3487.723611	-0.2856	0.1310
3487.726389	-0.2043	0.2856
3487.727778	-0.3360	-0.1653
3487.736806	-0.3449	0.2118
3487.738889	-0.3826	-0.0300
3487.740972	-0.5220	0.0450
3489.726389	0.5616	0.1715
3489.729167	0.5109	0.0513
3489.731250	0.3229	0.0937
3489.741667	0.4757	0.0152
3489.743750	0.3412	-0.0468
3489.746528	0.3644	0.0263
3493.702083	-0.0159	0.0170
3493.704167	0.0456	0.0378
3493.706250	0.0347	0.0521
3493.715278	0.0528	0.0879
3493.717361	0.0946	0.1004
3493.720139	0.0038	0.0922
3494.696528	0.1154	0.0914
3494.698611	0.1528	0.0855
3500.713889	-0.4027	0.2099
3500.716667	-0.4773	0.2311
3500.719444	-0.4424	0.2418

Io Residuals
Astrometric (MCDO)

EPOCH	α (")	δ (")
3050.968403	-1.1778	0.0407
3459.778299	0.0041	-0.3485
3461.766319	-0.2648	-0.2628
3486.662500	-0.3320	-0.0330
3515.793056	0.2076	0.1878
3517.793229	0.1664	0.1166

Io Residuals
Astrometric (USNO)

EPOCH	α (")	δ (")
1953.536458	0.2944	-0.2014

Europa Residuals
Radar (AREC)

EPOCH	Dop (Hz)
2690.725694	-64.5
2712.656250	125.6
2716.656250	111.4
3102.695775	-74.0
3107.676956	59.2
3119.642523	-27.4
3470.799306	-32.4
3474.790972	11.4

Europa Residuals
Astrometric (LMCC)

EPOCH	α (")	δ (")
2685.755556	-0.1557	-0.2388
2685.758333	-0.1324	-0.0281
2685.772222	-0.3969	-0.1560
2685.775000	0.0611	-0.1115
2714.649306	0.1707	-0.0625
2714.652083	0.1447	-0.0001
2714.654167	0.3206	0.0057
2714.658333	0.3104	0.0332
2714.660417	0.1202	0.0780
2714.662500	0.0728	-0.0365
2714.667361	0.1892	0.0833
2714.669444	0.0169	0.0119
2714.671528	0.1152	-0.0538
2717.658333	-0.3578	0.0516
2717.659722	-0.0321	0.1991
2717.663194	-0.2056	-0.0450
2719.646528	0.0213	-0.0762
2719.648611	-0.2390	-0.0793
2719.650694	-0.5044	0.1496
2719.654861	-0.0512	0.2566
2719.656944	-0.3997	0.3834
2719.659028	0.1261	-0.2336
2719.663194	-0.2880	0.1049
2719.665278	-0.5338	-0.0231
2719.667361	-0.1389	0.0225
2720.644444	0.7545	-0.0216
2720.651389	-0.0869	-0.2533
2720.653472	0.5111	3.0761
2721.638889	-0.2787	-0.0681
2721.640972	-0.3810	-0.2696
2721.643056	-0.8657	-0.4716
2721.647917	-0.1439	-0.0431
2721.650000	-0.5723	-0.4409
2721.652083	-0.8373	-0.2892
2721.658333	-0.3063	-0.3573
2721.660417	-0.3972	-0.5497
2721.662500	-0.7193	-0.3676
3095.733333	-0.7705	-0.2059
3095.739583	-0.5735	-0.3032
3096.691667	-0.0550	-0.0151
3096.693750	-0.1435	0.0500
3096.700000	-0.0706	0.0488
3096.701389	-0.0143	-0.0328
3099.698611	0.0957	-0.1141
3099.700694	0.2001	-0.1803
3099.702083	0.1511	-0.0273
3099.705556	0.1948	-0.0750
3099.706944	0.1862	-0.0178
3099.708333	0.1555	-0.0831
3101.691655	0.1308	0.3852
3101.695833	0.1555	0.3681
3101.700000	0.1243	0.1892
3101.703472	0.1061	0.3918
3113.678472	0.4100	-0.2108
3113.680556	0.4868	-0.1986
3113.682639	0.2841	0.0273
3113.686806	0.4368	-0.2669
3113.688889	0.3764	-0.0993
3113.690278	0.2423	-0.0603
3131.639583	-0.1161	-0.1562
3131.641667	-0.2532	-0.2960
3131.643056	-0.2252	-0.2658
3131.650000	-0.2746	-0.3540
3131.651389	-0.1069	-0.2955
3131.652778	-0.1539	-0.4066
3462.797222	-0.3922	0.5526
3462.800000	-0.4176	0.3508
3462.802778	-0.5132	0.3970
3462.811806	-0.3739	0.6690
3462.813889	-0.4993	0.5382
3462.815972	-0.5583	0.5304
3467.786111	-0.1795	0.0674
3467.805556	-0.3565	0.3241
3480.758333	-0.5202	0.2696
3480.761111	-0.4699	0.2358
3480.763889	-0.5561	0.1810

3480.772917	-0.4851	0.2752
3480.775694	-0.5633	0.3362
3480.778472	-0.4833	0.1732
3485.733333	0.1495	0.1580
3485.735417	-0.0829	0.1553
3485.747917	0.1871	0.1746
3485.750000	0.1610	0.1347
3487.723611	-0.0516	0.0488
3487.726389	-0.1171	0.0622
3487.727778	-0.2224	-0.1616
3487.736806	0.0054	0.1483
3487.738889	-0.1759	-0.0886
3487.740972	-0.1339	0.0246
3488.725000	-0.1296	0.1419
3488.727083	-0.1606	0.1900
3488.729167	-0.2180	-0.0538
3488.747917	-0.0607	0.1872
3488.750000	-0.1877	0.2910
3488.752083	-0.1589	-0.0050
3493.702083	-0.1469	0.0796
3493.704167	-0.1392	0.0867
3493.706250	-0.2000	0.0319
3493.715278	-0.1676	0.0808
3493.717361	-0.1157	0.0670
3493.720139	-0.1344	0.0617
3494.696528	0.0137	0.0432
3494.698611	0.0942	-0.0030
3500.713889	-0.5783	0.0950
3500.716667	-0.6160	0.0270
3500.719444	-0.5846	0.0824
3511.653472	-0.3455	-0.0202
3511.656250	-0.4458	-0.1235
3511.659028	-0.4718	-0.0324
3511.669444	-0.3323	-0.0163
3511.671528	-0.3855	0.0970
3511.673611	-0.2996	0.0075
3512.654167	-0.4649	-0.0873
3512.656944	-0.3952	-0.0812
3512.659028	-0.3797	-0.1749
3512.670139	-0.2241	-0.1115
3512.672222	-0.1950	-0.0792
3512.674306	0.2019	-0.1699

Europa Residuals
Astrometric (MCDO)

EPOCH	α (")	δ (")
3050.968403	-0.8727	0.1142
3459.778299	-0.0867	-0.3345
3461.766319	-0.1707	-0.3351
3486.662500	-0.6572	0.0299
3515.793056	0.3557	0.1283
3517.793229	-0.0557	0.1871

Europa Residuals
Astrometric (USNO)

EPOCH	α (")	δ (")
1953.536458	-0.2061	-0.2138
3166.536806	-0.2427	0.3591
3191.492708	-0.0079	-0.6138

G A N Y M E D E

Ganymede Residuals
Radar (AREC)

EPOCH	Dop (Hz)
2685.750000	-2.2
2686.743056	29.4
2717.656250	10.5
3100.701562	19.2
3104.676505	-7.1
3467.806944	30.5
3469.802778	-8.7
3472.795139	-48.3

Ganymede Residuals
Astrometric (LMCC)

EPOCH	α (")	δ (")
2685.755556	-0.1350	0.0557
2685.758333	-0.1329	0.0590
2685.772222	-0.1892	0.0231
2685.775000	-0.2285	-0.0038
2714.649306	-0.3178	-0.4379
2714.652083	0.0604	-0.0292
2714.654167	0.0054	-0.2058
2714.658333	0.1988	-0.2472

2714.660417	0.0418	-0.1815
2714.662500	-0.1733	0.0434
2714.667361	-0.0394	-0.0020
2714.669444	-0.1777	0.0223
2714.671528	0.0410	-0.0277
2716.646528	0.6667	0.3400
2716.649306	0.6297	0.3750
2716.652083	0.3852	0.3950
2716.656944	0.4440	0.1084
2716.660417	0.2323	0.2982
2716.662500	0.2312	0.1770
2716.667361	0.3712	0.1732
2716.669444	0.3286	0.0948
2716.671528	0.4193	-0.0097
2716.688194	0.6070	0.1546
2716.689583	0.4740	0.0074
2716.691667	0.5705	0.2094
2717.658333	-0.2408	0.1378
2717.659722	0.0664	0.3343
2717.663194	-0.0598	0.0084
2719.646528	-0.1105	-0.0715
2719.648611	-0.1840	-0.1957
2719.650694	-0.5424	-0.0757
2719.654861	-0.2312	0.1799
2719.656944	-0.3731	0.1704
2719.659028	-0.5133	-0.2919
2719.663194	-0.2233	0.2279
2719.665278	-0.3346	-0.0759
2719.667361	-0.5192	0.2625
2720.644444	0.0590	-0.0268
2720.651389	-0.1257	-0.0660
2720.653472	0.4946	2.5822
2721.638889	-0.3411	-0.2778
2721.640972	-0.1951	-0.2404
2721.643056	-0.4646	-0.0773
2721.647917	-0.2502	-0.2570
2721.650000	-0.1942	-0.3476
2721.652083	-0.9218	-0.2687
2721.658333	-0.3320	-0.0872
2721.660417	-0.2736	-0.5823
2721.662500	-0.4517	-0.2921
3095.733333	-0.6520	-0.0906
3095.739583	-0.5940	-0.0779
3096.691667	-0.0037	-0.0392
3096.693750	-0.0650	-0.0270
3099.698611	0.2650	-0.0796
3099.700694	0.3322	-0.1571
3099.702083	0.3098	-0.0223
3099.705556	0.2988	-0.0692
3099.706944	0.3157	-0.0891
3099.708333	0.3134	-0.1298
3101.691655	-0.2372	0.0259
3101.695833	-0.1463	0.2468
3101.700000	-0.2064	0.0384
3101.703472	-0.2348	0.2440
3131.639583	-0.1264	-0.0964
3131.641667	-0.1990	-0.2059
3131.643056	-0.0998	-0.1673
3131.650000	-0.2358	-0.2275
3131.651389	-0.1147	-0.1680
3131.652778	-0.1452	-0.2914
3462.797222	-0.0673	0.2257
3462.800000	-0.1913	0.1796
3462.802778	-0.1611	0.2167
3462.811806	0.0015	0.2146
3462.813889	-0.0680	0.1198
3462.815972	-0.2015	0.1911
3466.786111	-0.4636	-0.0305
3466.788194	-0.3314	0.0057
3466.790972	-0.3647	-0.0644
3467.786111	-0.0594	-0.0573
3467.805556	-0.2790	0.1331
3480.758333	-0.4108	0.1441
3480.761111	-0.3395	0.1029
3480.763889	-0.3215	0.0919
3480.772917	-0.3640	0.1168
3480.775694	-0.3262	0.0954
3480.778472	-0.3518	0.1092
3485.733333	0.2251	0.1479
3485.735417	0.0247	0.1976
3485.746528	0.1413	0.1598
3485.747917	0.2932	0.1273
3485.750000	0.2811	0.1992
3487.723611	-0.0564	-0.0817
3487.726389	-0.0235	-0.0259
3487.727778	-0.1675	-0.1474
3487.736806	-0.0050	0.0321
3487.738889	-0.0386	-0.1372
3488.725000	-0.1937	-0.0253
3488.727083	-0.0795	-0.0809
3488.729167	-0.2692	-0.0825
3488.747917	-0.1459	-0.0357
3488.750000	-0.1484	0.1214
3488.752083	-0.1738	-0.1385
3489.726389	-0.1746	0.1139
3489.729167	-0.1254	0.0406

3489.731250	-0.1297	0.0322
3489.741667	-0.0623	0.0671
3489.743750	-0.0897	-0.0170
3489.746528	-0.1846	0.0284
3493.715278	-0.5523	-0.0857
3493.717361	-0.4295	-0.0795
3493.720139	-0.3960	-0.0370
3494.696528	0.0325	0.0064
3511.653472	0.1117	0.0505
3511.656250	0.0249	-0.0191
3511.659028	-0.0428	0.0275
3511.669444	-0.0021	0.1883
3511.671528	0.0579	0.1737
3511.673611	-0.0242	0.1632
3512.654167	-0.0434	-0.0117
3512.656944	-0.0776	-0.0770
3512.659028	-0.0711	-0.1084

Ganymede Residuals
Astrometric (MCDO)

EPOCH	α (")	δ (")
3050.968403	-0.3975	0.2060
3459.778299	0.2415	-0.4129
3461.766319	-0.1521	-0.1807
3486.662500	-0.0950	0.2066
3515.793056	0.2639	0.1779
3517.793229	0.3809	0.0526

Ganymede Residuals
Astrometric (USNO)

EPOCH	α (")	δ (")
1953.536458	-0.1571	-0.4312
3166.536806	-0.1647	0.3772
3191.492708	0.5096	-0.6858

C A L L I S T O

Callisto Residuals
Radar (AREC)

EPOCH	Dop (Hz)
2683.756944	7.3
2684.739583	-4.5
2713.656250	-12.4
2715.656250	1.7
3070.793113	3.2
3096.710694	-13.1
3109.672801	4.6
3462.823611	-5.9
3468.803472	-1.9
3473.795139	8.7

Callisto Residuals
Astrometric (LMCC)

EPOCH	α (")	δ (")
2685.755556	-0.2444	0.2317
2685.758333	-0.0101	0.2400
2685.772222	-0.0590	0.1971
2685.775000	-0.3426	0.2545
2714.649306	-0.0922	-0.3329
2714.652083	0.0982	0.0605
2714.654167	-0.3016	-0.1497
2714.658333	-0.0393	-0.2951
2714.660417	-0.3412	0.1289
2714.662500	-0.0627	0.0640
2714.667361	-0.1399	-0.1544
2714.669444	-0.1266	-0.4570
2714.671528	-0.2120	-0.2845
2716.646528	0.5261	0.1657
2716.649306	-0.0845	-0.1193
2716.652083	-0.0364	0.5399
2716.656944	0.5051	0.0416
2716.660417	0.2216	0.2497
2716.662500	0.3220	0.2452
2716.667361	0.1320	0.0329
2716.669444	0.1313	0.0401
2716.671528	0.0067	0.0935
2716.688194	0.3739	0.1443
2716.689583	0.3138	-0.0944
2716.691667	0.1797	0.3027
2717.658333	0.3701	0.1319
2717.659722	0.5196	0.2883
2717.663194	0.3454	-0.0248
2719.646528	-0.2477	0.0342
2719.648611	-0.5358	-0.0453
2719.650694	-0.6107	-0.0896
2719.654861	-0.1337	-0.1527

2719.656944	-0.4104	0.4843
2719.659028	-0.1883	-0.3223
2719.663194	-0.4659	0.0665
2719.665278	-0.5611	-0.0488
2719.667361	-0.2381	0.0229
2720.644444	0.2004	-0.1258
2720.651389	-0.3125	-0.1187
2720.653472	-0.0313	2.8007
2721.638889	-0.4186	-0.3394
2721.640972	-0.4054	-0.5355
2721.643056	-0.7742	-0.1764
2721.647917	-0.3180	-0.0992
2721.650000	-0.3798	-0.3023
2721.652083	-0.8497	-0.2394
2721.658333	-0.6490	-0.0593
2721.660417	-0.4942	-0.4930
2721.662500	-0.5395	-0.6630
3095.733333	-0.0252	-0.0975
3095.739583	-0.0090	-0.1998
3096.691667	0.1296	-0.2070
3096.693750	0.0471	-0.2080
3096.700000	0.1701	-0.1917
3096.701389	0.0759	-0.2746
3099.698611	0.1580	-0.1428
3099.700694	0.2393	-0.2033
3099.702083	0.1582	-0.0949
3099.705556	0.1633	-0.1876
3099.706944	0.1946	-0.1370
3099.708333	0.2006	-0.0783
3101.691655	-0.3280	0.1048
3101.695833	-0.1524	0.2021
3101.700000	-0.1594	-0.0298
3101.703472	-0.3562	0.2370
3113.678472	0.2341	0.0847
3113.680556	0.1977	0.0874
3113.682639	0.1426	0.1201
3113.686806	0.2461	0.0507
3113.688889	0.0715	0.1085
3113.690278	0.1339	0.1124
3131.639583	-0.1337	-0.1584
3131.641667	-0.2134	-0.2663
3131.643056	-0.1172	-0.3448
3131.650000	-0.2303	-0.2790
3131.651389	-0.0807	-0.3143
3131.652778	-0.1547	-0.3137
3462.797222	-0.1478	0.1130
3462.800000	-0.1855	0.1704
3462.802778	-0.2297	0.1989
3462.811806	-0.0680	0.1011
3462.813889	-0.0994	0.0561
3462.815972	-0.2781	0.1093
3466.760417	-5.6218	0.6026
3466.762500	-5.6343	0.6639
3466.786111	-0.2783	0.1142
3466.788194	-0.3443	0.0980
3466.790972	-0.1980	-0.0891
3467.786111	-0.1581	-0.0180
3467.805556	-0.3903	0.2538
3480.758333	-0.1500	0.3393
3480.761111	-0.1070	0.3144
3480.763889	-0.1127	0.2896
3480.772917	-0.0715	0.3061
3480.775694	-0.0804	0.3473
3480.778472	-0.0536	0.2988
3485.733333	-0.0242	0.1398
3485.735417	-0.1161	0.1869
3485.746528	-0.2072	0.1394
3485.747917	0.0339	0.0765
3485.750000	-0.0283	0.2254
3487.723611	-0.1812	-0.0872
3487.726389	0.0274	-0.0518
3487.727778	-0.1508	-0.1135
3487.736806	-0.0774	0.0095
3487.738889	0.0474	-0.1776
3487.740972	-0.0674	0.1575
3488.725000	0.1099	-0.1120
3488.727083	0.1663	-0.1947
3488.729167	0.8358	-0.0803
3488.747917	-0.1725	-0.0453
3488.750000	0.0765	0.0211
3488.752083	0.3426	-0.2954
3489.726389	-0.2166	0.0477
3489.729167	-0.1213	-0.0040
3489.731250	-0.2730	0.1311
3489.741667	-0.0006	0.0110
3489.743750	-0.1256	-0.0304
3489.746528	0.9362	-0.0020
3493.702083	-0.0249	0.1181
3493.704167	0.0644	0.1326
3493.706250	0.0135	0.1401
3493.715278	0.0034	0.2210
3493.717361	-0.0266	0.1931
3493.720139	0.0058	0.1461
3494.696528	0.2353	0.0643
3494.698611	0.2795	0.0577
3500.713889	-0.4769	0.1288

3500.719444	-0.4809	0.1862
3511.653472	-0.1185	0.1230
3511.656250	-0.2338	-0.0686
3511.659028	-0.2624	0.0699
3511.669444	-0.1227	0.1360
3511.671528	-0.1002	0.1985
3511.673611	-0.0801	0.1502
3512.654167	-0.0595	-0.0856
3512.656944	-0.0255	-0.1518
3512.659028	0.0074	-0.1199

Callisto Residuals
Astrometric (MCDO)

EPOCH	α (")	δ (")
3050.968403	-0.5488	0.0820
3459.778299	0.6633	-0.3053
3461.766319	-0.5273	-0.0683
3486.662500	-0.8878	0.2902
3515.793056	0.2386	0.1278
3517.793229	-0.3305	0.1233

Callisto Residuals
Astrometric (USNO)

EPOCH	α (")	δ (")
1953.536458	0.1876	0.0625
3166.536806	-0.1956	0.2013
3203.502083	0.0627	0.1107

M U T U A L E V E N T S

Mutual Event Residuals
Io OCC Europa

EPOCH	t (s)	sep(%)
1843.881921	-0.264	-1.2248
1843.881944	1.857	-0.4211
1850.969340	-3.070	0.4209
1850.969363	-1.330	-0.7441
1858.056134	3.626	0.6231
1861.599086	-3.390	6.3152
1872.227685	-12.536	3.0555
1872.227847	1.464	-2.9339
1875.770405	-2.975	1.4413
1875.770417	-2.117	1.2690
1875.770463	2.048	2.6914
1875.770556	10.058	-1.6956
1882.855810	0.428	-0.1379
1886.398634	-3.240	0.3374
1886.398681	1.148	-0.0599
1889.941343	0.315	-0.4807
1897.027373	0.383	1.9119
1907.658437	2.953	1.4608
1907.658472	5.953	-1.1992
1911.202569	2.513	-0.2821
1914.747546	2.953	-1.0173
1914.747546	2.916	-0.2638
1921.838738	-1.002	2.2422
1921.838773	1.996	-1.0880
1921.838773	1.728	0.6801
1928.932859	3.896	1.2910
1932.480880	-4.456	-1.0936
1936.030822	5.890	-0.3290
1946.688611	2.190	1.1495
1946.688623	3.320	-0.9612
1946.688704	10.375	-0.4986
1950.246898	-3.832	3.1010
1953.809120	11.824	2.2021

Mutual Event Residuals
Europa OCC Io

EPOCH	t (s)	sep(%)
2037.522512	6.971	0.1784

Mutual Event Residuals
Ganymede OCC Europa

EPOCH	t (s)	sep(%)
1949.572975	13.554	-3.1621
1949.573125	26.901	0.8284
1956.754109	4.020	0.2996

Mutual Event Residuals
Io ECL Europa

EPOCH	t (s)	sep(%)
1889.934248	-2.064	6.3573
1897.032824	0.649	-1.2814
1907.683553	-2.158	-0.4724

1907.683576	-0.158	-0.4724
1911.234479	-2.610	-0.1458
1914.786424	-3.271	0.0297
1921.892164	-7.038	0.4888
1929.002211	-12.303	1.5633
1929.002234	-10.301	0.4833
1932.559317	-15.839	4.1880
1936.119792	-15.591	-0.2393
2018.560127	-3.533	-2.9436

Mutual Event Residuals
Europa ECL Io

EPOCH	t (s)	sep(%)
1991.471782	-7.143	-5.6259
1991.471794	-6.143	2.7241
1991.471806	-5.143	
1998.564687	-4.008	-0.3090
2002.111181	-2.985	-0.3426
2005.657662	-3.550	-8.4461
2016.297338	-4.612	2.8681
2030.484178	5.584	6.1720

Mutual Event Residuals
Io ECL Ganymede

EPOCH	t (s)	sep(%)
1944.999479	2.857	
1988.616574	-0.964	1.1376
1988.616701	10.041	-0.3724

Mutual Event Residuals
Ganymede ECL Io

EPOCH	t (s)	sep(%)
1991.654005	-0.982	-6.9875
1991.654016	0.018	3.1325
2006.527986	-0.808	-9.0091
2013.075868	8.228	3.3018

Mutual Event Residuals
Europa ECL Ganymede

EPOCH	t (s)	sep(%)
2031.029919	-11.373	-3.7300

Mutual Event Residuals
Ganymede ECL Europa

EPOCH	t (s)	sep(%)
1935.412535	-14.669	1.1282
1942.620428	-2.781	2.5718
1942.620440	-1.781	1.1718
1956.968553	-2.741	-1.1774
1956.968611	2.250	4.8826
1964.128935	4.251	-1.8766
1978.434583	1.075	-4.0612
1978.434606	3.074	-0.1512
1985.582685	-2.015	-1.8863
1985.582720	0.985	-0.9363
1999.873356	-2.034	
2021.299641	12.806	-1.3724
2028.439398	2.742	-0.6675

Mutual Event Residuals
Callisto ECL Io

EPOCH	t (s)	sep(%)
2018.060752	5.551	1.5401

Mutual Event Residuals
Europa ECL Callisto

EPOCH	t (s)	sep(%)
1977.020648	2.640	-4.0250
1993.645289	-7.483	

Mutual Event Residuals
Callisto ECL Europa

EPOCH	t (s)	sep(%)
1985.665046	7.943	3.8500
1985.665104	12.941	1.9900

Mutual Event Residuals
Ganymede ECL Callisto

EPOCH	t (s)	sep(%)
1960.000127	-3.247	-0.9335
2011.562199	-3.483	-1.4948

Mutual Event Residuals
Callisto ECL Ganymede

EPOCH	t (s)	sep (%)
1986.378831	-4.586	1.0141
2002.256829	7.955	1.5617

Jupiter Residuals
Normal Points

EPOCH	del (μs)
2020.500000	-31.36
2384.500000	46.29

Jupiter Residuals
Meridian (USNO)

EPOCH	α (")	δ (")
3183.466981	0.8711	-0.4238
3182.469493	0.2811	-0.6125
3180.474544	-0.1925	-0.5639
3177.482186	0.5821	-0.5207
3176.484750	-0.0137	-0.0580
3175.487324	0.3064	-0.0715
3174.489906	0.1790	-1.3129
3173.492498	0.4466	-0.2713
3170.500327	-0.0290	-0.6389
3169.502956	-0.1548	-0.1430
3160.527036	13.9619	-1.4242
3159.529760	0.6675	-0.9141
3157.535236	-0.2143	0.3461
3151.551896	-0.3749	-0.9127
3148.560354	-0.3179	-0.2267
3146.566040	0.5853	-0.0165
3145.568897	0.1515	0.0556
3143.574639	-0.3888	-0.0451
3142.577523	0.3804	-0.0344
3140.583320	-0.5949	0.3312
3139.586232	0.4891	0.0006
3135.597967	0.0881	-0.0326
3134.600922	1.0001	-0.5254
3127.621829	0.3319	0.4772
3126.624846	0.3972	
3118.649207	0.1259	-0.3851
3117.652277	-0.1722	-0.1236
3116.655352	0.6319	-0.8432
3115.658433	0.2048	0.1738
3114.661517	0.8742	0.0972
3113.664606	1.1549	0.2687
3112.667698	-1.0273	0.5211
3108.680103	0.5445	0.1680
3106.686321	1.2419	0.0072
3105.689433	0.2818	-0.0670
3103.695663	0.3130	-0.8179
3102.698779	0.1552	-0.2160
3101.701896	1.0249	0.5024
3099.708131	0.0415	-0.1600
3096.717480	0.4957	0.1689
3093.726820	0.7907	0.3499
3092.729929	0.5515	-0.2122
3090.736141	-0.4480	-0.4065
3088.742341	0.4064	-0.5523
3084.754700	-0.6258	-0.1692
3081.763923	0.1657	0.2784
3080.766988	0.4619	-0.2062
3079.770047	0.1783	-0.1101
3078.773100	0.4187	0.6336
3074.785253	0.6145	0.0664
3073.788275	1.2127	0.6647
3070.797297	-0.3433	-0.0008
3067.806251	1.3621	-0.0357
3066.809220	0.8696	-0.3517
3064.815133	0.2066	0.1423
3063.818077	0.5562	-0.3654
3062.821013	-0.5016	-0.4774
3061.823940	0.4185	-0.2617
3035.896786	0.4519	-0.3538
3034.899459	0.9235	
3033.902123	2.9042	0.1568
3030.910057	0.0919	-0.1017
3029.912684	0.6760	0.2419
3028.915301	0.8113	-0.0020
3027.917909	0.0812	-0.3338
3026.920509	0.7170	0.0232
3025.923099	0.3685	0.5032
3022.930816	0.1363	-0.2603
3021.933371	0.4095	0.8652
3013.953505	1.5250	-0.2652
3011.958456	0.0645	0.0683
3010.960919	-0.2486	-0.1081
3008.965823	1.0133	
2787.455447	0.7258	-0.0088
2786.457931	-0.1382	0.3308
2782.467945	0.7786	0.4721
2779.475539	-0.0368	0.4579
2771.496146	0.3361	0.4289
2770.498760	0.2549	0.2330
2769.501382	-0.0787	0.3711
2767.506652	0.5411	
2766.509300	1.4182	0.4617

2765.511957	-0.9721	
2763.517296	-1.1399	0.4320
2760.525371	0.4480	
2758.530798	0.3251	0.3468
2757.533525	-0.0752	0.1257
2752.547293	-0.1556	0.6089
2751.550073	-0.1051	0.3816
2749.555660	0.6414	0.7100
2748.558467	-0.2209	3.6957
2746.564107	-0.0793	0.3481
2745.566940	0.6495	
2744.569782	0.1136	0.7639
2742.575491	0.2670	0.3401
2741.578358	-0.2847	0.8498
2739.584116	0.5023	0.0046
2736.592814	0.5587	0.1026
2735.595729	0.3055	-0.4960
2734.598652	0.2668	0.4724
2733.601583	0.4146	
2732.604520	-0.0319	0.6569
2731.607466	0.5739	0.4185
2730.610418	0.3043	0.2473
2728.616344	-0.1244	0.6518
2727.619318	0.4395	1.0325
2723.631276	0.4541	0.5769
2721.637291	0.0444	0.0552
2719.643329	0.5078	0.6832
2717.649387	-0.0949	0.0418
2716.652424	0.4351	0.3634
2714.658509	0.2070	0.0953
2709.673788	0.7090	-0.2302
2708.676852	0.4970	0.6259
2707.679920	-0.0935	0.8439
2705.686061	0.0353	0.7142
2701.698361	0.6365	0.3477
2700.701439	-0.1977	0.4843
2699.704517	-0.0224	
2698.707595	0.8170	0.0545
2697.710674	1.2692	0.7537
2693.722981	0.7486	0.1115
2692.726055	0.0812	0.9103
2690.732197	0.0652	
2689.735265	-0.2015	0.4585
2686.744454	0.2024	0.4197
2684.750563	0.6548	0.1800
2683.753612	0.1059	0.2282
2682.756657	0.5397	0.2502
2672.786845	1.0770	0.1337
2668.798759	0.7365	
2665.807624	0.0038	
2654.839553	0.7068	0.3205
2653.842407	0.5317	0.0199
2652.845253	-0.4694	0.0216
2650.850920	1.2284	0.3765
2649.853740	0.0208	0.1740
2647.859356	1.0509	-0.0681
2643.870486	1.1064	0.3628
2642.873247	0.4778	0.0559
2637.886923	0.7127	0.1096
2634.895025	0.9167	0.4410
2633.897709	0.4639	0.6599
2626.916258	0.0472	0.3698
2625.918875	1.2104	0.1474
2624.921483	0.6017	0.5465
2622.926676	1.1226	-0.1989
2621.929260	1.5289	
2620.931836	0.5911	-0.1824
2619.934404	1.7581	-0.1838
2616.942063	1.0937	1.1026

BIBLIOGRAPHY

Aksnes, K. (1974). Mutual phenomena of Jupiter's Galilean satellites 1973-74. Icarus 21, 100.

---------- (1976). New formulation of de Sitter's theory of motion for Jupiter I-IV. I. Equations of motion and the disturbing function. (Center for Astrophysics Preprint Series 593).

Aksnes, K. and F.A. Franklin (1975). Mutual phenomena of the Galilean satellites in 1973. I. Total and near-total occultation of Europa by Io. Astron. J. 80, 56.

---------- (1976). Mutual phenomena of the Galilean satellites in 1973. III. Final results from 91 light curves. Astron. J. 81, 464.

Allen, C.W. (1973). Astrophysical Quantities (London: Athlone Press).

Anderson, J.D., G.W. Null, and S.K. Wong (1974). Gravity results from Pioneer 10 doppler data. J. Geophys. Res 79, 3661.

Ash, M.E. (1972). Determination of Earth Satellite Orbits. (M.I.T. Lincoln Laboratory Technical Note 1972-5).

Ash, M.E., D.B. Campbell, R.B. Dyce, R.P. Ingalls, G.H. Pettengill, and I.I. Shapiro (1971). Astronomical constants from analysis of inner-planet radar data. Bull. A.A.S. 3, 474.

Bergmann, P.G. (1976). Introduction to the Theory of Relativity (New York: Dover Publications, Inc.).

Brooks, C.E.P. (1969). Climate and Climatology. Encyclopaedia Britannica.

Brouwer, D. and G.M. Clemence (1961). Methods of Celestial Mechanics (New York: Academic Press).

Brown, B. (1977). The long period behavior of the orbits of the Galilean satellites of Jupiter. Celestial Mechanics 16, 229.

Buarque, J.A. (1978). Occultations of Jupiter Satellites. Pub. Astron. Soc. Pac. 90, 117.

Campbell, D.B., J.F. Chandler, S.J. Ostro, G.H. Pettengill, and I.I. Shapiro (1978). Galilean satellites: 1976 radar results Icarus 34, 254.

Campbell, D.B., J.F. Chandler, G.H. Pettengill, and I.I. Shapiro (1977). Galilean satellites of Jupiter: 12.6-centimeter radar observations Science 196, 650.

Chandler, J.F. (1975a). Application of ranging information to the celestial mechanics of Jovian satellites. (General Examination Paper, M.I.T.).

---------- (1975b). Studying the Galilean satellites by radar. (General Examination Paper, M.I.T.).

Chen D.-H., Wu Z.-X., Yang X.-Y., and Wang C.-B. (1978). A photometric study of mutual phenomena of Galilean satellites. Chinese Astron. 2, 13.

de Sitter, W. (1931). Jupiter's Galilean satellites. Mon. Not. Roy. Astron. Soc. 91, 706.

Divinskiy, M.L. (1974). Position observations of Jupiter and the Galilean Satellites. Astrometria i Astrofizika 22, 98.

Dyson, F.J. (1967). Experimental tests of general relativity. Radar. Relativity Theory and Astrophysics 1. Relativity and Cosmology, (Ehlers, ed.) 117-128. (Providence: American Mathematical Society).

Duxbury, T.C., T.V. Johnson, and D.L. Matson (1975). Galilean satellite mutual occultation data processing. Icarus 25, 569.

Fillius, R.W., C.E. McIlwain, and A Mogro-Campero (1975). Radiation belts of Jupiter: A second look. Science 188, 465.

Garfinkel, B. (1967). Astronomical refraction in a polytropic atmosphere. Astron. J. 72, 235.

Goldstein, R.M. and G.A. Morris (1975). Radar detection of Ganymede. Science 188, 1211.

Harris, D.L. (1961). Photometry and Colorimetry of planets and satellites. Planets and Satellites, (Kuiper and Middlehurst, eds.) 272-342. (Chicago: University of Chicago Press).

Hubbard, W.B. and T.C. Van Flandern (1972). Occultation of β Sco by Jupiter and Io. III. Astrometry. Astron. J. 77, 65.

Ianna, P.A. (1978). private communication.

Ianna, P.A., P. Seitzer, and F.H. Levinson (1979). Astrometric observations of the satellites of the outer planets. I. The Galilean satellites in 1977. Astron. J. 84, 429.

Johnson, T.V. (1971). Galilean satellites: Narrow band photometry 0.30 to 1.10 microns. Icarus 14, 94.

King, R.W. (1979). private communication.

Kovalevsky, J. and J.L. Sagnier (1977). Motions of natural satellites. Planetary Satellites, (Burns, ed.) 43-62. (Tucson: University of Arizona Press).

Landau, L.D. and E.M. Lifshitz (1962). The Classical Theory of Fields, 257-367. (Oxford: Pergamon Press).

Lieske, J.H. (1973). On the 3-7 commensurability between Jupiter's outer two Galilean satellites. Astron. & Astrophys. 27, 59.

---------- (1974). A Method of Revitalizing Sampson's Theory of the Galilean Satellites. Astron. & Astrophys. 31, 137.

---------- (1977a). Theory of Motion of Jupiter's Galilean Satellites. Astron. & Astrophys. 56, 333.

---------- (1977b). Additional FORTRAN subroutines for obtaining positions and partial derivatives of Jupiter's Galilean satellites. (JPL Engineering Memo 314-112).

---------- (1977c). Galilean satellites: Analysis of photometric eclipses. (JPL Engineering Memo 314-134).

Marsden, B.G. (1966). The motions of the Galilean satellites of Jupiter. Ph.D. Thesis, Yale University.

Morrison, D. (1973). Determination of radii of satellites and asteroids from radiometry and photometry. Icarus 19, 1.

Mulholland, J.D., G.F. Benedict, and P.J. Shelus (1979). Absolute and relative positions of Jupiter V (Amalthea) and the Galilean satellites 1976-1978. Astron. J. 84, 668.

Null, G.W., (1976). Gravity field of Jupiter and its satellites from Pioneer 10 and Pioneer 11 tracking data. Astron. J. 81, 1153.

Null, G.W., J.D. Anderson, and S.K. Wong (1975). Gravity field of Jupiter from Pioneer 11 tracking data. Science 188, 476.

Ostro, S.J. (1978). The structure of Saturn's rings and the surfaces of the Galilean satellites as inferred from radar observations. Ph.D. Thesis, M.I.T.

---------- (1979). private communication.

Pascu, D. (1977). Astrometric techniques for the observation of planetary satellites. Planetary Satellites, (Burns, ed.) 63-86. (Tucson: University of Arizona Press).

---------- (1978). private communication.

Peters, C.F. (1973). Table Mountain Satellite Observation: 1971-72. Astron. J. 78, 957.

Pettengill, G.H., I.I. Shapiro, and D.B. Campbell (1973). Proposal for radar observations of the Galilean satellites of Jupiter (using the Arecibo S-band radar).

Pierce, D.A. (1974). Observations of Jupiter's Satellites. I. Literature Search and Bibliography. (JPL Technical Memo 900-672).

---------- (1975). Computer format for photographic observations of natural satellites and planets. (JPL Engineering Memo 391-626).

---------- (1976). Observations of Jupiter's Satellites. (Supplement to JPL TM 900-672).

Reasenberg, R.D. (1974). Convergence indicator in PEP. Unpublished memorandum dated 1974 Jan 24.

---------- (1975a). The PEP a priori facility. Unpublished memorandum dated 1975 Jul 28.

---------- (1975b). Partial prereduction of the normal equations. Unpublished memorandum dated 1975 Jul 29.

Sampson, R.A. (1910). Tables of the Four Great Satellites of Jupiter (London: Wesley).

---------- (1921). Theory of the four great satellites of Jupiter. Mem. Roy. Astron. Soc. 63, 1.

Schild, A. (1967). Lectures on general relativity. Relativity Theory and Astrophysics 1. Relativity and Cosmology, (Ehlers, ed.) 1-104. (Providence: American Mathematical Society).

Shapiro, I.I. (1967). New method for the detection of light deflection by solar gravity. Science 157, 806.

Smith, E.J., L. Davis, D.E. Jones, P.J. Coleman, D.S. Colburn, P. Dyel, and C.P. Sonett (1975). Jupiter's magnetic field, magnetosphere, and interaction with the solar wind: Pioneer 11. Science 188, 451.

Soulie, G. (1972). Positions de Grosses Planetes et de la Lune. Astron. & Astrophys. Supp. 6, 311.

Standish, M.A. (1979). private communication.

Tausner, M.J. (1966). General Relativity and its Effects on Planetary Orbits and Interplanetary Observations. (M.I.T. Lincoln Laboratory Technical Report 425).

Thuillot, W. (1978). Application d'une integration numerique au systeme des satellites galileens avec comparaison a des observations. Doctoral Thesis, Pierre and Marie Curie University.

(1977) Transactions of the International Astronomical Union, 16B, (Muller and Jappel, eds.) 58. (Dordrecht: Reidel).

Vermilion, J.R., R.N. Clark, T.F. Greene, J.F. Seamans, and W.F. Yantis (1974). A low resolution map of Europa from four occultations by Io. Icarus 23, 89.

Vu, D.T. and J.L. Sagnier (1974). Mouvement des satellites galileens Jupiter: Mise sur ordinateur de la theorie de Sampson. (GRGS Bulletin 11).

Walker, R.L., J.W. Christy, and R.S. Harrington (1978). Positions of Planets and Natural Satellites. Astron. J. 83, 838.

Williamson, R.M. (1976). Photometric Observations of Mutual Eclipses and Occultations of the Galilean Satellites in 1973. Pub. Astron. Soc. Pac. 88, 73.

Wyckoff, S., A. Frohlich, and P. Wehinger (1977). Galilean Satellites: Photometry of Mutual Eclipses and Occultations. Pub. Astron. Soc. Pac. 86, 993.

BIOGRAPHICAL NOTE

John F. Chandler was born July 20, 1951 in Wilmington, Delaware, and he attended public schools there through high school graduation in 1969. In the summers of 1968 and 1969 he participated in National Science Foundation-sponsored summer science programs in modern algebra and computer programming and in archeology. Mr. Chandler won a National Merit Scholarship and a National Honor Society Scholarship and entered the Massachusetts Institute of Technology in September 1969. While at M.I.T. he majored in Earth and Planetary Science. During the summer of 1972 he worked at the National Radio Astronomy Observatory in Charlottesville, Virginia. Mr. Chandler was elected to Phi Beta Kappa. In 1973 he received the Bachelor of Science Degree and won a National Science Foundation Fellowship for graduate study. Since that time he has been enrolled in the M.I.T. graduate school in the Department of Earth and Planetary Science. On July 5, 1975 he married Bonnie Lee German in Cambridge, Massachusetts. She has received a B.A. from Wellesley College and an M.A.T. from Smith College, and she is presently the music secretary at M.I.T.